INVESTIGATING NUCLEAR TRANSPORT PROTEINS AS SECRETED CANCER BIOMARKERS

MICHAEL OBINNA OKPARA
OKPMIC002

Dissertation submitted in fulfilment of requirements for the degree of
MSc (Med) in Medical Biochemistry

in the
Division of Medical Biochemistry and Structural Biology

Department of
Integrative Biomedical Sciences

University of Cape Town

November 2018

Declaration

I, **Michael Obinna Okpara,** hereby declare that the work on which this thesis/dissertation is based is my original work (except where acknowledgements state otherwise) and that neither the whole work nor part of it has been, is being, or will be submitted for the award of another degree in this or any other university.

I have used the ***Nature*** journal style for citation and referencing. Each significant contribution to, and quotation in, this dissertation from the work(s) of other people has been attributed, cited and referenced.

I empower the University of Cape Town to reproduce for research either the whole or any portion of the contents in any manner whatsoever.

Signed: Signed by candidate

Date: November 24, 2018

Acknowledgements

All glory, praise and honour be to God Almighty who has been my stronghold throughout my stay in this great Institution. It is solely due to His benevolence that I have a life worth living and could complete this research project.

My very deep and immense gratitude goes to my parents (Mr and Mrs B. Okpara) and my lovely siblings for their unwavering moral support and prayers. I also appreciate my best friend, Eze Peace Ngozika, for always being there for me and for her words of encouragement.

Thank you to my supervisor, Professor Virna Leaner, for giving me the opportunity to study under her tutelage and for her guidance towards the completion of my study. I also thank my co-supervisor, Dr Pauline van der Watt for her inputs and suggestions.

I appreciate Associate Professor Denver Hendricks for his occasional pats on the back and words of encouragement.

Thank you to my laboratory mate, Aderonke Ajayi-Smith, for making the laboratory a delightful environment to work in.

I sincerely appreciate the tireless efforts of Mrs Hajira Guzgay and Mr Robert Samuels for ensuring that the laboratory was always up and running even on public holidays.

Thanks to Dr Clemens Hermann and Dr Bridget Calder for putting me through the mass spectrometry technique.

I appreciate Professor Iqbal Parker, Ms Arielle Rowe, and Mrs Shatha Omar for providing me with patient serum samples.

Lastly, I will like to specially acknowledge and thank the MasterCard Foundation Scholars Program at the University of Cape Town for providing the financial support needed to complete my study.

“You are my defender and protector. You are my God; in you I trust”

Psalms 91:2

Table of contents

Abbreviations

~	approximately
°C	degrees Celsius
%	percent
ABC	ammonium bicarbonate
ACN	acetonitrile
AP	affinity purification
AP-1	activator protein 1
AUC	area under the receiver operating characteristics curve
BCA	bicinchoninic acid
BRCA1	breast cancer 1
BSA	bovine serum albumin
BSL	biosafety level
CoCoA	coiled-coil co-activator
C18	octadecyl carbon chain
CA	cancer antigen
$CaCl_2$	calcium chloride
CREB	cAMP response element binding protein
CARP-1	cell cycle- and apoptosis-regulatory protein-1
CAS	Cellular apoptosis susceptibility protein
CaSki	human Caucasian epidermoid carcinoma of the cervix
CCAR1	cell division cycle and apoptosis regulator 1
cDNA	complementary deoxyribonucleic acid
CFIm	Cleavage factor Im
chk2	checkpoint kinase 2

cNLS	classical nuclear localisation signal
CO_2	carbon dioxide
co-IP	Co-immunoprecipitation
CPSF7	cleavage and polyadenylation specific factor 7
CREB	cAMP Response Element Binding Protein
CRM1	Chromosomal region maintenance protein 1
CSE1L	chromosome segregation 1-like protein
CT	computerized tomography
CTHRC1	collagen triple helix repeat containing 1
CT-1	Cobalt-60 gamma rays transformed WI-38
CV	coefficient of variation
CVF	cervicovaginal fluid
CYFRA 21-1	cytokeratin 19-fragments
DAPI	4', 6-diamidino-2-phenylindole
dH_2O	distilled water
DMEM	Dulbecco's Modified Eagle's Medium
DMSO	dimethylsulphoxide
DNA	deoxyribonucleic acid
DTT	dithiothreitol
EDTA	ethylenediaminetetraacetic acid
EGF	epidermal growth factor
EGR1	early growth response protein 1
ELISA	enzyme-linked immunosorbent assay
ER	endoplasmic reticulum
ERRP	EGF receptor-related protein

ESI	electrospray ionisation
FCS	fetal calf serum
FDA	Food and Drug Administration
FIP1L1	Pre-mRNA 3'-end-processing factor FIP1
g	Earth's gravitational force
GAPDH	Glyceraldehyde 3-phosphate dehydrogenase
GTPase	guanosine triphosphatase
HeLa	Henrietta Lacks
HER2	human epidermal growth factor receptor 2
HPV	human papillomavirus
HRP	horseradish peroxidase
hTERT RPE-1	human telomerase-immortalized retinal pigmented epithelial 1
IAA	iodoacetamide
IARC	International Agency for Research on Cancer
iBAQ	intensity-based absolute quantification
IBB	Importin β-binding domain
IgG	immunoglobulin G
ILVs	intraluminal vesicles
IP	immunoprecipitation
IPO5	importin-5
IPO7	importin-7
IP-MS	immunoprecipitation mass spectrometry
IP-WB	immunoprecipitation Western blot
J	Youden's index
kDa	kilodaltons

Kpnα	Karyopherin alpha
Kpnβ	Karyopherin beta
KYSE30	human oesophageal squamous cell carcinoma cell line
MALDI	matrix-assisted laser desorption ionisation
MAPK	mitogen-activated protein kinase
mRNA	messenger ribonucleic acid
MS	mass spectrometry
MVBs	multivesicular bodies
m/z	mass-to-charge ratio
Na_3VO_4	Sodium Orthovanadate
NF-kB p65	nuclear factor kappa-light-chain-enhancer of activated B cells
NES	nuclear export signal
NLS	nuclear localisation signal
NPCs	nuclear pore complexes
NSB1	Nijmegen breakage syndrome 1
NSCLC	non-small cell lung cancer
Ntf2	nuclear transport factor 2
Nups	nucleoporins
Nup214	nucleoporin 214
OSCC	oesophageal squamous cell carcinoma
Pap	Papanicolaou
PBS	phosphate buffered saline
PI	protease inhibitor
PET	positron-emission tomography
pre-mRNA	precursor messenger ribonucleic acid

PSA	prostate-specific antigen
Ran	Ras-related nuclear protein
RAC-1	Ras-related C3 botulinum toxin substrate 1
RanBP	Ran-binding protein
RanGDP	Ran-guanosine diphosphate
RanGTP	Ran-guanosine triphosphate
ROC	receiver operating characteristics curves
RPL7	ribosomal protein L7
RPL10	ribosomal protein L10
RPL13A	ribosomal protein L13A
RPS6	ribosomal protein S6
RPS4X	ribosomal protein S4, X isoform
RIPA	radioimmunoprecipitation assay
RNA	ribonucleic acid
rRNA	ribosomal ribonucleic acid
RT	room temperature
SCC-Ag	squamous cell carcinoma antigen
SD	standard deviation
SDS	Sodium dodecyl sulphate
SE	standard error
SEM	standard error of the mean
STIs	sexually transmitted infections
STRING	Search Tool for the Retrieval of Interacting Gene/protein
SV40	Simian virus 40
SVWI38	SV40-transformed lung fibroblasts

TMB	3,3’,5,5’-tetramethylbenzidine
TBST	Tris-buffered saline with tween-20
TNPO1	Transportin-1
TOF	time-of-flight
TPA	tissue polypeptide antigen
U	units
UTR	untranslated region
vs	versus
w/v	weight/volume
WHCO5	human oesophageal squamous cell carcinoma cell line
XPO1	exportin-1
XPO2	exportin-2
Y2H	yeast two-hybrids

Units

M	molar
mM	millimolar
mg	milligram
µg	microgram
ng	nanogram
L	litre
ml	millilitre
µl	microlitre
mm	millimetre

nm	nanometre
V	volts

Abstract

Previous studies in our laboratory using microarray gene expression analysis identified members of the nuclear transport protein family as significantly upregulated in cervical cancer biopsies compared to normal cervical epithelial tissues. These results were validated at both mRNA and protein levels, and similar upregulation observed in oesophageal cancer. Recent mass spectrometry (MS) analysis of cancer cell secreted proteins identified elevated levels of 13 members of the nuclear transport protein family in the secretomes of transformed, cervical cancer and oesophageal cancer cell lines. The nuclear transport proteins have functions in many cellular processes including proliferation, mitosis, maturation of RNA, activation of the actin cytoskeleton and restructuring of the nuclear envelope. In addition, they are required for the nuclear import and export of numerous cargo proteins such as transcription factors, oncoproteins and kinases, which often display deregulated activity in cancer cells.

The aims of this study were to 1) independently validate the MS data showing elevated levels of the nuclear transport proteins in the secretomes of cervical and oesophageal cancer cell lines, 2) investigate the diagnostic potential of members of the nuclear transport protein family using cervical and oesophageal cancer serum samples and 3) identify the potential binding partners of Kpnβ1, a key member of the nuclear transport protein family, in normal and cancer cells.

This study investigated the levels of endogenous expression and secretion of 8 members of the nuclear transport protein family; Kpnβ1, IPO5, IPO7, TNPO1, CRM1, CAS, Kpnα2 and Ran in a normal epithelial cell line (hTERT-RPE1) in comparison to transformed (SVWI38 and CT-1), cervical cancer (HeLa and CaSki) and oesophageal cancer (WHCO5 and KYSE 30) cell lines using Western blot analysis. Our data revealed differential endogenous expression in the cell lines. An analysis of the secretomes of the cell lines showed that all 8 proteins assayed were secreted at elevated levels by the transformed, cervical cancer and oesophageal cancer

cell lines compared to the normal cell line. These results validate previous MS data generated in our laboratory.

To investigate whether members of this protein family can be detected in the serum of cancer patients, ELISA for Kpnβ1, CRM1, Kpnα2 and CAS proteins were performed using commercially available ELISA kits. The results showed significantly elevated levels of Kpnβ1, CRM1 and CAS in the serum of cervical cancer patients compared to the non-cancer controls. Serum levels of Kpnβ1, CRM1, Kpnα2 and CAS were elevated in the oesophageal cancer patients compared to the non-cancer controls. To investigate the diagnostic potential of these proteins, logistics regression analysis was performed. Our results showed that CAS was the best performing individual candidate biomarker in discriminating between cervical cancer cases and non-cancer controls. It had the highest AUC (0.85±0.03) and highest sensitivity (55%) at 95% specificity compared to those of Kpnβ1 (AUC=0.77±0.04 with 35% sensitivity at 95% specificity), CRM1 (AUC=0.64±0.05 with 20% sensitivity at 95% specificity) and Kpnα2 (AUC=0.51±0.05 with <10% sensitivity at 95% specificity). The combination of Kpnβ1, CRM1, Kpnα2 and CAS as a panel of biomarkers had an improved AUC of 0.89 with a sensitivity of 100% at 60% specificity. In discriminating oesophageal cancer cases from the non-cancer controls, CAS (AUC=0.86±0.03 with 56% sensitivity at 95% specificity) similarly performed better compared to Kpnβ1 (AUC=0.62±0.05 with 15% sensitivity at 95% specificity), CRM1 (AUC=0.75±0.04 with 32% sensitivity at 95% specificity) and Kpnα2 (AUC=0.73±0.04 with 21% sensitivity at 95% specificity). The combination of Kpnβ1, CRM1, Kpnα2 and CAS as a panel of biomarkers had the highest diagnostic capacity with an AUC of 0.90 and 84% sensitivity at 86% specificity. These results suggest that individual members of the nuclear transport protein family have potential as diagnostic biomarkers for both cervical and oesophageal cancers, with a combination of Kpnβ1, CRM1, Kpnα2 and CAS being the best predictor.

Our investigation aimed at identifying the binding partners of Kpnβ1 in normal, cervical cancer and oesophageal cancer cell lines using immunoprecipitation coupled to mass spectrometry (IP-MS) identified 100 potential Kpnβ1 binding partners in hTERT-RPE1 normal cell extracts, 179 in HeLa cervical cancer cell extracts, 147 in WHCO5 cell extracts and 176 in KYSE30 oesophageal cancer cell extracts. VennDis JavaFX-based Venn and Euler diagram software was used to identify common and unique Kpnβ1 binding partners. 38 proteins were identified as common binding partners of Kpnβ1 in normal and cancer cells and 56 common binding partners of Kpnβ1 in the three cancer cell lines. Of these, 18 proteins were found to be unique to the three cancer cell lines and of these, 10 could be linked via protein-protein interaction mapping using STRING bioinformatic analysis. These include nucleoporin 214 (Nup214), Pre-mRNA 3'-end-processing factor FIP1 (FIP1L1), cell division cycle and apoptosis regulator 1 (CCAR1), cleavage and polyadenylation specific factor 7 (CPSF7), ribosomal protein L7 (RPL7), ribosomal protein L10 (RPL10), ribosomal protein L13A (RPL13A), ribosomal protein S6 (RPS6), ribosomal protein S4, X isoform (RPS4X) and Ras-related nuclear protein (Ran). Among these, FIP1L1, CCAR1 and CPSF7 have not been previously described as binding partners of Kpnβ1.

In conclusion, elevated levels of nuclear transport proteins in the extracellular environment of cancer cells and in cancer patient serum samples suggest that they have potential as diagnostic biomarkers for cervical and oesophageal cancers, with a combination of Kpnβ1, CRM1, Kpnα2 and CAS being the best predictor. In addition, this study shows that Kpnβ1 interacts with several different proteins in normal and cancer cells, with some of the interactions unique to cancer cells presenting as novel binding partners for further investigation.

CHAPTER 1

LITERATURE REVIEW

1.1. Global burden of cancer

Cancer is the uncontrolled growth and spread of cells, which can affect almost any part of the body[1]. It is a life-threatening disease and is a major cause of morbidity and mortality worldwide[2]. Cancer morbidity or mortality is a result of the ability of the cancer cells to metastasize[3]. According to a data survey available in the GLOBOCAN series of the International Agency for Research on Cancer (IARC), 14.1 million new cancer cases and 8.2 million cancer deaths were recorded worldwide in 2012[4]. The mortality rate of cancer worldwide is greater than those of malaria, HIV/AIDS, and tuberculosis combined[5]; it should, therefore, be given a global health priority. Cancer is projected to become a leading cause of morbidity and mortality in developing countries in the near future[6], with a projected increase from 6·1 million new cases in 2012 to 9·9 million new cases in 2030[4]. Even though developing countries bear the greater burden of cancer incidence and mortality, the resources made available in these countries in the fight against cancer remain limited, with 5% of all resources allotted to cancer care globally made available to developing countries[7].

In South Africa, almost 40 000 deaths from 58 000 cancer cases are recorded annually with cervical and oesophageal cancers ranking among the three major cause of cancer mortality[8]. It is thus imperative that systems be in place to improve primary health care by funding additional research geared towards early detection and diagnosis of cancer.

1.2. Cancer of the Cervix uteri

Cervical cancer arises from the abnormal growth of cells in the cervix which can spread to other parts of the body[9]. There are two major histological subtypes of cervical cancer: the adenocarcinomas and squamous cell carcinomas. Adenocarcinomas account for 15% of all cervical cancers while squamous cell carcinomas account for about 85%[10].

1.2.1. Cervical cancer burden in South Africa

In South Africa, cervical cancer has been reported to be the second most diagnosed cancer in women with an annual diagnosis of 7735 new cases. As the leading cancer-related cause of death among South African women, cervical cancer is responsible for approximately 4248 new cancer deaths annually[11]. South Africa is one of the countries with the highest cervical cancer incidence and mortality rates (Figures 1.1 and 1.2).

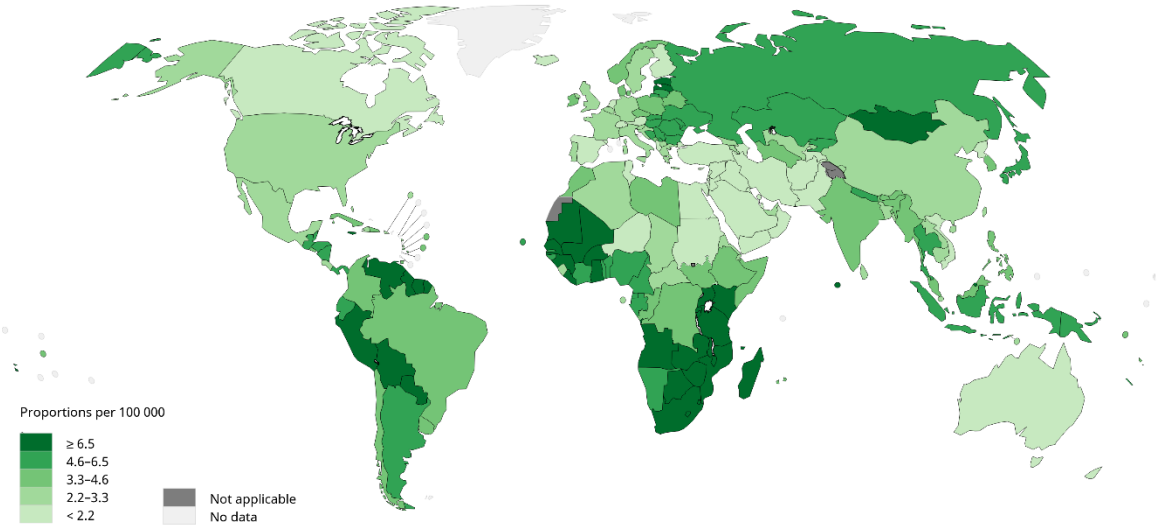

Figure 1.1. Incidence cumulative risk of cervical cancer. The map shows the probability of females that will be diagnosed with cervical cancer before the age of 75. GLOBOCAN 2018 URL: http://globocan.iarc.fr/Pages/Map.aspx#

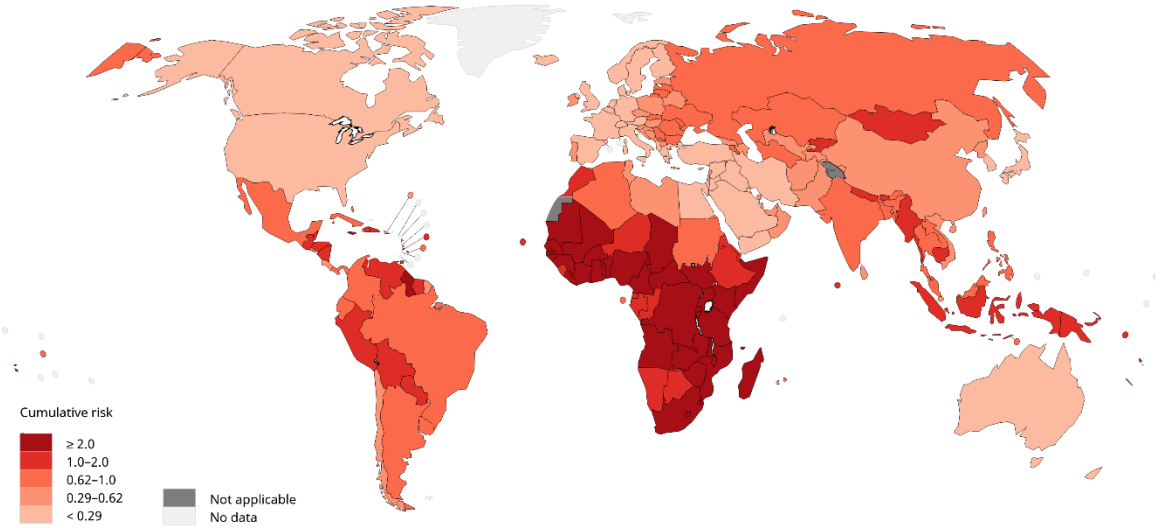

Figure 1.2. Mortality cumulative risk of cervical cancer. The map shows the probability of females dying from cervical cancer before the age of 75. GLOBOCAN 2018 URL: http://globocan.iarc.fr/Pages/Map.aspx#

1.2.2. Risk factors for cervical cancer

Human Papillomavirus (HPV) infection is the leading cause of cervical cancer, with infection by the high-risk HPV types 16, 18, 31 or 45 responsible for about 75% of all cervical cancers diagnosed each year[12,13]. Vaccinating girls against HPV before the onset of sexual activity would reduce the lifetime risk of cervical cancer by 40%[14]. HPV vaccines such as Gardasil (Merck and Company, Whitehouse Station, NJ) and Cervarix (GlaxoSmithKline, Brentford, UK) are commercially available, however, these are costly for citizens of many low-income countries including South Africa[15].

1.2.3. Screening/diagnostic methods for cervical cancer

There are different diagnostic tests that are performed in clinics for the detection of cervical cancer. The most common is the Papanicolaou (Pap) smear test or exfoliative cervicovaginal cytology. Others are the pelvic examination test (which is a visual and manual diagnostic test), colposcopy, endocervical curettage, loop electrosurgical procedure and imaging. The importance of these tests in diagnosing cervical cancer cannot be disputed as they have contributed to the management of cervical cancer in patients. However, there are some limits to the use of these diagnostic tests. For instance, the sensitivity of Pap smear tests to accurately detect cervical cancer is less than 50%, thereby giving false-negative results[16]. Colposcopy, endocervical curettage and loop electrosurgical procedures are very expensive and citizens of low-income countries struggle to afford them. Also, they are minimally invasive medical procedures which can cause some pain and damage to the body. Therefore, there is a need to discover diagnostic biomarkers with high sensitivity which can be measured in the blood for the detection of cervical cancer.

1.3. Cancer of the oesophagus

There are two histological subtypes of oesophageal cancer; adenocarcinoma and oesophageal squamous cell carcinoma (OSCC)[17]. Adenocarcinoma occurs within the distal third of the oesophagus and is formed from columnar epithelial cells; while OSCC occurs in the proximal region of the oesophagus and is formed from squamous epithelial cells[18]. There has been a rise in adenocarcinoma prevalence in the western world[19,20], but OSCC is more prevalent in developing countries[18].

1.3.1. Oesophageal cancer burden in South Africa

South Africa is known to have one of the highest incidences of oesophageal cancer in the world. Oesophageal cancer is the eighth most common cancer worldwide, and the sixth most common cause of death from cancer with about 80% of the cases worldwide occurring in developing countries. The mortality rate of oesophageal cancer in South Africa is reported to be 12.8 in every 100,000 men and 6.2 in every 100,000 women[2]. According to IARC, South Africa is one of the countries with the highest probabilities of individuals who will be diagnosed with oesophageal cancer and are expected to die from oesophageal cancer (Figures 1.3 and 1.4)

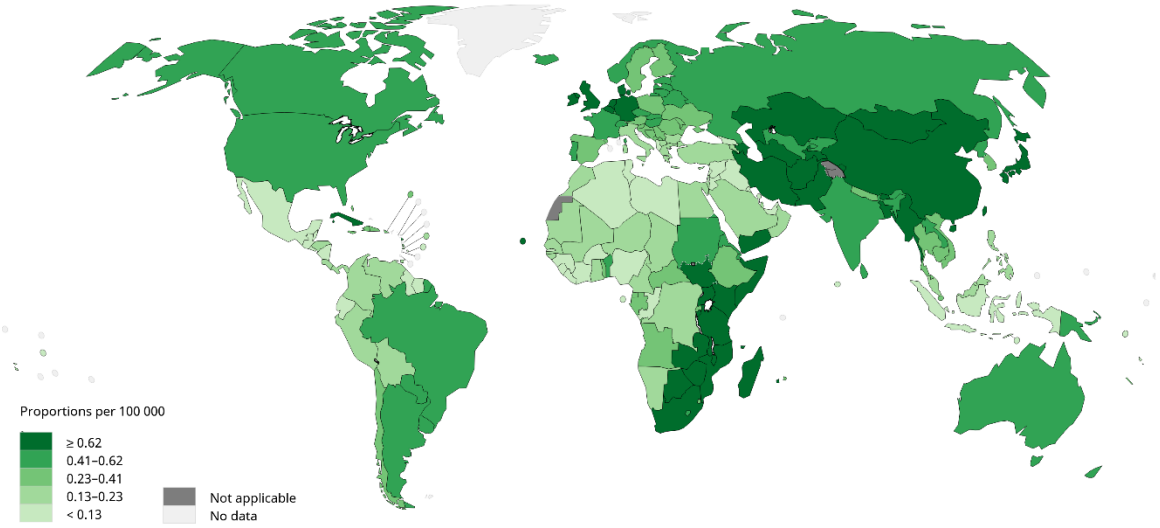

Figure 1.3. Incidence cumulative risk of oesophageal cancer. The map shows the probability of individuals that will be diagnosed with oesophageal cancer before the age of 75. GLOBOCAN 2018 URL: http://globocan.iarc.fr/Pages/Map.aspx#

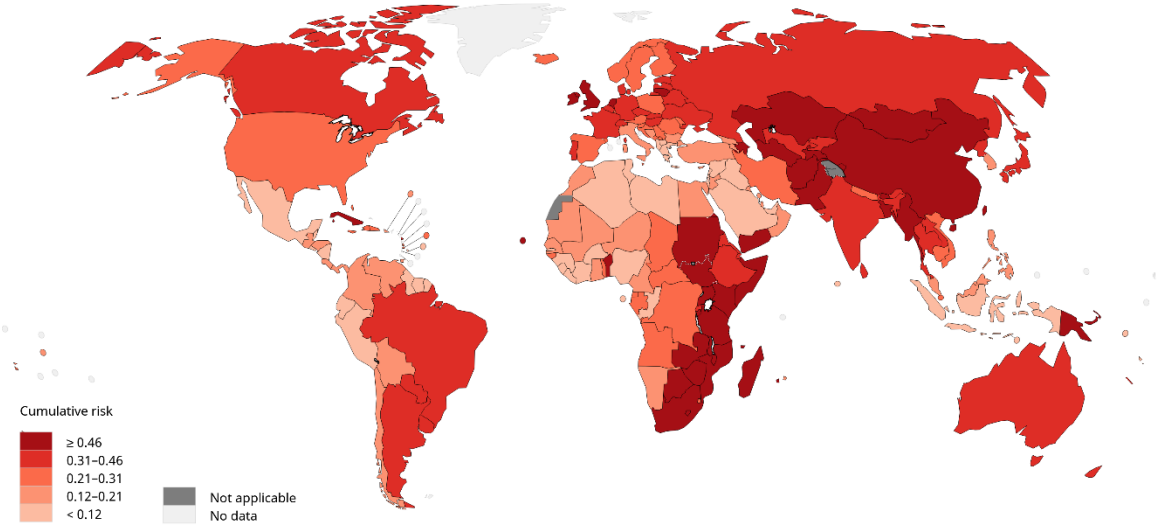

Figure 1.4. Mortality cumulative risk of oesophageal cancers. The map shows the probability of individuals dying from oesophageal cancer before the age of 75. GLOBOCAN 2018 URL: http://globocan.iarc.fr/Pages/Map.aspx#

1.3.2. Risk factors for oesophageal cancer

Smoking tobacco and opium are major risk factors for the development of oesophageal cancer, as carcinogenic compounds such as polycyclic aromatic hydrocarbons are produced. Alcohol consumption has also been implicated as a risk factor for oesophageal cancer[21–24]. Consumption of diets rich in starch but poor in fruits and vegetables is also a risk factor of oesophageal cancer[24,25]. Other risk factors of oesophageal cancer include diseases such as achalasia[26] and Plummer-Vinson syndrome[27].

1.3.3. Screening/diagnostic methods for oesophageal cancer

The diagnosis of oesophageal cancer involves some screening tests. The first diagnostic test conducted is a barium swallow examination called an oesophagogram to detect ulceration of the oesophagus. The presence of a stricture in the oesophagus hinders the progress of the barium which is monitored radiographically. Then upper endoscopy can be performed to examine the oesophageal lining by passing an endoscope down the digestive tract. During an upper endoscopy, biopsies can be taken for further examination. If the biopsies indicate the growth of tumours, then other tests such as endoscopic ultrasound, computerized tomography (CT) scan and/or positron-emission tomography (PET) scan will be done to determine if the tumour has metastasized[28]. As these diagnostic procedures are very expensive and usually involve exposing the body to some radioactive materials during the scans, it becomes imperative to discover blood-based diagnostic biomarkers for the diagnosis of oesophageal cancer.

1.4. Biomarkers and their applications in cancer

According to the National Cancer Institute, a biomarker is a biological molecule found in blood, other body fluids, or tissues that is a sign of a normal or abnormal process, or of a condition or disease[29], such as cancer. A biomarker may also be used to see how well the body

responds to a treatment for a disease or condition[29]. Cancer biomarkers can be any of the following; proteins, metabolites, deoxyribonucleic acid (DNA), messenger ribonucleic acid (mRNA), or processes such as apoptosis, angiogenesis or proliferation[30].

Biomarkers have the potential to be tools for the early diagnosis of diseases and for the monitoring of high-risk populations. Their discovery in cancer research is receiving considerable interest as it is anticipated that biomarkers could have an impact on the global cancer burden. Furthermore, they enhance the discovery and development of targeted therapeutics[31]. Biomarkers which can be monitored from readily accessible fluids have thus become the focus of much research.

1.4.1. Classification of cancer biomarkers

There are three classes of biomarkers: predictive, prognostic and diagnostic biomarkers. Predictive biomarkers can predict the possible response of patients before a specific therapeutic intervention is administered. Prognostic biomarkers give an indication of the chances of a patient responding to therapy after the disease is diagnosed and they predict the possibility of a disease or recurrence of the disease. Diagnostic biomarkers are used to detect the presence of a type of cancer in patients[30].

1.4.2. Qualities of an ideal diagnostic biomarker

An ideal diagnostic biomarker should be present in a measurable amount in body fluids – such as serum – even at the early stage of the disease[32]. Its detection must be extremely accurate to ensure proper clinical management of patients. Testing for an ideal biomarker should be safe, easy and relatively cheap to conduct so that the developing countries can easily access it. High sensitivity and specificity for the disease in question is another quality of an ideal biomarker, so as to minimize false-positive and false-negative values when the disease is tested for[33–36].

1.4.3. Blood as a source of secreted cancer biomarkers

As the human blood carries out its primary function of transportation, it encounters different organs, tissues and cells, hence making it an attractive source for discovering biomarkers for several diseases. Cancer cells are known to secrete proteins into their extracellular environment[37] and many secreted proteins from cancer cells can enter the blood circulation and could serve as potential therapeutic targets and diagnostic biomarkers[38]. A benefit of blood as a source of secreted protein biomarkers is that it encounters virtually all cells in the organism. Even tissue-related proteins can be released into the bloodstream due to specific secretion, shedding from the surface, or non-specific leakage[39]. As a source of cancer biomarkers, blood is advantageous as it is easily accessible, its collection is minimally invasive, low risk and inexpensive[40]. Although significant amounts of albumin and other proteins in blood serum present potential difficulties when analysing blood serum for potential biomarkers, it still remains the optimal sample to investigate from the perspective of biomarker discovery[38].

Blood samples have been used to identify biomarkers of many human diseases including Alzheimer's disease[41], Parkinson's disease[42], preeclampsia[43], breast cancer[44], and prostate cancer[45]. Before a blood cancer biomarker can be approved for use in clinical settings, extensive clinical validation must be carried out, hence, only a few blood-based cancer biomarkers have been approved by the Food and Drug Administration (FDA) for use in clinical practice (Table 1.1)[46]. As there are currently no FDA approved cervical and oesophageal cancer biomarkers, it becomes imperative to discover secreted proteins which have the potential of becoming cervical and oesophageal cancer biomarkers.

Table 1.1. List of FDA approved blood-based protein cancer biomarkers currently used in clinical practice

Biomarkers	Cancer type	Methodology for quantification	Year first approved
Pro2PSA	Prostate	Immunoassay	2012
ROMA (HE4+CA-125)	Ovarian	Immunoassay	2011
OVA1 (multiple proteins)	Ovarian	Immunoassay	2009
HE4	Ovarian	Immunoassay	2008
Fibrin/fibrinogen degradation product (DR-70)	Colorectal	Immunoassay	2008
AFP-L3%	Hepatocellular	HPLC, microfluidic capillary electrophoresis	2005
Circulating Tumor Cells (EpCAM, CD45, cytokeratins 8, 18+, 19+)	Breast	Immunomagnetic capture/ immune-fluorescence	2005
CA19-9	Pancreatic	Immunoassay	2002
CA-125	Ovarian	Immunoassay	1997
CA15-3	Breast	Immunoassay	1997
CA27.29	Breast	Immunoassay	1997
Free PSA	Prostate	Immunoassay	1997
Thyroglobulin	Thyroid	Immunoassay	1997
Alpha-fetoprotein (AFP)	Testicular	Immunoassay	1992
Total PSA	Prostate	Immunoassay	1986
Carcino-embryonic antigen	Not specified	Immunoassay	1985

1.5. Mechanism of protein secretion

Synthesized proteins are assembled by ribosomes as they move into the endoplasmic reticulum (ER) and they are able to associate with rough ER through an ER-signal peptide[47]. These proteins undergo four essential modifications – glycosylation, formation of disulphide bonds, folding of polypeptide chains and specific proteolytic cleavage – before they are secreted into the extracellular space of the cell. The translational process is completed in the ER where newly synthesized proteins are either incorporated into transport vesicles that combine together to form *cis*-Golgi vesicles or they remain in the ER as structural proteins or enzymes[47]. As the *cis*-Golgi cisterna changes to *trans*-Golgi cisterna, membrane-bound and luminal proteins undergo post-translational modifications. These modified proteins are then ready for secretion into the extracellular environment via any of the described classical or non-classical protein secretion pathways (Figure 1.5).

Some proteins move to the cell surface via micro-vesicles and are secreted in this manner into the extracellular environment[47]. Secretory vesicles can bind to the plasma membrane and ensure the release of the luminal proteins into the extracellular environment[48]. Other proteins are translocated across the plasma membrane into the extracellular space[48]. The synthesis of exosomes can also serve as a mechanism through which proteins can be secreted into the extracellular environment[48].

Exosomes (40-100 nm in diameter) are a group of small extracellular vesicles which contain RNAs, lipids and proteins[49]. There is evidence that suggests that body fluids from cancer patients contain more exosomes than body fluids from non-cancer subjects[50,51]. Additionally, the existence of circulatory RNAs and proteins in exosomes have made them a promising target for cancer biomarkers discovery with over 4000 different exosomal proteins already identified from purified exosomes[52]. As a subset of the secretome, the exosome is enriched with proteins

which would have been classified as low abundance proteins in the total secreted proteins, thus, making cancer cell-derived exosomes a good source for the discovery of diagnostic biomarkers[53]. Some of the protein groups that have been identified in exosomes from both cancer patient samples and *in vitro* cell lines include membrane trafficking and cytoskeletal proteins, heat-shock proteins, major histocompatibility complexes, signal transducers and many others[54].

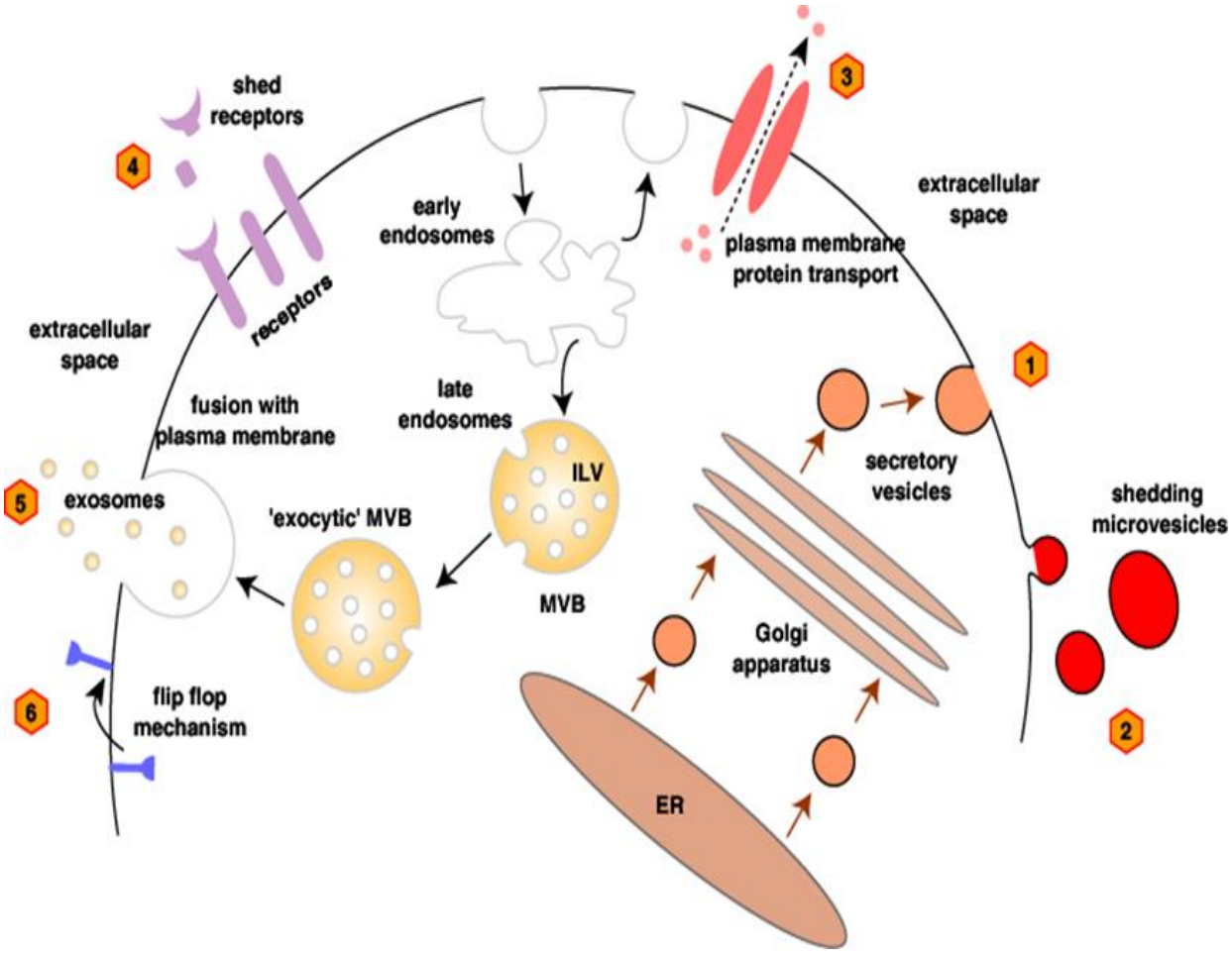

Figure 1.5. Mechanism of protein secretion. Protein secretion in cells occurs through classical or non-classical pathways. (1) classical secretion via the ER/Golgi apparatus (2) plasma membrane blebbing (3) translocation across the plasma membrane (4) receptor-mediated protein secretion (5) exosomal secretion where intraluminal vesicles (ILVs) which are accumulated within multivesicular bodies (MVBs) are moved to the plasma membrane and released into the extracellular environment as exosomes (6) flip-flop secretory mechanism. http://mathivananlab.org/images/Protein_Secretion.png[55].

1.6. Secreted proteins and their potential as cancer biomarkers

All proteins released by a cell, a tissue, or an organ via a classical or non-classical protein secretion pathway are known as the secretome[56–58]. It has been reported that about one-tenth of the entire human genome encodes secreted proteins[56]. The secreted proteins of a cell, tissue, or organ may include growth factors, immune regulatory cytokines, chemokines, hormones, other paracrine signalling molecules, cell motility factors, and extracellular matrix-degrading proteases[59,60] and their secretion may be an indication of pathological conditions[61].

The study and analysis of the cancer secretome are essential for the discovery of cancer biomarkers[56,60,62,63], as it has been reported that cancer cells secrete proteins into their extracellular environment[37]. Conditioned media containing secreted proteins from cultured cancer cells could also serve as a source for biomarkers discovery[64]. Recent studies have been conducted on conditioned media for the discovery of diagnostic biomarkers using mass spectrometry (MS) in diverse cancers including glioblastoma[65], thyroid[66], colorectal[67], breast[68], pancreatic[69], head and neck[70] and lung cancer[71].

The analysis of secreted proteins in conditioned media *in vitro* poses some challenges as the low concentration of these secreted proteins demands that concentration steps are required. These may lead to partial loss of the proteins contained in the supernatant[72]. Another challenge encountered during the analysis of secreted protein in conditioned media is the possible "release" of intracellular proteins which become contaminants in the conditioned media[56,73,74]. This could be because of cell lysis and/or cell death as these cells are incubated in serum-free media. Optimizing sample preparation steps such as the time of serum starvation[74,75] and cell seeding concentrations have been recommended to reduce the contamination of conditioned media by intracellular proteins to a bearable minimum[71,76].

Studies aimed at identifying secreted biomarkers for cervical and oesophageal cancers have been carried out. A recent study using enzyme-linked immunosorbent assay (ELISA) techniques identified collagen triple helix repeat containing 1 (CTHRC1) and squamous cell carcinoma antigen (SCC-Ag) as novel potential diagnostic biomarkers for cervical cancer[77]. In another study, proteomics techniques were used to discover 16 candidate markers with only alpha-actin-4 and pyruvate kinase isozyme M1/M2 identified as the most promising biomarkers for detecting cervical cancer[78]. A different study aimed at discovering diagnostic biomarkers for oesophageal cancer identified cytokeratin 19-fragments (CYFRA 21-1), tissue polypeptide antigen (TPA) and SCC-Ag as potential biomarkers for OSCC[79]. However, these biomarkers have limited use as they have low sensitivity and specificity. Thus, there is a need to continue research to identify biomarkers which could enhance early detection and better cancer diagnosis.

Previous studies performed in our laboratory identified nuclear transport proteins as potential biomarkers for cervical and oesophageal cancers. This was achieved through the use of cDNA microarray technology to profile normal cervical epithelial tissues and cervical cancer biopsies, obtained from South African patients. van der Watt *et al*. (2009) discovered that the genes encoding the nuclear transport proteins were expressed at significantly elevated levels in the cancer biopsies compared to the normal tissues[80]. Verification of nuclear transport proteins upregulation was performed at the protein level and both cervical and oesophageal cancer cells were found to display elevated levels of members of the nuclear transport protein family.

Based on the findings of van der Watt *et al*. (2009), a hypothesis-driven biomarker discovery in cancer cells secretomes was performed in our laboratory using MS. An inclusion list comprising 31 nuclear transport proteins was generated using Skyline, and an inclusion on versus inclusion off runs were performed. An analysis of the secretomes of normal, transformed

and cancer cells showed a general increase in the abundance of 13 members of the nuclear transport protein family from normal to transformed to cancer cells (A. Wishart, MSc dissertation, 2017[†]). We, therefore, hypothesized that these nuclear transport proteins could be potential biomarkers for the diagnosis of cervical and oesophageal cancers.

1.7. The nuclear transport protein family

Facilitated transport of numerous proteins is achieved via the action of nuclear transport proteins. The superfamily of nuclear transport proteins consists of the Karyopherin beta (Kpnβ)/Importin beta family, the Karyopherin alpha (Kpnα)/Importin alpha family of adaptor proteins and Ran protein (which provides the energy required for nuclear-cytoplasmic transport). The Kpnβ family forms the major class of soluble transport receptors. Its members interact with some import and/or export cargo proteins and certain ribonucleic acids (RNA) across the nuclear envelope. Thus far 20 genes encoding Kpnβ family members in the human genome have been identified including ten proteins involved in nuclear import, seven proteins involved in nuclear export, two bidirectional transporters and one transporter that remains uncharacterised[81].

The nuclear import proteins – generally known as importins – bind their cargo in the cytoplasm and transport the cargo into the nucleus. An import function has been demonstrated for almost all the importins and they include: Kpnβ1 (also known as importin-β or importin-β1 or p97)[82], Kpnβ2 (also called transportin-1 (TNPO1) or importin-β2)[83], transportin-2 (also referred to as importin-β2b)[84], Kpnβ3 (also called Ran-binding protein (RanBP)5 or importin-β3 or importin-5 (IPO5))[85], importin-4[86], importin-7 (IPO7) (also called RanBP7)[85], importin-8[87], importin-9[86], importin-11[88], and importin-12 (also known as transportin-SR or transportin-3)[89].

[†] A Wishart. "Investigating secreted biomarkers for cancer: the potential of the nuclear transport proteins." University of Cape Town, 2017.

The seven transport proteins that have been reported to mediate transportation of cargoes from the nucleus to the cytoplasm include: Chromosomal region maintenance protein 1 (CRM1) or exportin-1 (XPO1)[90], Cellular apoptosis susceptibility protein (CAS) (also known as chromosome segregation 1-like protein (CSE1L) or exportin-2 (XPO2))[91], exportin-5[92], exportin-6[93], exportin-7[94], RanBP17 and exportin-t[95]. Meanwhile, Importin-13[96] and exportin-4[97,98] have been reported to mediate both nuclear import and export of cargoes, while RanBP6 is yet to be characterized.

Though most of these Kpnβ proteins are capable of mediating nuclear-cytoplasmic transport independently, few, such as Kpnβ1, often interact with an adaptor protein before they can bring about the transport of protein cargoes. These adaptor proteins make up the other subgroup of the karyopherin superfamily, known as the Kpnα or importin alpha family. The characterized human Kpnα proteins include Kpnα1 (importin α5), Kpnα2 (importin α1), Kpnα3 (importin α4), Kpnα4 (importin α3), Kpnα5 (importin α6) and Kpnα6 (importin α7)[99].

1.8. Mechanisms of nuclear-cytoplasmic transport

The translocation of molecules to and from the nucleus or cytoplasm is limited by the nuclear envelope, a double-membrane structure in which large pore structures named nuclear pore complexes (NPCs) are embedded. Each NPC is made up of approximately (~)50 – 100 different proteins, called nucleoporins (Nups)[100,101]. Proteins smaller than 20–30 kDa can pass through the NPC via passive diffusion while larger proteins require facilitated transport to gain access into or out of the nucleus[101].

Kpnβ1-mediated nuclear transport occurs via active transport and the energy is provided by Ras-related nuclear protein (Ran), a small Ras-like guanosine triphosphatase (GTPase)[102]. In the classical nuclear import pathway, the cargo protein is recognized by Kpnα through its nuclear localisation signal (NLS). They bind to Kpnβ1, thereby forming a cargo:Kpnα:Kpnβ1

trimeric complex, which localizes to the nuclear envelope[103]. Ran-guanosine triphosphate (RanGTP) then binds after translocation through the NPC, inducing the allosteric destabilization and release of the import cargo and Kpnα. Kpnα is recycled back to the cytoplasm by its own nuclear exporter, CAS. Kpnβ1 is separately transported back to the cytoplasm, bound by RanGTP. Back in the cytoplasm, RanGTP is hydrolysed to Ran-guanosine diphosphate (RanGDP) and Kpnβ1 is released for its next cycle (Figure 1.6). RanGDP is transported back into the nucleus via its import factor, nuclear transport factor 2 (Ntf2)[102].

In the classical nuclear export pathway, the cargo protein is recognized by the exportin through its nuclear export signal (NES). RanGTP then binds to stabilize the complex which is translocated into the cytoplasm through the NPC. The hydrolysis of RanGTP to RanGDP causes the complex to dissociate, thereby releasing the cargo protein into the cytoplasm (Figure 1.6). Unlike the case of numerous NLSs, only one NES which is recognised by CRM1 has been characterised to date[104].

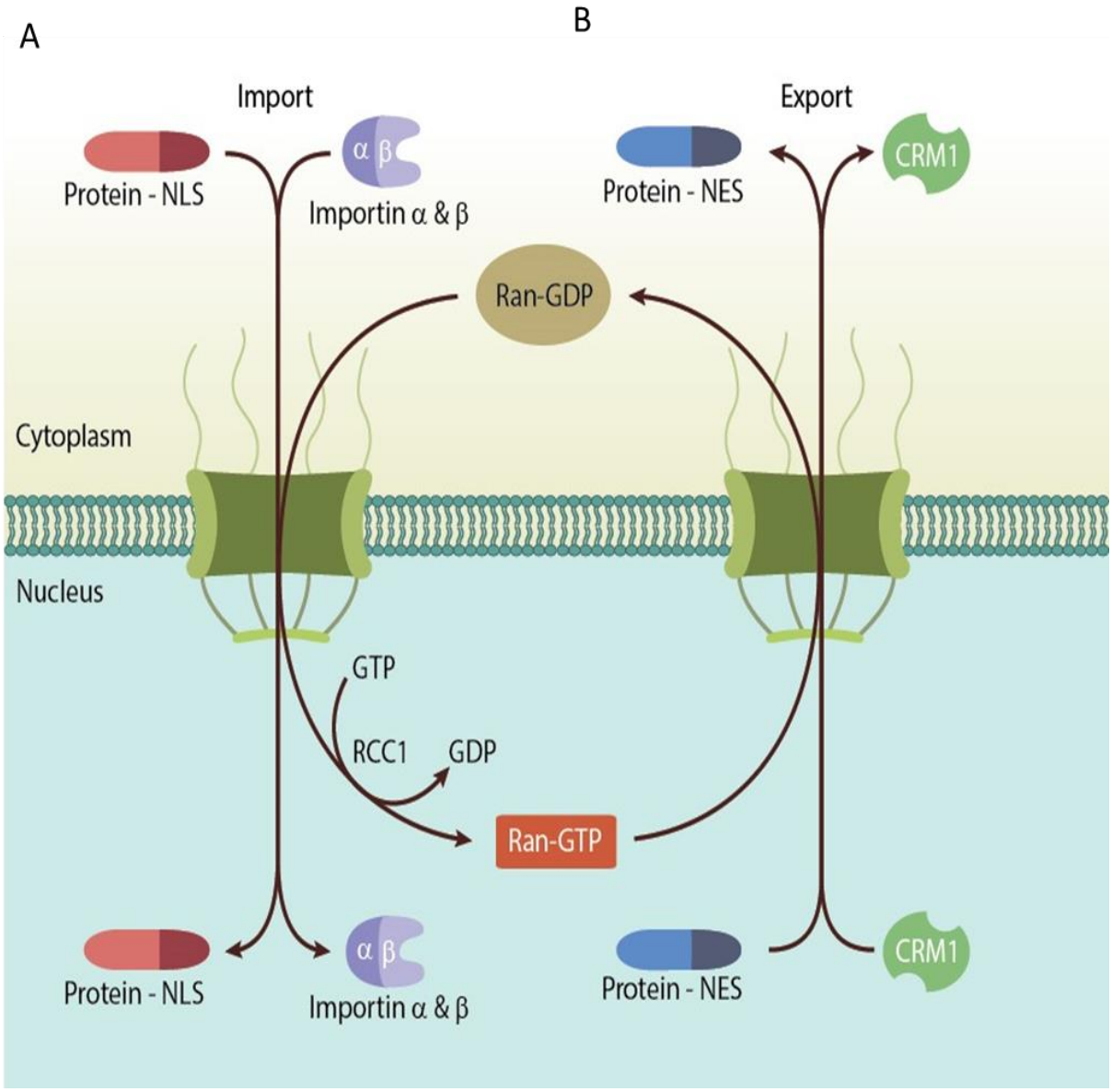

Figure 1.6. Classical nuclear import/export pathways. **A)** Kpnα is an adaptor protein which binds with Kpnβ1 and facilitates the binding of the cargo protein through its nuclear localisation signal (NLS) region of amino acids. This trimeric complex is now able to translocate from the cytoplasm into the nucleus through the NPC. The binding of RanGTP to this complex in the nucleus causes the dissociation of the cargo protein from the complex. Kpnα is shuttled back into the cytoplasm by CAS protein to repeat the transport cycle (not shown). **B)** the NES on the cargo protein enhances the binding of CRM1 which then binds to RanGTP to stabilise the complex. This trimeric complex then translocates from the nucleus into the cytoplasm through the NPC. RanGAP1 and RanBP1 catalyst (not shown) hydrolyse RanGTP to a RanGDP form which causes the complex to dissociate, thus releasing the cargo protein. RanGDP is then shuttled back to the nucleus by Ntf2 (not shown) and converted back into RanGTP by Rcc1 to maintain the directionality of the transport cycle. Figure adapted from MBInfo, (2014)[105].

1.9. Potential of nuclear transport proteins as cancer biomarkers

Generally, the rate of nuclear-cytoplasmic transport increases as cells change from quiescence to proliferating to transformed cells[106]; hence leading to an increased level of certain Kpnβ proteins in transformed cells[106]. Our laboratory previously showed that Kpnβ1 is overexpressed in cervical cancer tissue and cell lines compared to normal cervical tissue and normal cervical epithelial cells[80]. As the primary importer of cargoes into the nucleus, the concentration of Kpnβ1 in the cell determines the rate of nuclear import[107]. In classical cases, Kpnβ1 depends on its adaptor protein, Kpnα to bring about its import function[103]. CRM1 is the principal exporter of cargoes from the nucleus into the cytoplasm[90] and has been reported to be overexpressed in pancreatic cancer[108], cervical cancer[80], osteosarcoma[109], ovarian cancer[110] and glioma[111]. The energy required to carry out this facilitated nuclear-cytoplasmic transport is provided by Ran, a small Ras-like GTPase[102]. So it is not surprising that the Ran protein has also been found to be overexpressed in actively proliferating and transformed cells[112,113].

Previous MS analysis of the secretomes of normal, transformed, cervical cancer and oesophageal cancer cell lines performed in our laboratory revealed that these nuclear transport proteins, and others, were secreted at an elevated level by cancer cells compared to normal cells (A. Wishart, MSc dissertation, 2017[‡]). There is evidence to suggest that proteins secreted by cancer cells could accumulate in the serum or other bodily fluids such as urine, cervicovaginal fluid (CVF) and saliva[37]. For instance, Kpnα2 has been shown to be secreted into serum and can be a potential biomarker for non-small cell lung cancer (NSCLC) and OSCC[114,115]. This study will, therefore, focus on investigating the potential of nuclear transport proteins as secreted cancer biomarkers.

[‡] A Wishart. "Investigating secreted biomarkers for cancer: the potential of the nuclear transport proteins." University of Cape Town, 2017.

Furthermore, considering the nuclear import/export functions performed by nuclear transport proteins, it is expected that they may interact with one another and/or with many other proteins in the cell. Identifying and comparing their potential binding partners in normal and cancer cells could lead to the discovery of other potentially relevant cancer biomarkers as well as potential anti-cancer therapeutic targets.

1.10. Immunoprecipitation-mass spectrometry (IP-MS) as a tool for studying protein-protein interactions

Different proteins are known to perform different roles in an organism. In many cases, two or more proteins can interact with one another to perform a function. This is because proteins scarcely perform their cellular/biological functions alone but require an association with other molecules or proteins. For instance, there are reports which suggest that during the classical nuclear import of cargo proteins, Kpnβ1 interacts with Kpnα2 to perform its nuclear import function[103]. Given that there are over 17,008 confident protein identifications in the human proteome[116], it is expected that several proteins would dynamically interact with one another during cellular/biological processes. Identifying the interactions between a target protein and its binding partners is key to understanding the functions which the target protein performs in cellular/biological processes.

In the past, the genetic method (yeast two-hybrid (Y2H)) was employed in the study of protein-protein interactions. Despite the simplicity and rapidity of the Y2H method, it has a very high false-positive rate and less than 50% reliability rate. In recent times, biochemical methods (immunoprecipitation (IP) and affinity purification (AP)) have found application in the identification of binding partners of a target protein. These biochemical methods can now be coupled to MS-based high throughput proteomics to increase the number of identified binding partners while reducing the false-positive rate of the identified binding partners[117].

IP is an antigen-antibody technique which involves precipitating a target protein from the proteome of a cell, tissue or an organism. This could be achieved using antibody-conjugated beads specific to the target protein to form a complex with the target protein then subsequently eluting the target protein from the complex[118]. MS can then be used to identify proteins which were co-immunoprecipitated with the target protein as its binding partners.

The advent of MS as a technique used in proteomics has ensured a marked improvement in the analysis of peptides and proteins[119] when compared to the Western blot (WB) technique. MS involves the characterisation of ionised peptides based on their mass-to-charge ratio (*m/*z) for the identification of proteins[120,121].

The most important components of a mass spectrometer are the ion source, the mass analyser and the ion transducer/detector (Figure 1.7)[121,122]. The ion source is responsible for the ionisation of peptides[123]. There are basically two methods of ionisation used for proteomic MS – matrix-assisted laser desorption ionisation (MALDI) and electrospray ionisation (ESI)[124–128]. These ions are then sorted based on their *m/z* by the mass analyser. There are three major types of mass analysers – ion trapping instruments (e.g. orbitrap), quadrupole and time of flight (TOF). Lastly, an ion transducer or detector – usually an electron multiplier – records the intensities of each ion of a given *m/z* ratio, producing a mass spectrum which can then be used to determine the molecular composition or structure of each ion as well as relative abundances[122,129].

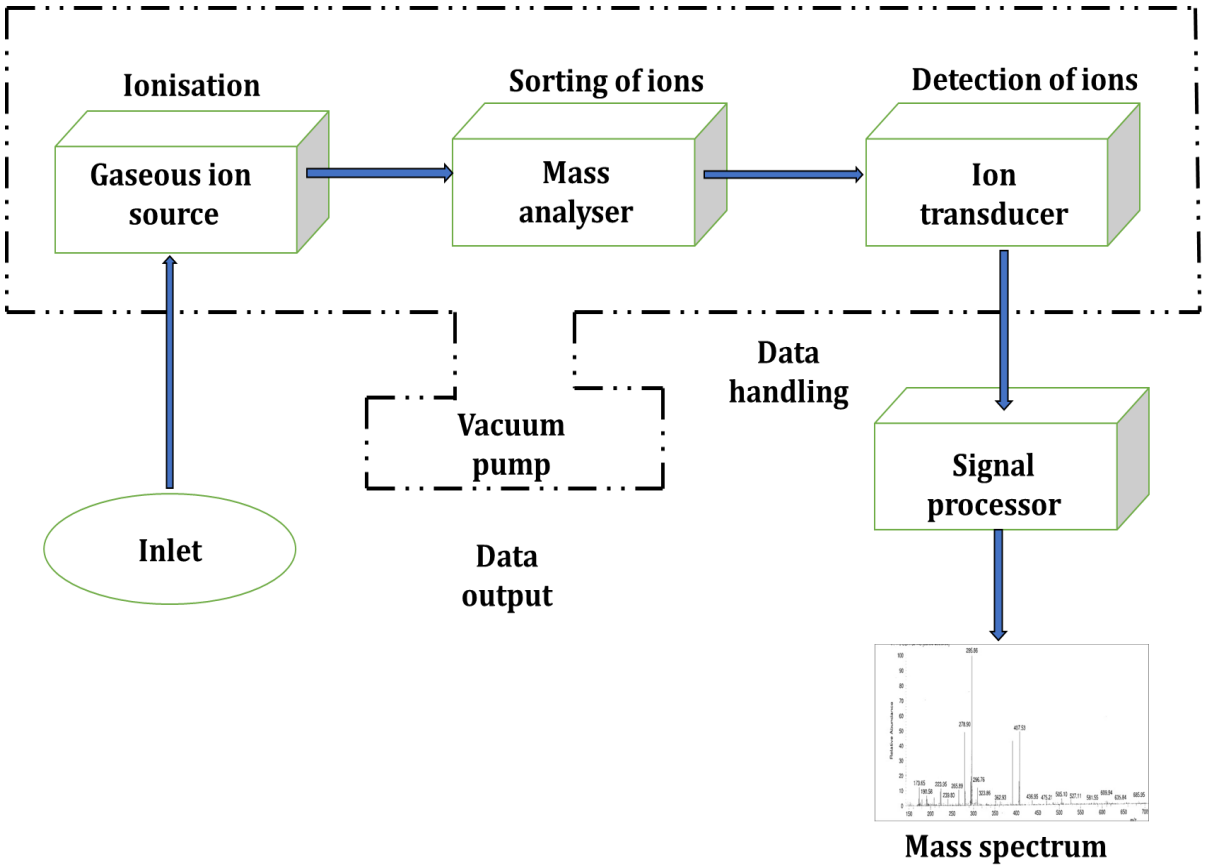

Figure 1.7. Schematic representation of mass spectrometer overview. The sample for analysis is introduced through the inlet and passes through the three major components of a mass spectrometer, a gaseous ion source, a mass analyser, and an ion transducer/detector. A mass spectrum which can be used to determine the molecular composition or structure of each ion is then produced after the signals have been processed by the signal processor. Figure adapted from Lee *et al.* (2005)[122].

1.11. Potential of Kpnβ1 binding partners as cancer therapeutic targets and biomarkers

Kpnβ1 is the principal nuclear importer of cargo proteins in the cell and performs several roles in biological/cellular processes. The various roles which Kpnβ1 plays suggest that numerous proteins might be interacting with Kpnβ1 as binding partners. Identifying the binding partners of Kpnβ1 in cancer cells would help in understanding the role/importance of these binding partners in cancer and help to discover potential anti-cancer therapeutic targets and novel cancer biomarkers.

Protein-protein interaction studies have been carried out to identify the binding partners of Kpnβ1 with some of these studies describing other functions of Kpnβ1 apart from its nuclear import function. Some of the functions shared by Kpnβ1 and its reported binding partners include regulation of spindle assembly during mitosis by counter-regulating Ran[130–133], activation of the actin cytoskeleton[134], ER-degradation of misfolded proteins[135], permeability of NPCs[136], RNA binding/processing[137] and restructuring of the nuclear envelope and NPCs[138,139].

There is also evidence to show that other nuclear transport proteins are similarly involved in many other functions. For instance, CRM1 (which is the principal nuclear export protein) is reported to share some functions with its binding partners. Some of these shared functions are seen in the role they play in autophagy, post-translational transport to peroxisome, ribosome maturation, transport of regulatory proteins, and degradation of mRNA[140].

Apart from identifying the binding partners and the possible functions which a target protein shares with its binding partners, IP-MS studies can also be used to discover potential anti-cancer therapeutic targets and biomarkers. Kpnβ1 is an essential protein in the survival of cancer cells[80]; and as such, it will be interesting to identify proteins which interact with it in cancer cells. One way to do this would be to identify the binding partners of Kpnβ1 in normal

and cancer cells. Then the binding partners of Kpnβ1 identified in cancer cell lines but absent in the normal cell line will be further studied as potential anti-cancer therapeutic targets or biomarkers.

1.12. Aim and objectives

The aim of the project was to investigate the potential of nuclear transport proteins as secreted cancer biomarkers.

The objectives of this study were to:

1) compare the level of expression of intracellular and secreted nuclear transport proteins in normal, transformed, cervical cancer and oesophageal cancer cell lines

2) investigate the presence and level of Kpnβ1, CRM1, Kpnα2 and CAS in serum samples obtained from non-cancer subjects, cervical cancer and oesophageal cancer patients

3) identify the binding partners of Kpnβ1 in normal, cervical cancer and oesophageal cancer cell lines using an IP-MS approach.

CHAPTER 2

MATERIALS AND METHODS

2.1. Materials

2.1.1. Cells and cell lines

Human telomerase-immortalized retinal pigmented epithelial 1 (hTERT RPE-1) cell line, SV40-transformed WI38 lung fibroblasts (SVWI38) cell line and human cervical carcinoma cell lines, Henrietta Lacks (HeLa) and human Caucasian epidermoid carcinoma of the cervix (CaSki), used for this study were purchased from American Type Culture Collection (ATCC, Rockville, MD, USA). Cobalt-60 gamma rays transformed WI38 lung fibroblast (CT-1) cell line is as referred to in Namba *et al*. (1980)[141]. Human oesophageal squamous cell carcinoma (WHCO5) cell line was originally established from a South African patient with OSCC and was acquired from Professor Rob Veale at the University of Witwatersrand[142] while human oesophageal squamous cell carcinoma (KYSE30) cell line was acquired from Deutsche Sammlung von Mikroorganismen und Zellkulturen (DSMZ) (Berlin, Germany).

2.1.2. Serum samples

Ethics approval for blood collection and patient consent were established before the study began (Ethics Reference Number HEC040/2005 – Genetic markers for susceptibility to oesophageal cancer). In collaboration with Professor Iqbal Parker at the University of Cape Town (UCT), blood serum samples were obtained from 73 non-cancer subjects, 74 cervical cancer and 73 oesophageal cancer patients.

2.1.3. ELISA kits

ELISA kits for human Kpnβ1 (Catalogue number: SEE752Hu), human CRM1/XPO1 (Catalogue number: LS-F9390-1) and human Kpnα2 (Catalogue number: SEE748Hu) were purchased from The Cloud-Clone Corp., (Houston, TX77494, USA). Meanwhile, the ELISA kits for human CAS/XPO2 (Catalogue number: MBS9316513) were purchased from MyBiosource, Inc. (San Diego, CA 92195-3308, USA).

The intra-assay coefficient of variation (CV) for the Kpnβ1, CRM1/XPO1 and Kpnα2 ELISA kits was <10% while the inter-assay CV was <12%. However, the intra-assay CV and inter-assay CV for the CAS/XPO2 ELISA kits were <15%.

2.2. Methods

2.2.1. Tissue cell culture

Cell suspensions contained inside cryovials which were stored in liquid nitrogen were thawed in a water bath at 37 degrees Celsius (°C) until defrosted. The content of the cryovial (1 millilitre (ml) cell suspension) was emptied into 100 millimetres (mm) tissue culture dish and 10 ml of appropriate medium was added depending on the cells in the suspension. Dulbecco's Modified Eagle's Medium (DMEM) (Gibco®, Life Technologies, Carlsbad, CA, USA) supplemented with penicillin (100 Units (U)/ml), streptomycin (100 microgram (μg)/ml) and 10% fetal calf serum (FCS) (HyClone Laboratories, UT, USA) were the components of the growth medium for SVWI38, CT-1, HeLa, CaSki, WHCO5, and KYSE30. However, hTERT-RPE1 cell lines were grown in DMEM/F-12 (1:1) nutrient mixture (Gibco®, Life Technologies, Carlsbad, CA, USA) supplemented with penicillin (100 U/ml), streptomycin (100 μg/ml), 10% FCS and 0.01 milligram (mg)/ml hygromycin B (Sigma Aldrich). The medium was changed the following day. All cells were grown in their appropriate medium and were maintained in a

humidified incubator at 37 °C and in 5% carbon dioxide (CO_2). The medium was changed every 48 hours until the cells reached 85-90% confluency before they were subcultured.

2.2.2. Subculturing of cells

5 ml of 0.05% trypsin-ethylenediaminetetraacetic acid (EDTA) was added to cells in 100 mm tissue culture dishes and was incubated at 37 °C for 3 minutes (The recipes for solutions used in this study are provided in Appendix III). 5 ml of the appropriate medium was added to neutralise the trypsin-EDTA. The mixture was transferred into a 12 ml tube and was centrifuged at a speed of 500 x Earth's gravitational force (*g*) for 3 minutes at room temperature (RT) in an Ortoalresa Digtor 21R centrifuge (28864 Ajalvir, Madrid, Spain). The supernatant was discarded, and the cell pellet was re-suspended in 5 ml of fresh medium. 1 ml of the cell suspension was then pipetted into five 100 mm tissue culture dishes containing 10 ml of the appropriate medium.

2.2.3. Cells freezing and storage

Briefly, cells were treated as per subculture protocol (section 2.2.2). Upon re-suspension in 5 ml of medium, 500 microlitres (µl) of dimethylsulphoxide (DMSO) (Calbiochem®, Merck) was added. This was properly mixed, and 5 ml of the cell suspension was aliquoted into 5 cryovials. These were initially put in a -80 °C freezer for 24 hours, and then one frozen cell suspension in a cryovial was defrosted and tested for Mycoplasma. The cells were only stored in the liquid nitrogen tank if they were Mycoplasma negative, otherwise, they were discarded.

2.2.4. Mycoplasma test

Mycoplasma is a prokaryotic organism that is a frequent contaminant of cell cultures and can render experiments invalid. This test was carried out to ensure that the cells were Mycoplasma free before using them for experiments or storing them in the liquid nitrogen tank. Briefly, cells

were cultured in penicillin and streptomycin free medium for 72 hours and were trypsinized. 30 µl of cell suspension was pipetted onto a sterilised coverslip before 3 ml of penicillin and streptomycin free medium was added. The cells were then cultured for another 24 hours. The medium was removed in a dark environment and the cells were fixed with methanol for 10 minutes at -20 °C. This was washed with phosphate buffered saline (PBS) followed by addition of 1 ml PBS containing 100 nanograms (ng)/ml 4', 6-diamidino-2-phenylindole (DAPI) and incubated at RT for 5 minutes. Another wash with PBS was done before the coverslip was mounted onto a slide with mowiol. The slide was left to dry overnight in the dark at RT. The slide was then examined under the fluorescent microscope the next day for the presence of Mycoplasma. Mycoplasma positive cells would have a speckled cytoplasm/membrane while Mycoplasma negative cells would have a clear cytoplasm with bright blue nuclei. Only Mycoplasma negative cells were used for this study.

2.2.5. Protein harvest and quantitation

2.2.5.1. Protein harvest from whole cells

The Cell Signalling radioimmunoprecipitation assay (RIPA) protocol (Cell Signalling technology, #9806, Danvers, MA, USA) was used for protein extraction from whole cells. Cells were grown to ~80% confluency before the medium was aspirated with a sterile Pasteur pipette. The cells were washed twice with 5 ml of ice-cold PBS to remove any residual medium and then lysed using RIPA buffer containing 1x protease inhibitor (PI) (Roche, Mannheim, Germany) and 0.1 molar (M) Sodium Orthovanadate (Na_3VO_4) (Merck, Kenilworth, NJ 07033 U.S.A) to inhibit the action of phosphatases. A sterile rubber scraper was used to scrape the cells off the bottom of the tissue culture dish before the cells were transferred to Eppendorf tubes (Eppendorf, Hamburg, Germany). The lysates were sonicated on ice for 10 seconds and then centrifuged at 18000 x *g* for 10 minutes at 4 °C in an Ortoalresa Biocen 22R centrifuge

(28864 Ajalvir, Madrid, Spain). The supernatant was transferred to fresh Eppendorf tubes and stored at -80 °C for future use.

2.2.5.2. Protein harvest from serum-free culture medium

Cells were grown to ~70% confluency in 100 mm tissue culture dishes. Then they were rinsed with warm PBS before they were washed twice with serum-free medium (0% FCS) and incubated in 7.5 ml of serum-free medium at 37 °C for 24 hours. 15 ml of the serum-free culture medium was transferred into a 50 ml tube and then centrifuged at 500 x *g* for 15 minutes at 4 °C in an Ortoalresa Digtor 21R centrifuge (28864 Ajalvir, Madrid, Spain). The supernatant was transferred into Amicon Ultra-15 centrifugal filter unit (Merck Millipore Ltd, Darmstadt, Germany) for a series of centrifugation to concentrate the protein. The supernatant was centrifuged at 2000 x *g* for 40 minutes at 4 °C and the filtrate was discarded. 13 ml of distilled water (dH_2O) was added to the concentrate and was centrifuged at 2000 x *g* for 40 minutes at 4 °C. 5 ml of dH_2O was added to the concentrate and was centrifuged at 2000 x *g* for 40 minutes at 4 °C. Finally, 1 ml of dH_2O was added to the concentrate and was centrifuged at 2000 x *g* for 30 minutes at 4 °C. The final concentrate was transferred to fresh Eppendorf tubes then 25 µl of 10x PI and 2.5 µl of 0.1M Na_3VO_4 were added to 250 µl of the concentrate and stored at -80 °C for future use.

2.2.5.3. Preparation of patient serum samples

Blood sample collection was performed according to the university's ethics regulations. Briefly, whole blood samples were collected in red top Vacutainer blood collection tubes (BD Biosciences, Franklin Lakes, NJ, USA) by the research nurse. The tubes were inverted several times and incubated at RT for 1 hour until pellets formed at the bottom of the tubes. The blood samples were centrifuged at 2000 x *g* for 10 minutes at 4 °C and the supernatant (serum) was removed by pipetting and stored in cryovials at -20 °C. All serum sample preparations were

performed in the tissue culture biosafety level (BSL) II section of the Cancer Molecular and Cell Biology laboratory (Wernher & Beit Building South, International Centre for Genetic Engineering and Biotechnology, UCT). Refer to Table 3.1 for the demographic and clinicopathological information of the patients.

2.2.5.4. Protein quantification

Protein concentrations were determined using a Pierce® bicinchoninic acid (BCA) protein assay kit (product #23225, Thermo Fisher, San Jose, CA, USA) according to the manufacturer's instructions. In principle, the presence of protein results in the reduction of Cu^{2+} to Cu^{+}, which further reacts with the BCA to give an intense purple colour that can be measured at a particular wavelength[143–145]. Absorbance was read at 595 nanometres (nm) on a BioTek EL800 absorbance plate reader (BioTek, Winooski, VT, USA) using the Gen5 software. A standard curve was plotted using the bovine serum albumin (BSA) standards and protein concentration of each unknown protein sample was determined via extrapolation.

2.2.5.5. Kpnβ1, CRM1, Kpnα2 and CAS ELISA

ELISA kits for human Kpnβ1, CRM1, Kpnα2 and CAS were used to quantitate Kpnβ1, CRM1, Kpnα2 and CAS in patient serum samples according to the manufacturer's instruction manual with slight modifications. Serum samples for Kpnβ1, CRM1 and Kpnα2 analysis were diluted in 0.01M PBS, pH 7.15, while serum samples for CAS analysis were diluted in sample diluent provided by the manufacturer. The dilution factors used for quantitating Kpnβ1, CRM1, Kpnα2 and CAS were 1:5, 1:2, 1:2 and 1:2, respectively.

For Kpnβ1, all reagents, standards and samples were brought to RT. 100 µl of serially diluted standard and 100 µl of diluted samples were pipetted into each of the microtiter plate wells which were pre-coated with biotin-conjugated antibody specific to Kpnβ1 and were incubated at 37 °C for 2 hours. The solutions were aspirated, then 100 µl of Detection Reagent A, which

is avidin conjugated to horseradish peroxidase (HRP), was pipetted into each well and the plate was incubated at 37 °C for 1 hour. These were aspirated and washed three times with 1x wash solution. Thereafter 100 µl of Detection Reagent B was pipetted into each well and the plate was incubated at 37 °C for 1 hour. These were aspirated and washed five times with 1x wash solution. 90 µl of 3,3',5,5'-tetramethylbenzidine (TMB) substrate solution was pipetted into each well and the plate was incubated at 37 °C for 20 minutes. Only the wells that contained Kpnβ1, biotin-conjugated antibody and HRP-conjugated avidin exhibited a blue colour formation when the TMB substrate was added. 50 µl of stop solution was added. This changed the colour of the mixture from blue to yellow and the intensity of colour formation was measured spectrophotometrically at a wavelength of 450 nm using a BioTek EL800 absorbance plate reader (BioTek, Winooski, VT, USA). A standard curve was generated by plotting concentrations of standards against the optical density (O.D) readings. Finally, the concentration of Kpnβ1 in each patient serum sample was determined via extrapolation. The same principle was applied for quantitation of CRM1, Kpnα2 and CAS in patient serum samples.

2.2.6. Western blots Analysis

2.2.6.1. Gel preparations and electrophoresis

Sodium dodecyl sulphate (SDS) polyacrylamide gels were prepared with the 4% stacking gel on top of the 10% separating gel and were cast in 1.5 mm glass plates. The analysis was performed according to the Abcam® protocol (technical resource: western blotting – a beginner's guide, Abcam, Cambridge, UK). 10-15 µg of the extracted protein sample, along with 4x Laemli loading dye containing 10% β-mercaptoethanol, was denatured by heating the sample in a heating block at 90 °C for 5 minutes. These mixtures were loaded into the wells of the stacking gel, along with a lane of 5 µl of Colour Prestained Protein Standard broad range

11-245 kilodaltons (kDa) (New England Biolabs, Ipswich, MA, USA, Catalogue number: P7712) as a marker of molecular weight (see Appendix IV, Figure B.1). The electrophoresis tank was filled with 1x running buffer and the gel was run at 170 volts (V) for 60 minutes or until the dye front had run off the bottom of the gel.

2.2.6.2. Electrotransfer

The protein was transferred from the gel unto a HyBond™-ECL™ nitrocellulose membrane (Amersham, Buckinghamshire, UK) by placing them in between sponges and filter papers in cassettes. The order of arrangement was cassette, sponge, filter paper, gel, membrane, filter paper, sponge, and cassette, such that the protein was transferred onto the membrane (towards the positive electrode). The electrophoresis transfer tank (Biorad) was filled with ice-cold 1x transfer buffer and the transfer was done at 185 V for 80 minutes.

2.2.6.3. Blocking and antibody incubation

Thereafter the HyBond™-ECL™ nitrocellulose membrane was blocked in 5% weight/volume (w/v) fat-free powder milk (dissolved in Tris-buffered saline with Tween-20 (TBST)) by shaking for 1 hour at RT. Blocking is done to prevent non-specific background binding of the primary and/or secondary antibodies to the membrane. The membrane was incubated in the appropriate primary antibody at 4 °C for 16 hours. The membrane was washed thrice with TBST for 5 minutes with shaking and then incubated in the appropriate HRP-conjugated secondary antibody at RT for 1 hour (see Table 2.1). After secondary antibody incubation, the membrane was washed thrice with TBST for 5 minutes.

Table 2.1. Antibody concentrations and incubation conditions for WB

Primary antibody	Company, Catalogue number	Primary antibody condition	Secondary antibody	Secondary antibody condition	Substrate	Protein size (kDa)
Rabbit Anti-NTF97/ Importin beta antibody	Abcam ab45938	1:5000 2.5% milk in TBST	Goat anti-rabbit (Biorad)	1:5000 2.5% milk in TBST	LumiGlo® (KPL)	97
Rabbit anti-Crm1 (H-300) antibody	Santa Cruz Biotechnology sc-5595	1:1000 2.5% milk in TBST	Goat anti-rabbit (Biorad)	1:5000 2.5% milk in TBST	LumiGlo® (KPL)	115
Rabbit anti-KPNA2 antibody	Abcam Ab97580	1:2000 2.5% milk in TBST	Goat anti-rabbit (Biorad)	1:5000 2.5% milk in TBST	LumiGlo® (KPL)	52
Mouse anti-CAS antibody	Sigma-Aldrich SAB1400055	1:1000 2.5% milk in TBST	Goat anti-mouse (Biorad)	1:5000 2.5% milk in TBST	LumiGlo® (KPL)	110
Mouse anti-Ran antibody	Sigma-Aldrich R4777	1:1000 2.5% milk in TBST	Goat anti-mouse (Biorad)	1:5000 2.5% milk in TBST	LumiGlo® (KPL)	27
Mouse anti-TNPO 1 antibody	Sigma-Aldrich T0825	1:1000 2.5% milk in TBST	Goat anti-mouse (Biorad)	1:5000 2.5% milk in TBST	LumiGlo® (KPL)	101
Rabbit anti-IPO5 antibody	Sigma-Aldrich SAB4200179	1:1000 2.5% milk in TBST	Goat anti-rabbit (Biorad)	1:5000 2.5% milk in TBST	LumiGlo® (KPL)	125
Rabbit anti-importin-7 (H-78) antibody	Santa Cruz Biotechnology sc-134913	1:500 2.5% milk in TBST	Goat anti-rabbit (Biorad)	1:5000 2.5% milk in TBST	LumiGlo® (KPL)	120
Mouse anti-GAPDH (0411) antibody	Santa Cruz Biotechnology sc-47724	1:10000 5% milk in TBST	Goat anti-mouse (Biorad)	1:5000 5% milk in TBST	LumiGlo® (KPL)	37

Rabbit anti-β-tubulin (H-235) antibody	Santa Cruz Biotechnology sc-9104	1:500 2.5% milk in TBST	Goat anti-rabbit (Biorad)	1:2000 5% milk in TBST	LumiGlo® (KPL)	55
Mouse anti-Vimentin (V9) antibody	Santa Cruz Biotechnology sc-6260	1:500 5% milk in TBST	Goat anti-mouse (Biorad)	1:5000 5% milk in TBST	LumiGlo® (KPL)	54
Rabbit anti-NF-kB p65 (H-286) antibody	Santa Cruz Biotechnology (sc-7151)	1:250 5% milk in TBST	Goat anti-mouse (Biorad)	1:3000 5% milk in TBST	LumiGlo® (KPL)	65
Rabbit anti-cJun (D)	Santa Cruz Biotechnology (sc-44)	1:250 5% BSA	Goat anti-mouse (Biorad)	1:5000 5% milk in TBST	LumiGlo® (KPL)	39

2.2.6.4. Visualization

Visualisation of blots was performed using LumiGLO® chemiluminescent substrate system (KPL, Lot No. 130575, Milford, MA, USA) in a dark room using medical X-ray blue film AGFA (Ref EWPKK, AGFA HealthCare NV, Mortsel, Belgium), developer (G150, AGFA HealthCare NV, Mortsel, Belgium) and fixer (G354, AGFA HealthCare NV, Mortsel, Belgium). Briefly, membranes were incubated in the respective substrate for 1 minute at RT and exposed to medical X-ray blue film, which was subsequently developed in a bath of the developer, rinsed in clean water, fixed in a bath of fixer, rinsed in clean water, and then dried at RT to show protein bands.

2.2.6.5. Stripping of membranes

Whenever there was a need to probe for another protein on the same membrane, the membrane was stripped for re-probing especially if the primary antibodies were produced in the same animal model. The membrane was rinsed thrice with TBST before it was incubated in 10% acetic acid at RT for 10 minutes with shaking. Then it was rinsed thrice with TBST. The blocking, antibody incubation and visualization steps were then carried out as described in sections 2.2.6.3 and 2.2.6.4 above.

2.2.6.6. Staining of gel

The gel was stained with Coomassie blue stain to show equal loading of protein and/or to show the protein profile along each lane. Briefly, 20 ml of Coomassie blue stain was added to the freshly run gel inside a 150 mm tissue culture dish and was shaken gently for 1 hr at RT. The gel was then rinsed twice in dH_2O before 20 ml of Coomassie destaining solution and a sponge were added. These were shaken for 16 hours at RT, then the gel was rinsed in dH_2O before it was transferred onto a glass slab and photos of the gel were taken.

2.2.6.7. Densitometry analysis

The protein bands that were developed on the medical X-ray film (section 2.2.6.4) were scanned and converted into Joint Photographic Experts Group (JPEG) images. These were then converted to greyscale using Paint.NET version 4.0.9 software (Microsoft, Redmond, WA, USA). These greyscale images were opened using ImageJ software (National Institutes of Health, MD, USA) and the background was corrected using a rolling ball radius of 50 for all images. The gel analyser tool was used to select bands and to plot the lanes, and the wand tool was used to enclose the area under each peak. The areas were measured, and the values exported to Excel (Microsoft, Redmond, WA, USA) for further analysis.

2.2.7. Immunoprecipitation for Kpnβ1

Intracellular protein was harvested from whole cell lysates as described in section 2.2.5.1 but using non-denaturing lysis buffer in the place of RIPA buffer to conserve the binding partner interactions. 1000 µg of intracellular protein was divided equally into 2 Eppendorf tubes, one with "IgG isotype" as the negative control and the other with antibody for pull-down. Each of these samples was subjected to preclearing by adding 50 µl of protein A agarose (High Affinity) conjugated beads (Abcam, Catalogue number: ab193255) then incubated at 4 °C for 45 minutes with gentle rocking. The samples were centrifuged at 18000 x *g* for 10 minutes at 4 °C in an Ortoalresa Biocen 22R centrifuge (28864 Ajalvir, Madrid, Spain), then the supernatants were transferred to fresh Eppendorf tubes. 50 µg of Anti-Karyopherin β1 (H-7) AC agarose conjugated antibody at 500 µg/ml, 25% agarose (Santa Cruz Biotechnology, Catalogue number: sc-137016 AC) was added to the sample for pull-down while 50 µl of protein A agarose (High Affinity) conjugated beads and 15 µl of Rabbit (DA1E) mAb IgG isotype control (Cell Signalling technology, Catalogue number: 3423) was added to the "IgG isotype" control sample. We used a monoclonal Kpnβ1 antibody conjugated to beads for the pull-down assays to increase the specificity of the antibody to the target protein and increase the specificity of protein-protein interactions. This is because using a polyclonal antibody conjugated to beads would cause more non-specific associations thereby giving numerous false binding partners[146,147].

Afterwards, the samples were incubated at 4 °C overnight with gentle rocking. The samples were centrifuged at 18000 x *g* for 3 minutes at 4 °C, and the supernatants were aspirated. The bead pellets were washed five times with 450 µl of ice-cold 1x PBS containing 50 µl of 10x PI. Washing was done by centrifuging at 10000 x *g* for 3 minutes at 4 °C with the supernatant discarded after each wash. The bead pellets were then subjected to further treatment for either IP-MS or immunoprecipitation Western blot (IP-WB) analysis.

2.2.7.1. Immunoprecipitation mass spectrometry (IP-MS)

The washed bead pellets for IP-MS were taken to the Applied Proteomic and Biology Laboratory (Wernher & Beit Building North, Institute of Infectious Disease and Molecular Medicine, UCT) for MS analysis of the samples. The protein samples were first digested into peptides using the in-solution digestion method and were desalted using the octadecyl carbon chain (C18) paper before they were run on the Q Exactive Mass Spectrometer.

2.2.7.1.1. In-solution digestion

30 µl of denaturation buffer was used to elute the protein bound to the washed bead pellets from section 2.2.7 by vortexing for 5 minutes. 1 mM dithiothreitol (DTT) reduction buffer was added and this was incubated at RT for 1 hour to break the disulphide bonds of cysteine into free sulfhydryl groups[148]. 5 mM iodoacetamide (IAA) (Amresco Biochemicals and Life Science products) was added and this was incubated in the dark at RT for 1 hour. IAA is an alkylating agent which forms S-carboxyamidomethyl-cysteine when it reacts with the free sulfhydryl groups of cysteine residues. This reaction is crucial because S-carboxyamidomethyl-cysteine cannot be oxidized to re-form disulphide bonds, and as such, more sites within the protein will be exposed to the digestion enzyme for cleavage[148]. The samples were then diluted with 4 volumes of 20mM ammonium bicarbonate (ABC) (Sigma Aldrich) and 20 mM calcium chloride ($CaCl_2$) (Sigma Aldrich). ABC and $CaCl_2$ were added to reduce the concentration of urea in the sample. Trypsin (New England Biolabs, Ipswich, MA, USA) was added to the samples with a protein to trypsin ratio of 50:1 and were incubated at RT overnight for digestion of protein into peptides. The digestion was stopped by adding formic acid at 0.1% final concentration.

2.2.7.1.2. Desalting of peptides

Purification and concentration of the digested peptides were performed by desalting the peptides with C18 stage tips. The stage tips were prepared with Empore™ Octadecyl solid phase extraction disks (Supelco, SIGMA, St Louis, MO, USA). Briefly, C18 papers were pierced into yellow pipette tips and were activated by adding 300 µl of solvent B (80% acetonitrile (ACN) and 0.1% formic acid), then centrifuging at 3000 x *g* for 2 minutes at RT in a Jouan A14 microcentrifuge (Saint-Herblain, Pays de la Loire, France). Next, the activated C18 paper was equilibrated twice with 100 µl of solvent A (2% ACN and 0.1% formic acid) by centrifuging at 3000 x *g* for 2 minutes at RT. The sample was added into the stage tip and was centrifuged at 3000 x *g* for 2 minutes at RT. Peptides in the sample were bound to the C18 paper while the salt solution flowed through the C18 paper. A glass vial was inserted into a fresh Eppendorf tube and the stage tip was inserted into the glass vial through the lid of the Eppendorf tube such that the peptides will be eluted into the glass vial. The bound peptides on the C18 paper were then eluted thrice into the glass vial by centrifuging 50 µl of solvent C (60% ACN and 0.1% formic acid) through the C18 paper at 3000 x *g* for 2 minutes at RT. The eluate in the glass vial was dried in a speed vac at RT until the peptides were pelleted. The dried peptides were resuspended in 30 µl of solvent A and this was run on the Q Exactive Mass Spectrometer (Thermo Fisher, San Jose, CA, USA).

2.2.7.2. Immunoprecipitation Western blot

The washed bead pellets from section 2.2.7. were resuspended in 35 µl of 2x loading buffer without bromophenol blue. 10 µg of the original protein was added to 35 µl of 2x loading buffer as a "non-treated" positive control. All samples were then boiled at 95 °C for 5 minutes and centrifuged at 18000 x *g* for 3 minutes at RT in an Ortoalresa Biocen 22R centrifuge (28864 Ajalvir, Madrid, Spain). 1 µl of 1% bromophenol blue was added to the supernatants and 35 µl

of each sample was run on a gel for WB analysis of the pulled down Kpnβ1. After probing for Kpnβ1, the membrane was subjected to a stripping protocol as described in section 2.2.6.5. and was probed for the binding partners of Kpnβ1.

For all IP-WB analysis, Abcam Veriblot for IP Detection Reagent (HRP) (Catalogue number: ab131366) was used as a secondary antibody with a dilution of 1:2500 in 5% milk in TBST. Abcam Veriblot for IP Detection Reagent (HRP) was used in place of the secondary antibodies listed in Table 2.1 because it only detects native antibodies. Hence, the detection of heavy and light chain immunoglobulin G (IgG) will be reduced provided the "IgG isotype" control and pull-down samples were fully denatured.

A schematic representation of the experimental design for this study is shown in Figure 2.1.

2.2.8. Bioinformatics and statistical analyses

2.2.8.1. Analyses of WB and ELISA data

Microsoft Excel 2016, GraphPad Prism software version 5.01 (GraphPad Software Inc., San Diego, CA, USA) and CombiROC web application tool (www.combiroc.eu)[149] were used for statistical analyses of WB and ELISA. WB experiments were performed in triplicate or quadruplicate and their corresponding densitometry were represented as the mean ± standard error of the mean (SEM), except where stated otherwise. The student's t-test was used to compare the levels of protein expression and secretion between the normal cell line and transformed and cancer cell lines; and *p*-values less than 0.05 (indicated by *) were considered statistically different. The non-parametric Mann-Whitney *U*-test was used for comparisons in ELISA results based on clinical characteristics; while *p*-values less than 0.05 were considered statistically different. The receiver operating characteristics (ROC) curves for each candidate biomarker and their combinations were constructed by plotting sensitivity (true positive rate)

against 1-specificity (false positive rate) by assuming that each value is a possible cut-off point. The area under the receiver operating characteristics curve (AUC) was computed as an index to determine the ability of each biomarker to discriminate between cases and controls. An optimal cut-off value was determined for each candidate biomarker by selecting the cut-off value which corresponded to the highest Youden's index (J)[150,151]. J is calculated as:

$$J = 1 - (\text{false positive rate} + \text{false negative rate})$$

$$J = 1 - ((1 - \text{specificity}) + (1 - \text{sensitivity}))$$

$$J = 1 - (1 - \text{specificity} + 1 - \text{sensitivity})$$

$$J = 1 - 1 + \text{specificity} - 1 + \text{sensitivity})$$

$$J = \text{sensitivity} + \text{specificity} - 1$$

2.2.8.2. Analyses of IP-MS data

All MS data were processed using the MaxQuant (version 1.5.4.1.) and the Perseus statistical software package (version 1.5.5.3.). VennDis JavaFX-based Venn and Euler diagram software created by Ignatchenko *et al.*[152] was used to generate Venn diagrams for the overlap of identified potential binding partners of Kpnβ1 in cells extracts. Lastly, the STRING (Search Tool for the Retrieval of Interacting Gene/protein) protein-protein interaction mapping tool (www.string-db.org)[153] was used to indicate interactions between Kpnβ1 and its binding partners.

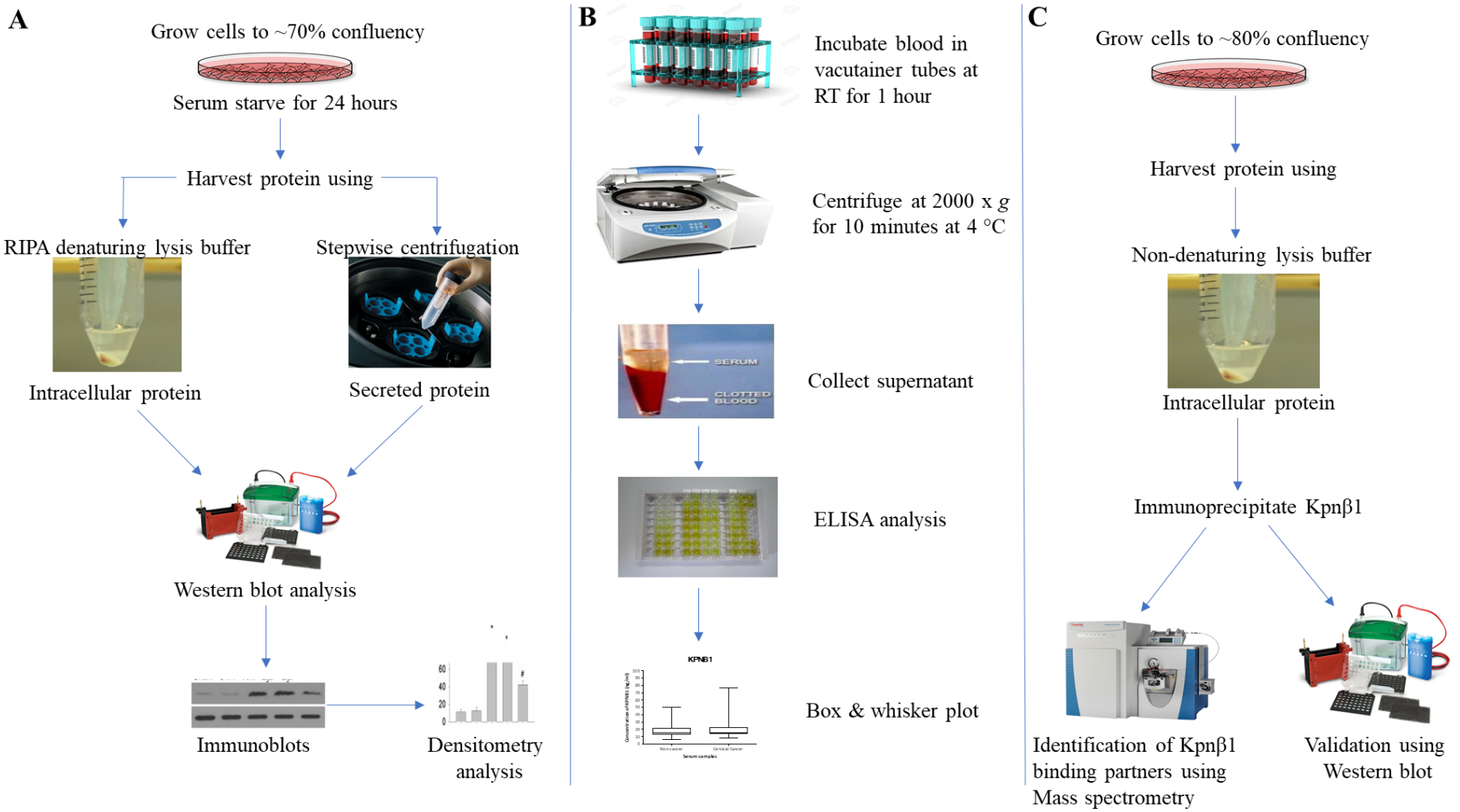

Figure 2.1. Workflow of experimental design. A) Cells were grown to ~70% confluency and were serum-starved. Intracellular and secreted proteins were harvested using RIPA and step-wise centrifugation respectively. The level of expression of nuclear transport proteins as represented on immunoblots was quantified and compared using densitometry. **B)** Drawn blood was incubated at RT and centrifuged. The supernatants (serum) were then analysed using ELISA. **C)** Cells were grown to ~80% confluency and intracellular protein was harvested in non-denaturing lysis buffer. Kpnβ1 was immunoprecipitated and its binding partners were identified using MS analysis and validated using WB.

CHAPTER 3

INVESTIGATING THE POTENTIAL OF SECRETED NUCLEAR TRANSPORT PROTEINS AS CANCER BIOMARKERS

3.1. Introduction

A study previously done in our laboratory using microarray analysis identified elevated expression of the nuclear transport proteins, Kpnβ1, CRM1 and Kpnα2 in cervical cancer biopsies compared to non-cancer cervical tissues[80]. Research by other groups have shown that members of the nuclear transport protein family are overexpressed in different cancers. Kpnβ1 has been reported to be overexpressed in gastric[154] and breast cancer[155]. CRM1, the principal nuclear exporter of cargo proteins and RNAs from the nucleus to the cytoplasm, has also been reported to be overexpressed in pancreatic cancer[108], osteosarcoma[109], ovarian cancer[110] and glioma[111]. The adaptor protein, Kpnα2 has been shown to be upregulated in colon cancer[156], upper tract urothelial carcinoma[157], gastric cancer[158], ovarian cancer[159] and meningioma[160]. CAS has been reported to be overexpressed in prostate cancer[161] and human hepatocellular carcinoma[162].

Our laboratory also conducted an MS analysis of the secretomes of normal, transformed, cervical cancer and oesophageal cancer cell lines by generating an inclusion list of 31 nuclear transport proteins using Skyline. The result showed an increase in the abundance of 13 members of the nuclear transport protein family from normal to transformed to cancer cell lines (A. Wishart, MSc dissertation, 2017[§]). Furthermore, there is other evidence to suggest that

[§] A Wishart. "Investigating secreted biomarkers for cancer: the potential of the nuclear transport proteins." University of Cape Town, 2017.

nuclear transport proteins may have potential as cancer biomarkers. A study by Wang *et al.* (2011) showed that Kpnα2 is present in the secretome of lung cancer cell lines and they also identified Kpnα2 as a potential biomarker for NSCLC[114]. In 2014, Ma and Zhao reported that Kpnα2 is a promising biomarker for OSCC[115]. In another study, Kpnα2 was reported to have potential as a diagnostic serum biomarker for epithelial ovarian carcinoma[163]. CAS has been reported to be secreted by melanoma cells and present in the serum samples of metastatic cancer patients[164].

Based on our data showing that Kpnβ1, CRM1 and Kpnα2 have elevated expression in cervical cancer[80] and the MS analysis of cancer cells secretomes done in our laboratory (A. Wishart, MSc dissertation, 2017[**]), we hypothesized that multiple members of the nuclear transport protein family may have potential as cancer biomarkers.

In this study, we aimed to independently validate the inclusion MS data using WB analysis to compare the intracellular and secreted levels of 8 members of the nuclear transport protein family (Kpnβ1, IPO5, IPO7, TNPO1, CRM1, CAS, Kpnα2 and Ran) in the normal immortalized epithelial cell line (hTERT-RPE1) as a non-cancer control, transformed cell lines (SVWI38 and CT-1), cervical cancer cell lines (HeLa and CaSki) and oesophageal cancer cell lines (WHCO5 and KYSE30). The study was extended to include patient serum samples and the ELISA method was used to investigate the levels of Kpnβ1, CRM1, Kpnα2 and CAS in serum samples of a cohort of non-cancer subjects (as control), cervical cancer and oesophageal cancer patients.

[**] A Wishart. "Investigating secreted biomarkers for cancer: the potential of the nuclear transport proteins." University of Cape Town, 2017.

3.2. Results

3.2.1. Expression of intracellular nuclear transport proteins in cultured normal, transformed, cervical cancer and oesophageal cancer cell lines

We commenced this study by investigating the expression level of 8 members of the nuclear transport protein family in normal, transformed and cancer cell lines. Normal epithelial (hTERT-RPE1), transformed (SVWI38, CT-1), cervical cancer (HeLa, CaSki), and oesophageal cancer (WHCO5 and KYSE30) cell lines were grown to ~70% confluency and were serum-starved for 24 hours to minimize cell autolysis. Intracellular proteins were harvested from the whole cell lysates as described in section 2.2.5.1. WB analysis was used to evaluate the intracellular levels of Kpnβ1, IPO5, IPO7, TNPO1, CRM1, CAS, Kpnα2 and Ran in each cell line. Glyceraldehyde 3-phosphate dehydrogenase (GAPDH) was used to control for even protein loading.

The results showed that all the nuclear transport proteins were expressed by the normal, transformed, cervical cancer and oesophageal cancer cell lines but at differential levels of expression (Figure 3.1). The band for CAS in the CaSki cell line was of a different mobility than CAS in all the other cell lines. This must have been due to some post-translational modification during the synthesis of CAS protein in CaSki cell line. The quantification of experiments performed in triplicate is shown in Figure 3.2. For proteins with double bands, only the band which is of the same mobility with other protein bands for other cell lines was quantified.

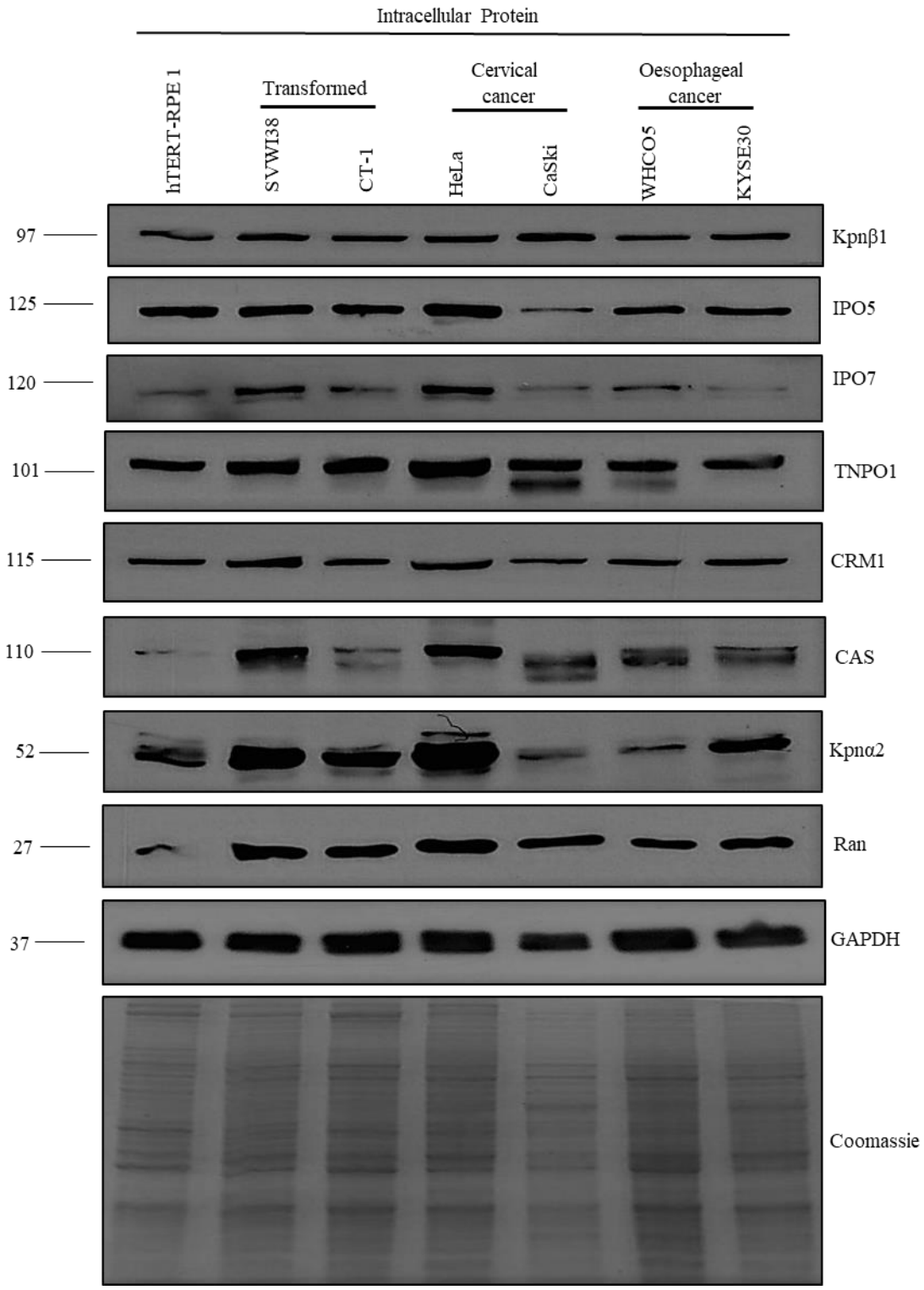

Figure 3.1. Expression of intracellular nuclear transport proteins in cultured normal, transformed, cervical cancer and oesophageal cancer cell lines. WB analysis of intracellular Kpnβ1, IPO5, IPO7, TNPO1, CRM1, CAS, Kpnα2 and Ran in the normal immortalized epithelial cell line (hTERT-RPE1), transformed cell lines (SVWI38 and CT-1), cervical cancer cell lines (HeLa and CaSki) and oesophageal cancer cell lines (WHCO5 and KYSE30). Each lane contained 15 μg of whole cell lysate protein. GAPDH was used as a loading control and Coomassie staining was performed to show the protein profile along each lane. Results shown are representative of experiments performed in triplicate.

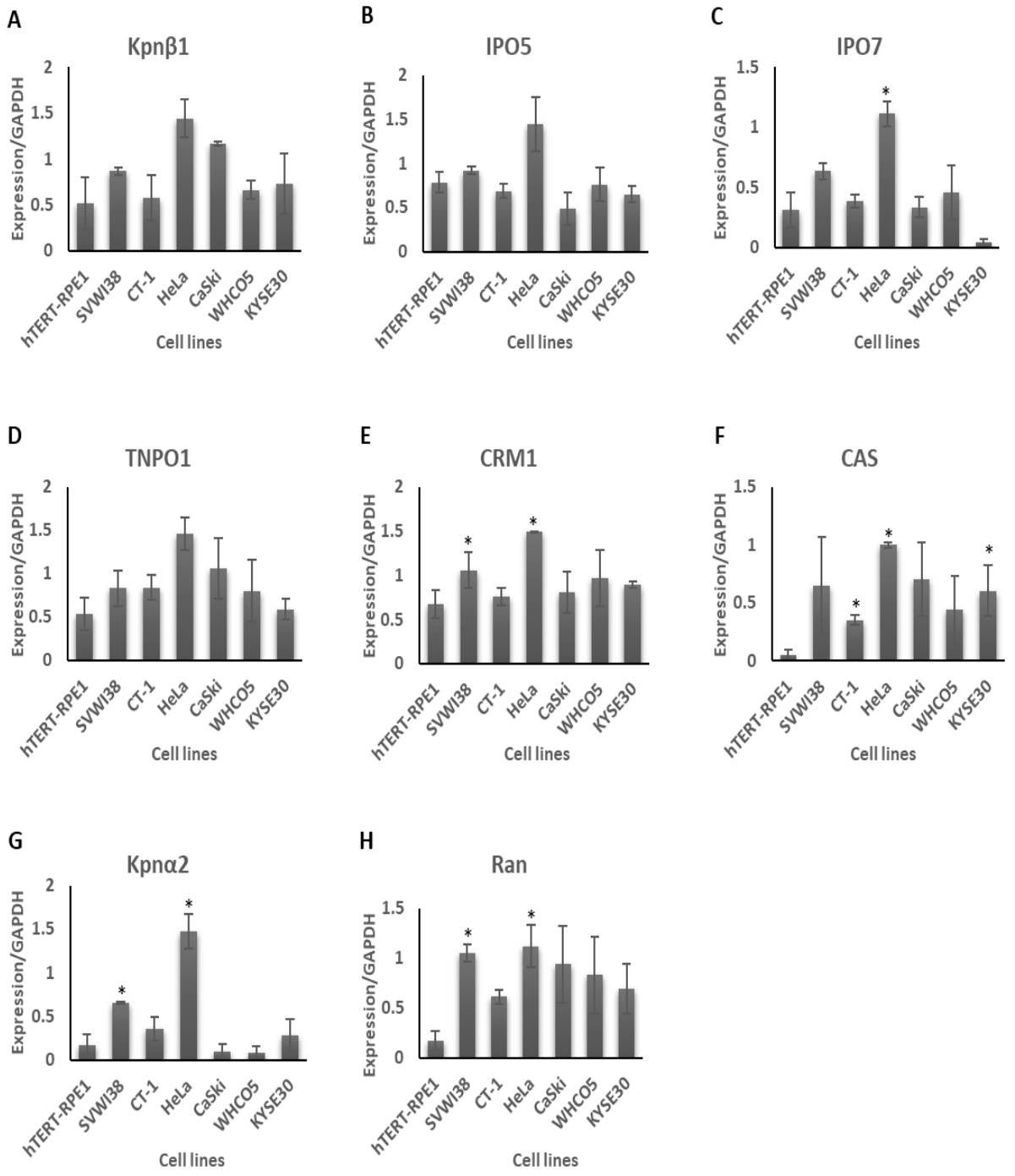

Figure 3.2. Densitometry quantification of intracellular nuclear transport proteins in cultured normal, transformed, cervical cancer and oesophageal cancer cell lines. Image J was used to quantify the intensity of the bands from WB and was represented as Expression/GAPDH of: **A)** Kpnβ1 **B)** IPO5 **C)** IPO7 **D)** TNPO1 **E)** CRM1 **F)** CAS **G)** Kpnα2 and **H)** Ran. Results shown represent the mean ± SEM of experiments performed in triplicate. The student's t-test was used to compare the levels of protein expression and **P*<0.05 was considered statistically different.

3.2.2. Secretion of nuclear transport proteins by cultured normal, transformed, cervical cancer and oesophageal cancer cell lines

Having shown that Kpnβ1, IPO5, IPO7, TNPO1, CRM1, CAS, Kpnα2 and Ran were expressed, though differentially, in normal, transformed, cervical cancer and oesophageal cancer cell lines (Figures 3.1 and 3.2), we next investigated whether hTERT-RPE1, SVWI38, CT-1, HeLa, CaSki, WHCO5 and KYSE30 secreted these proteins into their extracellular environment. Cell lines were grown to ~70% confluency and were serum-starved for 24 hours to minimize cell autolysis and cytosolic contamination of the cell secretome. Secreted proteins were harvested from the serum-starved culture media from the same population of cells from which intracellular proteins were harvested. The serum-starved culture media were subjected to a step-wise centrifugation process as described in section 2.2.5.2. in order to concentrate the secreted proteins. WB analysis was used to evaluate the level of Kpnβ1, IPO5, IPO7, TNPO1, CRM1, CAS, Kpnα2 and Ran in the secretomes of hTERT-RPE1, SVWI38, CT-1, HeLa, CaSki, WHCO5 and KYSE30.

The results showed little to no detection of all 8 nuclear transport proteins in the secretome of hTERT-RPE1 cells with higher levels in the transformed, cervical cancer and oesophageal cancer cell lines although at varying levels (Figure 3.3). β-tubulin, which is not secreted from cells, was included to eliminate intracellular protein contamination as a confounding factor, while the Coomassie stained gel showed the protein profile for all cell lines. The quantification of experiments performed in quadruplicate is shown in Figure 3.4. These findings suggest that the detection of nuclear transport proteins in the extracellular environment of cells associates with the transformed and cancer state.

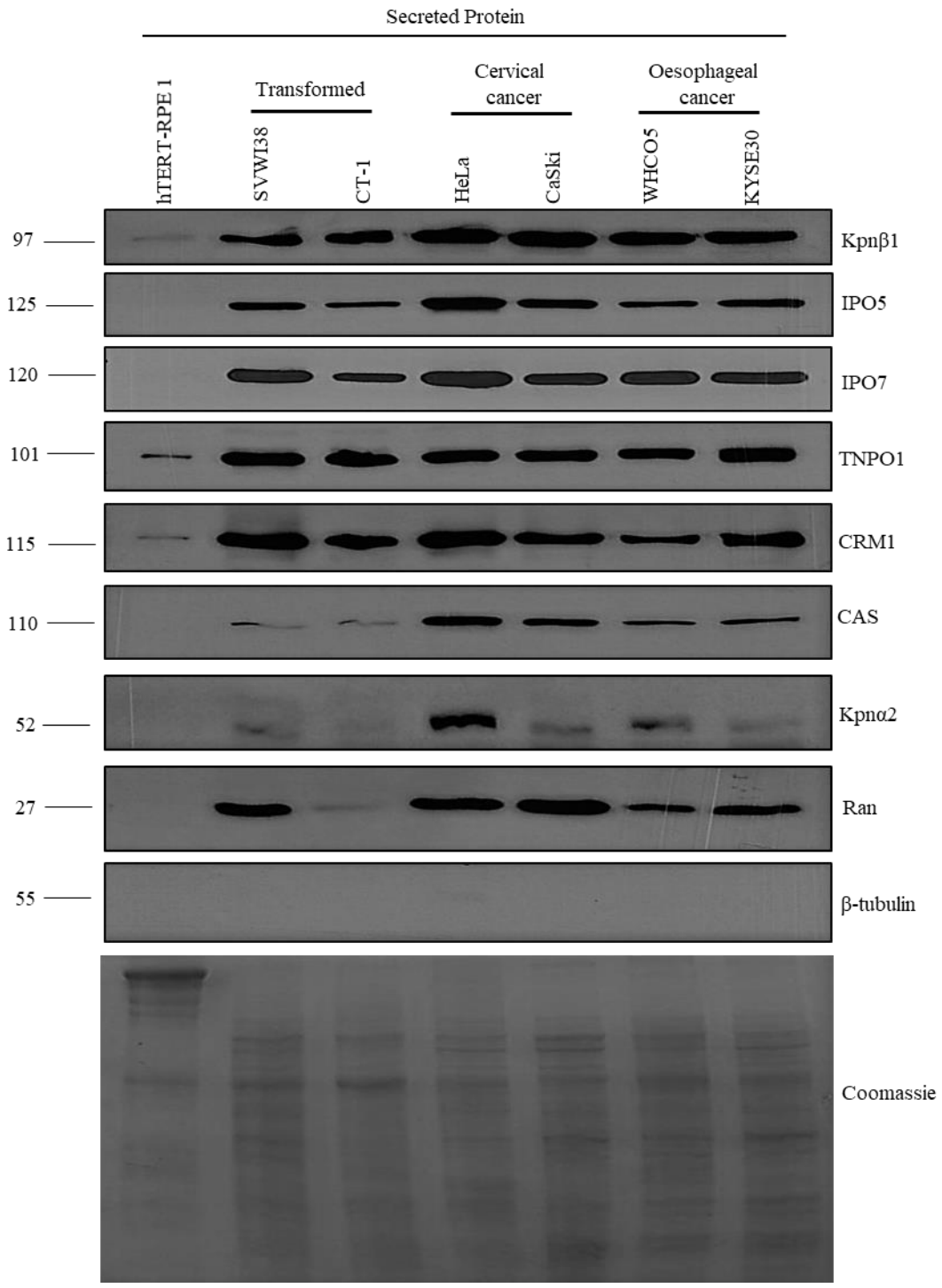

Figure 3.3. Secretion of nuclear transport proteins by cultured normal, transformed, cervical cancer and oesophageal cancer cell lines. WB analysis of Kpnβ1, IPO5, IPO7, TNPO1, CRM1, CAS, Kpnα2 and Ran secreted by the normal immortalized epithelial cell line (hTERT-RPE1), transformed cell lines (SVWI38 and CT-1), cervical cancer cell lines (HeLa and CaSki) and oesophageal cancer cell lines (WHCO5 and KYSE30). Each lane contained 15 µg of secreted protein. Coomassie staining was performed to show the protein profile along each lane. β-tubulin was used to monitor cytosolic contamination of the cell secretome. Results shown are representative of experiments performed in quadruplicate.

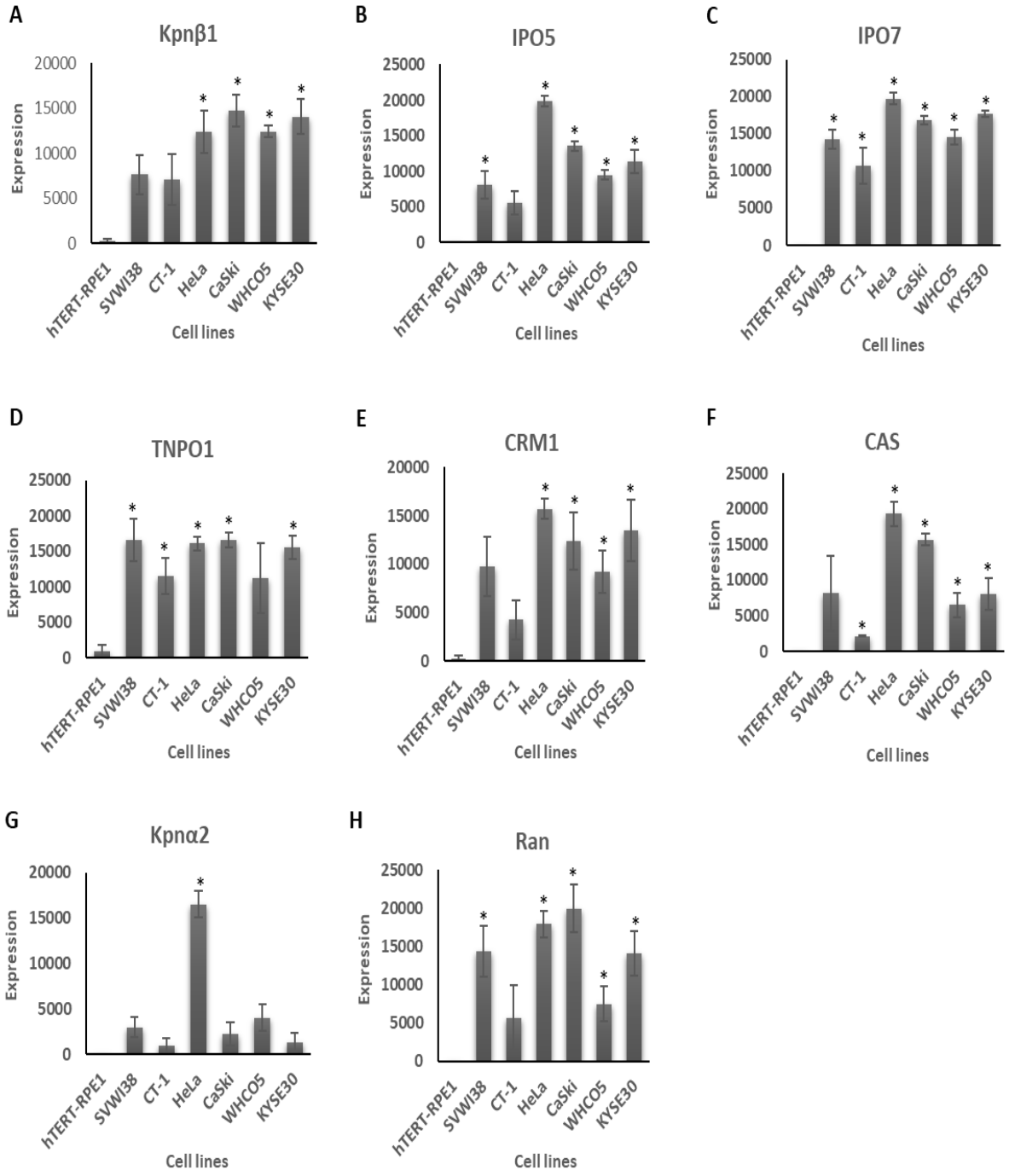

Figure 3.4. Densitometry quantification of secreted nuclear transport proteins by cultured normal, transformed, cervical cancer and oesophageal cancer cell lines. Image J was used to quantify the intensity of the bands from WB and was represented as Expression of: **A**) Kpnβ1 **B)** IPO5 **C)** IPO7 **D)** TNPO1 **E)** CRM1 **F)** CAS **G)** Kpnα2 and **H)** Ran. Results shown represent the mean ± SEM of experiments performed in quadruplicate. The student's t-test was used to compare the levels of protein secretion and **P*<0.05 was considered statistically different.

In addition to the 8 nuclear transport proteins, we also monitored the secretion of Vimentin by normal, transformed, cervical cancer and oesophageal cancer cell lines. The result showed that there is a higher level of Vimentin in the secretomes of hTERT-RPE1 and SVWI38 compared to the cervical and oesophageal cancer cell lines (Figures 3.5A and B). This result serves as an indication that the elevated levels of nuclear transport proteins in the secretomes of transformed and cancer cell lines is not due to the overall elevation of secreted proteins in transformed and cancer cells.

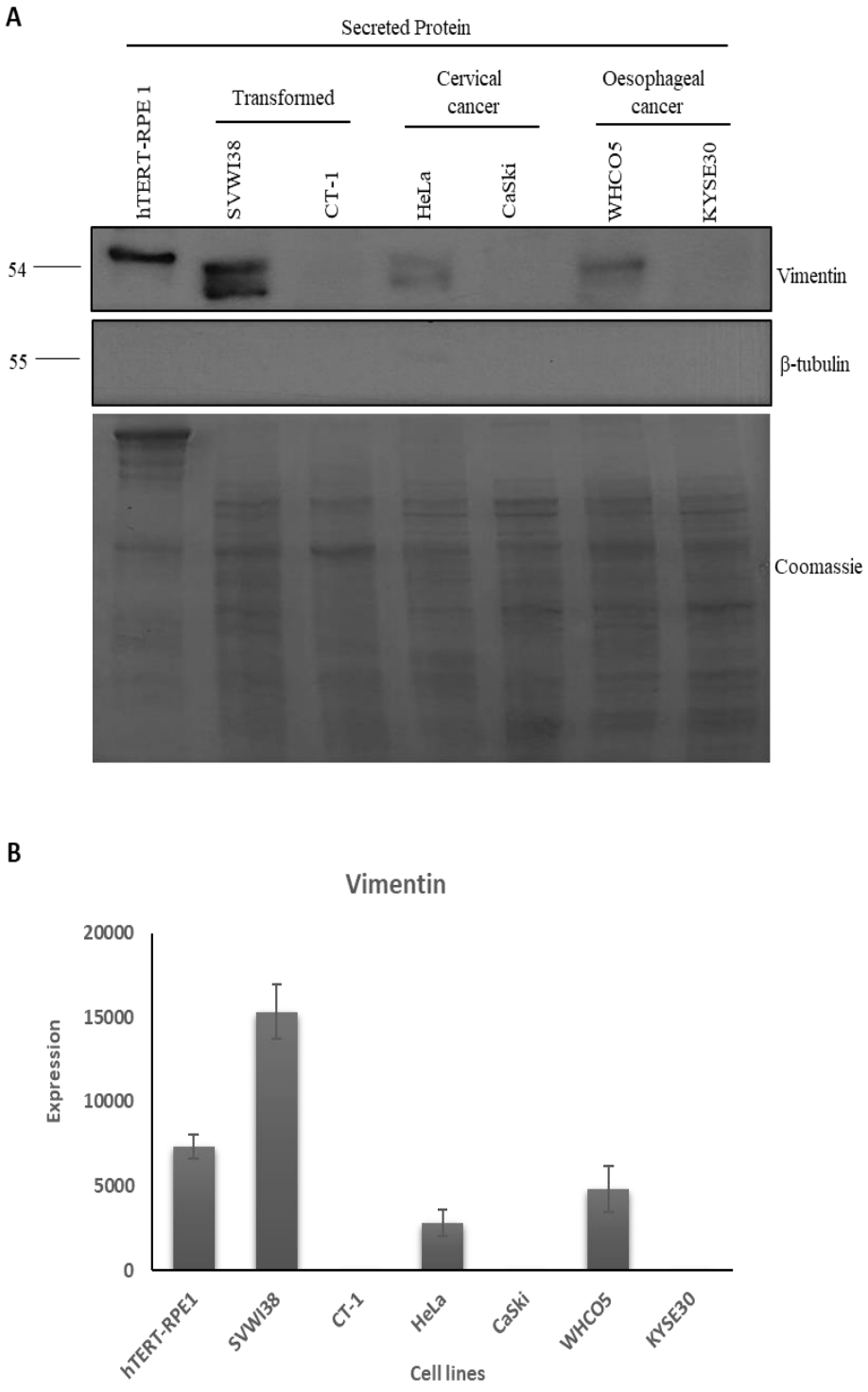

Figure 3.5. Secretion of Vimentin by cultured normal, transformed, cervical cancer and oesophageal cancer cell lines. A) WB analysis of Vimentin secreted by normal immortalized epithelial cell line (hTERT-RPE1), transformed cell lines (SVWI38 and CT-1), cervical cancer cell lines (HeLa and CaSki) and oesophageal cancer cell lines (WHCO5 and KYSE30). Each lane contained 15 µg of secreted protein. Coomassie staining was performed to show the protein profile along each lane. β-tubulin was used to monitor cytosolic contamination of the cell secretome. Results shown are representative of experiments performed in quadruplicate. **B)** Densitometry quantification of secreted Vimentin. Image J was used to quantify the intensity of the bands from WB and was represented as Expression of Vimentin. Results shown represent the mean ± SEM of experiments performed in quadruplicate.

3.2.3. ELISA analysis of Kpnβ1, CRM1, Kpnα2 and CAS in patient serum

Having established that multiple members of the nuclear transport protein family are secreted by transformed, cervical and oesophageal cancer cell lines into their extracellular environment at a higher level compared to the normal cell line, we sought to investigate the presence of Kpnβ1, CRM1, Kpnα2 and CAS in human serum samples. These are the nuclear transport proteins for which commercially manufactured ELISA kits were available at the time of the study. This was done to determine if our cell culture *in vitro* findings could be validated using *ex vivo* human serum samples from non-cancer subjects and cancer patients.

A total of 220 serum samples were analysed in this study; 73 serum samples were obtained from non-cancer subjects (as controls), 74 serum samples were obtained from cervical cancer patients and 73 were from oesophageal cancer patients. The demographic and clinicopathological information of the non-cancer subjects, cervical and oesophageal cancer patients are given in Table 3.1.

Table 3.1. Study set and clinicopathological features of subjects

Characteristics	Control (n = 54)	Cervical cancer (n = 74)	Control (n = 73)	Oesophageal cancer (n = 73)
Gender				
Male (%)	0 (0)	0 (0)	19 (26.0)	43 (58.9)
Female (%)	54 (100)	74 (100)	54 (74.0)	30 (41.1)
Age				
Mean (SD)	48.2 (16.7)	54.1 (12.3)	48.8 (16.3)	59.1 (10.51)
Median (Range)	43.5 (17-84)	53.0 (30-87)	46 (17-84)	61 (28-83)
Stage				
I (%)		4 (5.4)		0 (0)
II (%)		19 (25.7)		1 (1.4)
III (%)		46 (62.2)		36 (49.3)
IV (%)		4 (5.4)		4 (5.5)
N/A (%)		1 (1.4)		32 (43.8)
Differentiation				
Well (%)		4 (5.4)		5 (6.8)
Moderate (%)		34 (45.9)		44 (60.3)
Poor (%)		10 (13.5)		5 (6.8)
N/A (%)		26 (35.1)		19 (26.0)
Smoker				
No (%)	40 (74.1)	36 (48.6)	43 (58.9)	20 (27.4)
Yes (%)	14 (25.9)	35 (47.3)	30 (41.1)	53 (72.6)
N/A (%)	0 (0)	3 (4.1)	0 (0)	0 (0)
Alcohol intake				
Heavy (%)	1 (1.9)	17 (23.0)	12 (16.4)	31 (42.5)
Light (%)	13 (24.1)	6 (8.1)	18 (24.7)	19 (26.0)
No (%)	39 (72.2)	25 (33.8)	40 (54.8)	18 (24.7)
N/A (%)	1 (1.9)	26 (35.1)	3 (4.1)	5 (6.8)
Race				
Black (%)	21 (38.9)	47 (63.5)	29 (39.7)	50 (68.5)
Mixed (%)	33 (61.1)	27 (36.5)	44 (60.3)	23 (31.5)
Place of birth				
Eastern Cape (%)	11 (20.4)	41 (55.4)	13 (17.8)	48 (65.8)
Western Cape (%)	41 (75.9)	29 (39.2)	54 (74.0)	23 (31.5)
Others (%)	2 (3.7)	4 (5.4)	6 (8.2)	2 (2.7)

*N/A stands for not available

3.2.3.1. ELISA analysis of Kpnβ1 in patient serum

The serum concentration of Kpnβ1 in a cohort of 73 non-cancer subjects, 74 cervical cancer patients and 73 oesophageal cancer patients was determined using ELISA. 54 of the 73 non-cancer subjects were females and were used as the control group for comparison to the cervical cancer cases, whereas all 73 non-cancer subjects were used as the control group for comparison to the oesophageal cancer cases (Table 3.1). After doing some preliminary ELISA experiments to determine the optimal dilution factor for preparing the serum samples, a 1:5 dilution factor was used.

The result showed significantly elevated Kpnβ1 levels in serum from cervical cancer patients (P<0.0005) compared to the non-cancer controls (Figure 3.6A). Similarly, serum Kpnβ1 was significantly higher in patients with oesophageal cancer (P<0.05) compared to the non-cancer controls (Figure 3.6B). As shown in Table 3.2, the mean ± standard deviation (SD), median and range concentrations of serum Kpnβ1 in non-cancer controls versus (vs) cervical cancer patients are 16.1±10.2 ng/ml vs 33.0±21.9 ng/ml, 14.1 ng/ml vs 22.6 ng/ml and 0 – 57.3 ng/ml vs 8.5 – 84.6 ng/ml, respectively. For non-cancer controls vs oesophageal cancer cases, the mean±SD, median and range concentrations of serum Kpnβ1 are 16.5±10.1 ng/ml vs 22.5±15.0 ng/ml, 14.3 ng/ml vs 15.3 ng/ml and 0 – 57.3 ng/ml vs 5.8 – 82.0 ng/ml, respectively.

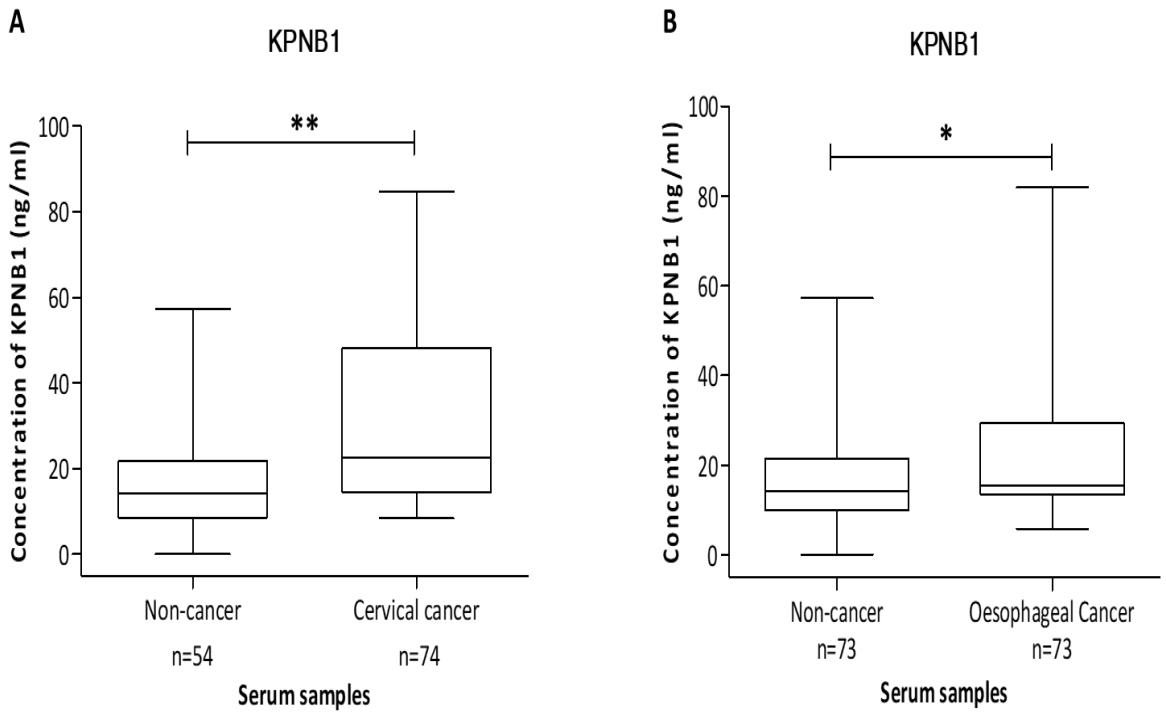

Figure 3.6. Serum level of Kpnβ1 in non-cancer subjects, cervical cancer and oesophageal cancer patients. ELISA was used to determine the concentration (ng/ml) of serum Kpnβ1 and comparisons were made between **A)** 54 non-cancer controls and 74 cervical cancer cases, **B)** 73 non-cancer controls and 73 oesophageal cancer cases. Data are represented as box and whisker plots. Non-parametric Mann-Whitney *U*-Test was used to compare between the non-cancer subjects and the cancer cases (**P*<0.05 and ***P*<0.0005).

Table 3.2. Mean, median and range concentration of serum Kpnβ1 for non-cancer and cancer cases

Descriptive statistics	Control (n = 54)	Cervical cancer (n = 74)	Control (n = 73)	Oesophageal cancer (n = 73)
Mean±SD (ng/ml)	16.1±10.2	33.0±21.9	16.5±10.1	22.5±15.0
Median (ng/ml)	14.1	22.6	14.3	15.3
Range (ng/ml)	0 – 57.3	8.5 – 84.6	0 – 57.3	5.8 – 82.0

3.2.3.2. ELISA analysis of CRM1 in patient serum

The serum concentration of CRM1 in a cohort of 73 non-cancer subjects, 74 cervical cancer patients and 72 oesophageal cancer patients was determined using ELISA. Again, 54 of the 73 non-cancer subjects were females and were used as the control group for comparison to the cervical cancer cases (Table 3.1). After performing some optimization experiments, a 1:2 dilution factor was used for patient serum sample preparation.

The serum level of CRM1 was significantly elevated in patients with cervical cancer ($P<0.05$) compared to the non-cancer controls (Figure 3.7A). Similarly, serum CRM1 was significantly higher in patients with oesophageal cancer ($P<0.0005$) compared to the non-cancer controls (Figure 3.7B). The mean±SD, median and range concentrations of serum CRM1 in non-cancer controls versus cervical cancer patients are 451.1±504.9 pg/ml vs 1082.2±1433.0 pg/ml, 214.3 pg/ml vs 483.7 pg/ml and 0 – 1469.4 pg/ml vs 0 – 5504.5 pg/ml, respectively. For non-cancer controls vs oesophageal cancer cases, the mean±SD, median and range concentrations of serum CRM1 are 384.8±488.1 pg/ml vs 1176.9±1147.0 pg/ml, 136.2 pg/ml vs 817.8 pg/ml and 0 – 1538.3 pg/ml vs 0 – 4759.8 pg/ml, respectively (see Table 3.3). Interestingly, the average CRM1 serum concentration (across patient groups) was ~30-fold less than the average serum concentration of Kpnβ1.

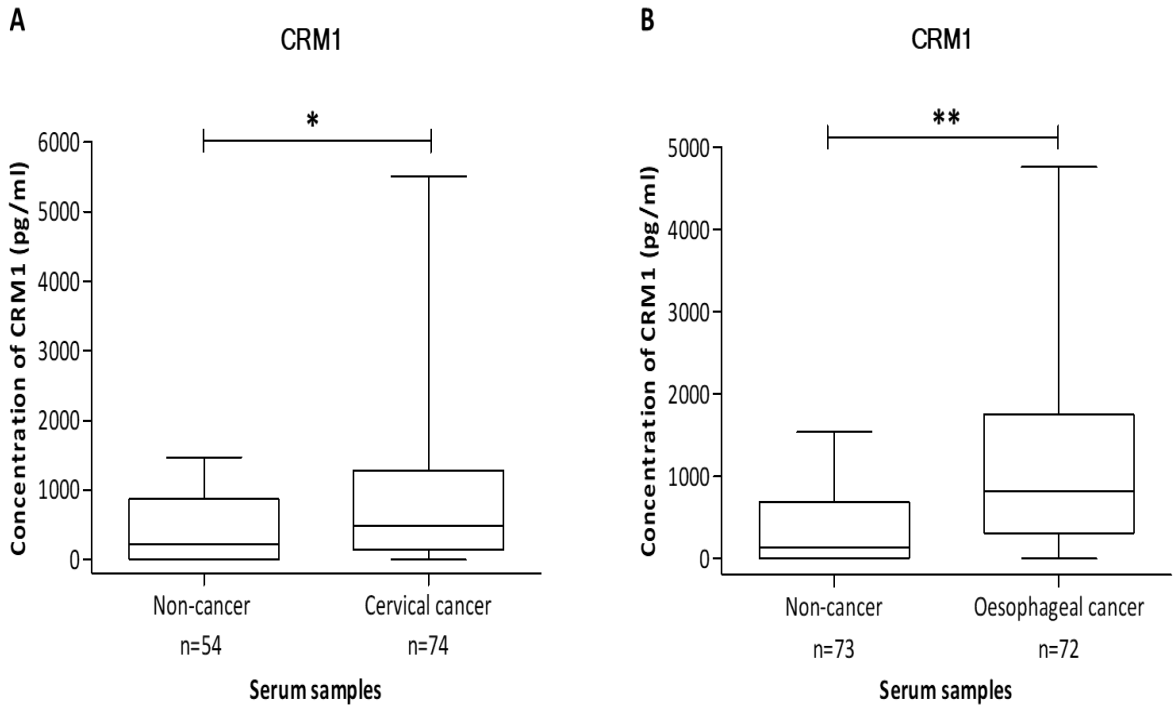

Figure 3.7. Serum level of CRM1 in non-cancer subjects, cervical cancer and oesophageal cancer patients. ELISA was used to determine the concentration (pg/ml) of serum CRM1 and comparisons were made between **A)** 54 non-cancer controls and 74 cervical cancer cases, **B)** 73 non-cancer controls and 72 oesophageal cancer cases. Data are represented as box and whisker plots. Non-parametric Mann-Whitney *U*-Test was used to compare between the non-cancer subjects and the cancer cases (*P<0.05 and **P<0.0005).

Table 3.3. Mean, median and range concentration of serum CRM1 for non-cancer and cancer cases

Descriptive statistics	Control (n = 54)	Cervical cancer (n = 74)	Control (n = 73)	Oesophageal cancer (n = 72)
Mean±SD (pg/ml)	451.1±504.9	1082.2±1433.0	384.8±488.1	1176.9±1147.0
Median (pg/ml)	214.3	483.7	136.2	817.8
Range (pg/ml)	0 – 1469.4	0 – 5504.5	0 – 1538.3	0 – 4759.8

3.2.3.3. ELISA analysis of Kpnα2 in patient serum

Next, we measured the level of serum Kpnα2 in a cohort of 73 non-cancer subjects, 74 cervical cancer patients and 72 oesophageal cancer patients using ELISA. 54 of the 73 female non-cancer subjects were used as the control group for comparison to the cervical cancer cases (Table 3.1). Preliminary ELISA experiments were done to determine the optimal dilution factor for the serum samples and a 1:2 dilution factor was used to prepare the serum samples for ELISA.

Unlike Kpnβ1 and CRM1, the serum level of Kpnα2 in patients with cervical cancer and in the non-cancer control group showed no statistical difference (Figure 3.8A). However, serum Kpnα2 was significantly elevated in patients with oesophageal cancer (P<0.0005) compared to the non-cancer controls (Figure 3.8B). Table 3.4 shows the mean±SD, median and range concentrations of serum Kpnα2 in non-cancer controls versus cervical cancer patients are 235.8±304.0 pg/ml vs 231.8±304.2 pg/ml, 139.3 pg/ml vs 118.8 pg/ml and 0 – 1319.8 pg/ml vs 0 – 1363.4 pg/ml, respectively. Also, the mean±SD, median and range concentrations of serum Kpnα2 in non-cancer controls vs oesophageal cancer cases are 198.2±276.4 pg/ml vs 455.8±405.2 pg/ml, 126.5 pg/ml vs 268.1 pg/ml and 0 – 1319.8 pg/ml vs 6.0 –1434.5 pg/ml, respectively. The average serum concentration of Kpnα2 was ~80-fold less than that of Kpnβ1.

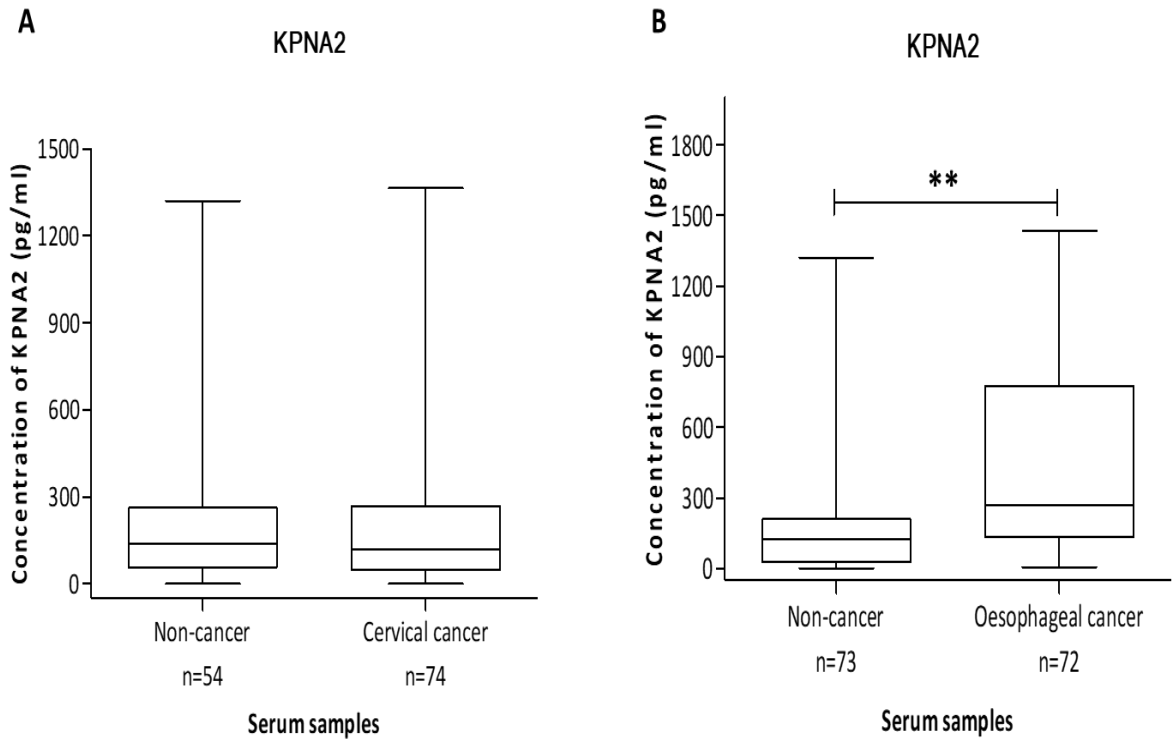

Figure 3.8. Serum level of Kpnα2 in non-cancer subjects, cervical cancer and oesophageal cancer patients. ELISA was used to determine the concentration (pg/ml) of serum Kpnα2 and comparisons were made between **A)** 54 non-cancer controls and 74 cervical cancer cases, **B)** 73 non-cancer controls and 72 oesophageal cancer cases. Data are represented as box and whisker plots. Non-parametric Mann-Whitney *U*-Test was used to compare between the non-cancer subjects and the cancer cases (***P*<0.0005).

Table 3.4. Mean, median and range concentration of serum Kpnα2 for non-cancer and cancer cases

Descriptive statistics	Control (n = 54)	Cervical cancer (n = 74)	Control (n = 73)	Oesophageal cancer (n = 72)
Mean±SD (pg/ml)	235.8±304.0	231.8±304.2	198.2±276.4	455.8±405.2
Median (pg/ml)	139.3	118.8	126.5	268.1
Range (pg/ml)	0 – 1319.8	0 – 1363.4	0 – 1319.8	6.0 –1434.5

3.2.3.4. ELISA analysis of CAS in patient serum

The serum level of CAS in a cohort of 73 non-cancer subjects, 74 cervical cancer patients and 70 oesophageal cancer patients was measured using ELISA. Again, the 54 female serum samples of the 73 non-cancer subjects served as the control group for comparison against the cervical cancer cases (Table 3.1). A 1:2 dilution factor was used to prepare the serum samples for ELISA after preliminary optimization experiments had been done.

The results showed that the level of serum CAS was significantly elevated in patients with cervical cancer (P<0.0005) compared to the non-cancer controls (Figure 3.9A). Similarly, serum CAS was significantly raised in patients with oesophageal cancer (P<0.0005) compared to the non-cancer controls (Figure 3.9B). The increases in serum CAS levels in the cancer compared to non-cancer groups were greater than those observed for Kpnβ1, CRM1 or Kpnα2. As shown in Table 3.5, the mean±SD, median and range concentrations of serum CAS in non-cancer controls versus cervical cancer patients are 0.8±1.9 ng/ml vs 11.7±13.4 ng/ml, 0 ng/ml vs 6.2 ng/ml and 0 – 8.6 ng/ml vs 0 – 61.3 ng/ml, respectively. For non-cancer controls vs oesophageal cancer cases, the mean±SD, median and range concentrations of serum CAS are 0.9±2.3 ng/ml vs 10.0±12.3 ng/ml, 0 ng/ml vs 5.4 ng/ml and 0 – 13.6 ng/ml vs 0 – 61.0 ng/ml, respectively. The average serum concentration of CAS was more similar to that of Kpnβ1, being only 4-fold less.

Collectively, these results suggest that Kpnβ1, CRM1 and CAS have potential as biomarkers for cervical cancer, while Kpnβ1, CRM1, Kpnα2 and CAS tracks with oesophageal cancer.

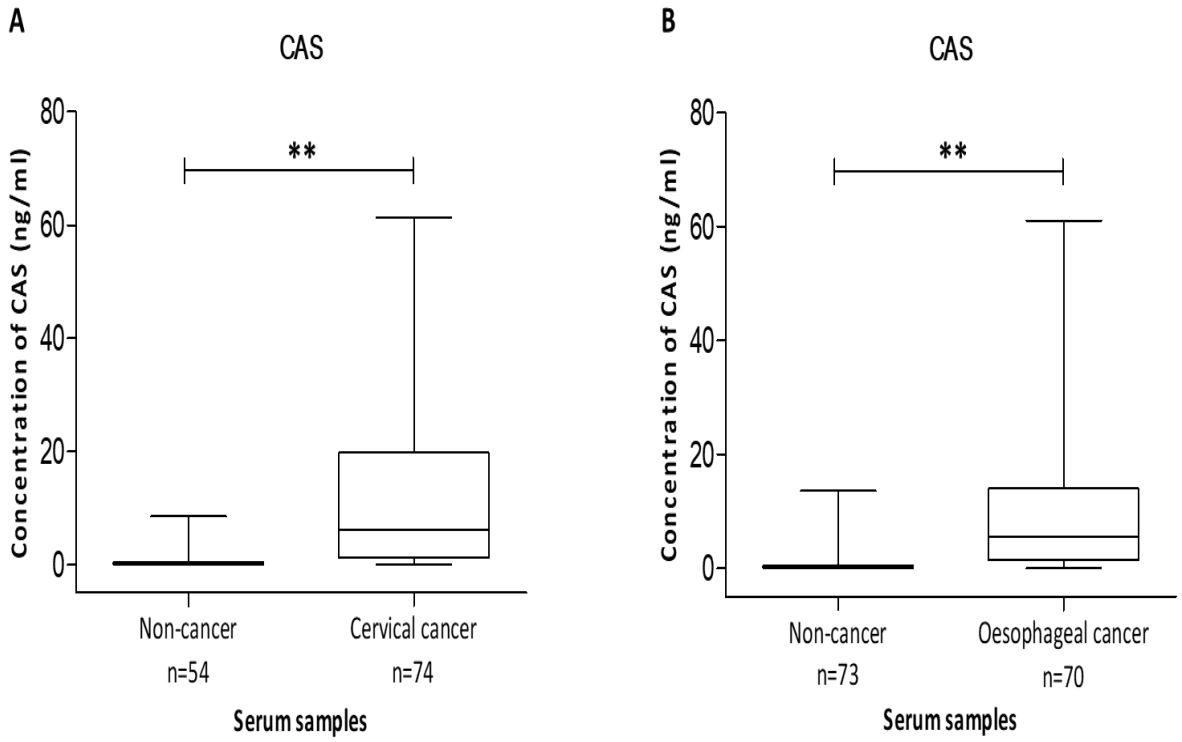

Figure 3.9. Serum level of CAS in non-cancer subjects, cervical cancer and oesophageal cancer patients. ELISA was used to determine the concentration (ng/ml) of serum CAS and comparisons were made between **A)** 54 non-cancer controls and 74 cervical cancer cases, **B)** 73 non-cancer controls and 70 oesophageal cancer cases. Data are represented as box and whisker plots. Non-parametric Mann-Whitney *U*-Test was used to compare between the non-cancer subjects and the cancer cases (**P*<0.05 and ***P*<0.0005).

Table 3.5. Mean, median and range concentration of serum CAS for non-cancer and cancer cases

Descriptive statistics	Control (n = 54)	Cervical cancer (n = 74)	Control (n = 73)	Oesophageal cancer (n = 70)
Mean±SD (ng/ml)	0.8±1.9	11.7±13.4	0.9±2.3	10.0±12.3
Median (ng/ml)	0	6.2	0	5.4
Range (ng/ml)	0 – 8.6	0 – 61.3	0 – 13.6	0 – 61.0

3.2.3.5. Candidate biomarkers levels according to clinicopathological features

Next, we sought to determine whether serum Kpnβ1, CRM1, Kpnα2 and CAS levels correlated with clinicopathological features. Not all patient information required for these comparisons was available and for many cases, the necessary information was recorded as "not available" in the database (N/A in Table 3.1). Stage information for approximately half of the oesophageal cancer cases was not available with only 1 case recorded as early-stage (stages I/II combined). This coincides with the late detection of oesophageal cancer and thus limited the number of early early-stage samples. However, there was sufficient information to make cervical cancer comparisons according to cancer stage.

The results showed that serum Kpnβ1 was significantly elevated in samples from early-stage cervical cancer cases (stages I/II combined) versus non-cancer controls ($P<0.0005$). Similarly, the level of serum Kpnβ1 in late-stage cases (stages III/IV combined) was higher compared to the non-cancer controls ($P<0.0005$). Comparison of early-stage to late-stage cases showed no statistical difference (Figure 3.10A).

The level of serum CRM1 was similarly significantly higher in early-stage cervical cancer cases compared to the non-cancer controls ($P<0.05$). Comparison between the late-stage cases and the non-cancer controls also showed a significant increase in the level of CRM1 in the late-stage cases ($P<0.05$). There was no statistical difference in the level of serum CRM1 when the early-stage cases were compared to the late-stage cases (Figure 3.10B).

There was no statistical difference between the level of serum Kpnα2 in early-stage cervical cancer cases and non-cancer control cases. Comparison between the late-stage cases and non-cancer controls also showed no statistical difference. Similarly, a within cases comparison showed no statistical difference (Figure 3.10C). This is consistent with the finding that serum Kpnα2 was unchanged between non-cancer and cervical cancer patient groups (Figure 3.8A).

A comparison between early-stage cervical cancer cases and non-cancer controls showed that serum CAS was significantly elevated in the early-stage cervical cancer cases ($P<0.0005$). Similarly, serum CAS in the late-stage cervical cancer cases was significantly higher compared to the non-cancer control cases ($P<0.0005$). However, there was no statistical difference when early-stage cases were compared to late-stage cases (Figure 3.10D).

These results show that Kpnβ1, CRM1 and CAS protein levels in patient serum samples are already elevated in the early stages of cervical cancer progression, hence these proteins show potential as early diagnostic markers of the disease.

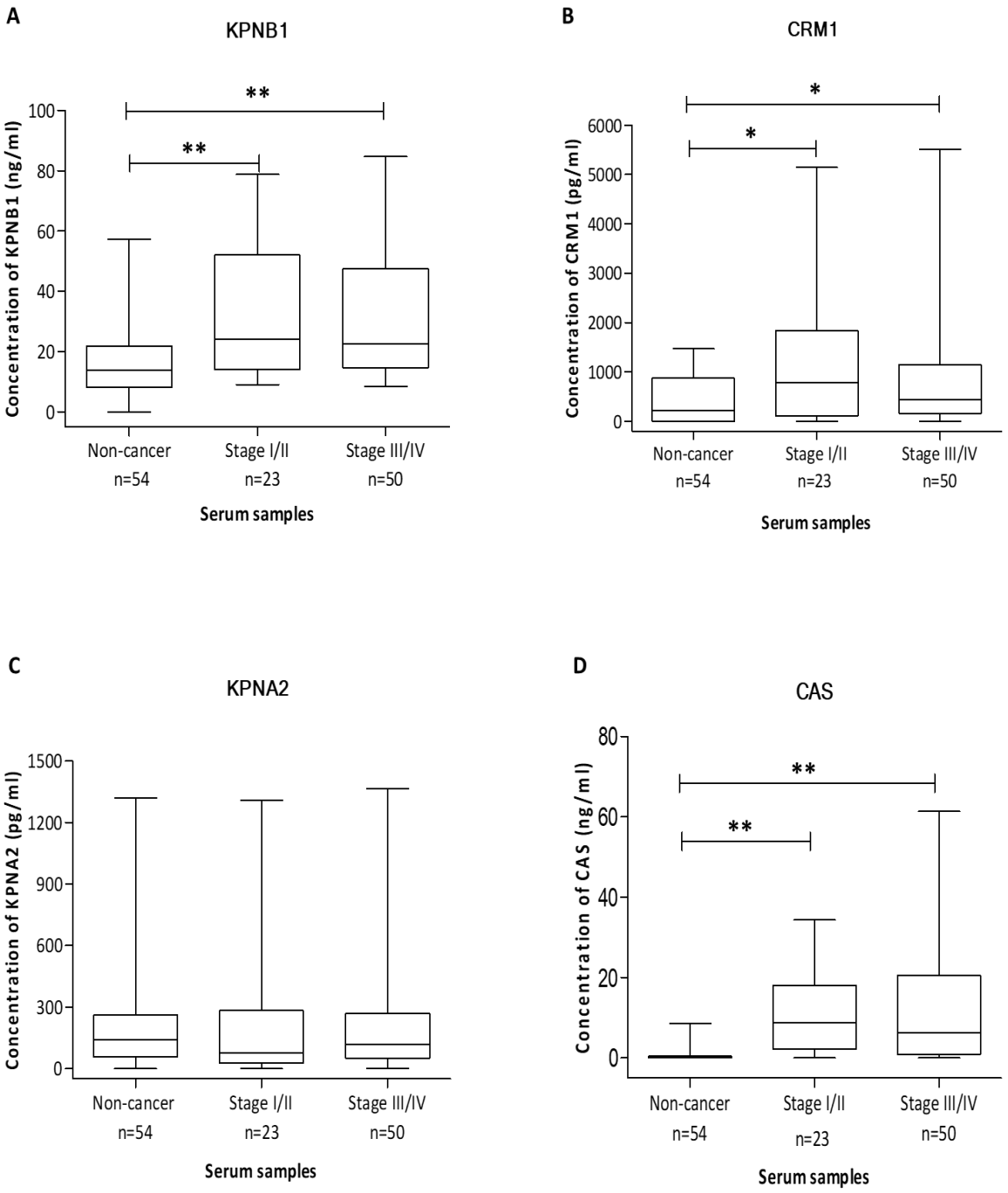

Figure 3.10. Efficacy of candidate biomarkers for early detection of cervical cancer. Serum levels of **A)** Kpnβ1, **B)** CRM1, **C)** Kpnα2 and **D)** CAS in non-cancer controls were compared to those in patients with early-stage and late-stage cervical cancer. Data are represented as box and whisker plots (**P*<0.05 and ***P*<0.0005).

3.2.3.6. Receiver operating characteristics curves (ROC) for candidate biomarkers

Our data using patient serum samples suggest that Kpnβ1, CRM1 and CAS have potential as biomarkers for cervical cancer and that Kpnβ1, CRM1, Kpnα2 and CAS have potential as biomarkers for oesophageal cancer. To measure the potential of these proteins as biomarkers, statistical determination of the likelihood of the proteins to distinguish between disease-positive and disease-negative states is required.

Plotting ROC curves and calculating the AUC for each candidate biomarker can be used as an index for determining the ability of the candidate biomarker to distinguish between disease-positive and disease-negative cases. The ROC curve is a graphical illustration of the trade-off between sensitivity (true-positive rate) and 1–specificity (false-positive rate). Sensitivity is the proportion of patients who are disease-positive that are correctly identified by the diagnostic test. Specificity is the proportion of patients who are disease-negative that are correctly identified by the diagnostic test[165]. To maximize the ability of the diagnostic test to identify disease-positive states while maximizing its ability to correctly identify disease-negative states, the sensitivity of each candidate biomarker was determined at 95% specificity. AUC is an index which is derived from the ROC curve and it ranges from 0 to 1. The closer the AUC is to 1, the better the overall performance of the candidate biomarker to distinguish between disease-positive and disease-negative states[166–168].

In this study, we performed a logistics regression analysis by plotting ROC curves to analyse the ability of Kpnβ1, CRM1, Kpnα2, CAS and their combination to discriminate cervical cancer and oesophageal cancer cases from non-cancer controls (Figure 3.11A and B). The AUC for each candidate biomarker investigated in this study showed that CAS (AUC=0.85±0.03 with 55% sensitivity at 95% specificity (P<0.0001)) is the best individual candidate biomarker for discriminating between cervical cancer cases and non-cancer controls. Table 3.5 shows the

AUC ± standard error (SE), *P*-value for the AUC, sensitivity at 95% specificity and the optimal cut-off value for each candidate biomarker for the cervical cancer cases. CAS (AUC=0.86±0.03 with 56% sensitivity at 95% specificity ($P<0.0001$)) also showed the best ability to discriminate between oesophageal cancer cases and the non-cancer controls. Table 3.6 shows the AUC±SE, *P*-value for the AUC, sensitivity at 95% specificity and the optimal cut-off value for each candidate biomarker for the oesophageal cancer cases.

A combinatorial analysis of the candidate biomarkers was done using the CombiROC web application tool to determine the biomarker combinations that will best discriminate between the cancer cases and the non-cancer controls. The CombiROC web application tool computes the sensitivity and specificity of all possible biomarker combinations and displays the AUC, sensitivity and specificity of the best performing biomarker combination[149]. A combination of Kpnβ1, CRM1, Kpnα2 and CAS displayed the highest diagnostic capacity for cervical cancer with a combined AUC of 0.89 and 100% sensitivity at 60% specificity. Similarly, a combination of Kpnβ1, CRM1, Kpnα2 and CAS outperformed all other biomarker combinations in discriminating oesophageal cancer cases from non-cancer controls with a combined AUC of 0.90 and 84% sensitivity at 86% specificity.

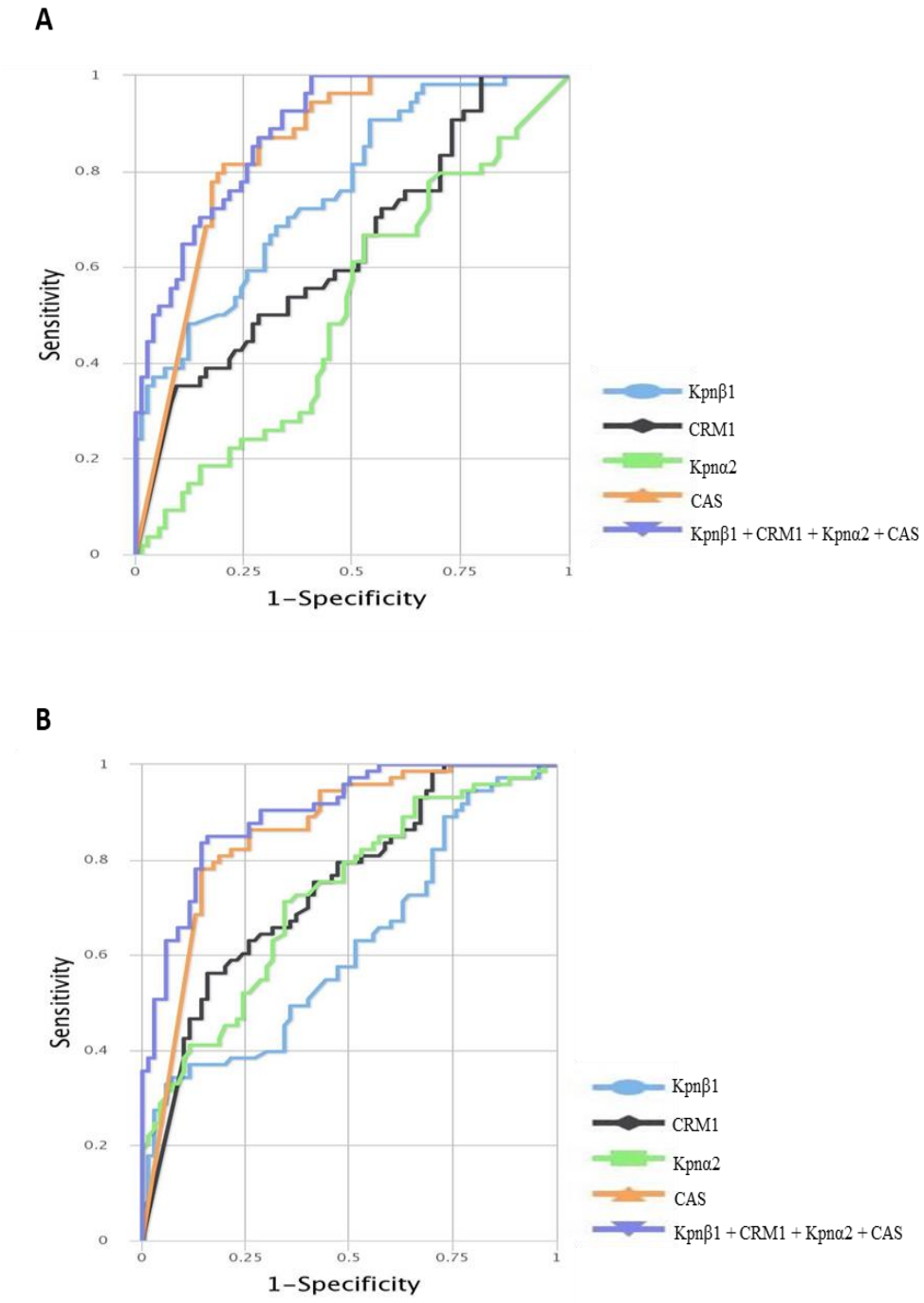

Figure 3.11. ROC curve analysis for candidate biomarkers. A) The ability of Kpnβ1, CRM1, Kpnα2, CAS and their combination to discriminate cervical cancer cases from non-cancer controls. **B)** The ability of Kpnβ1, CRM1, Kpnα2, CAS and their combination to discriminate oesophageal cancer cases from non-cancer controls.

Table 3.6. Classification performance of the candidate biomarkers in the cervical cancer cases

Candidate biomarkers	AUC±SE (95% Confidence interval)	*p*-value for AUC	Sensitivity (%) at 95% specificity	Cut-off
Kpnβ1 (ng/ml)	0.77±0.04 (0.66 – 0.85)	<0.0001	35	>13.83
CRM1 (pg/ml)	0.64±0.05 (0.54 – 0.74)	<0.01	20	>16.65
Kpnα2 (pg/ml)	0.51±0.05 (0.41 – 0.61)	0.82	<10	>89.24
CAS (ng/ml)	0.85±0.03 (0.78 – 0.91)	<0.0001	55	>0.67

Table 3.7. Classification performance of the candidate biomarkers in the oesophageal cancer cases

Candidate biomarkers	AUC±SE (95% Confidence interval)	*p*-value for AUC	Sensitivity (%) at 95% specificity	Cut-off
Kpnβ1 (ng/ml)	0.62±0.05 (0.53 – 0.72)	<0.01	15	>11.61
CRM1 (pg/ml)	0.75±0.04 (0.67 – 0.83)	<0.0001	32	>192.80
Kpnα2 (pg/ml)	0.73±0.04 (0.65 – 0.81)	<0.0001	21	>174.40
CAS (ng/ml)	0.86±0.03 (0.79 – 0.92)	<0.0001	56	>0.46

3.3. Discussion

In this study, the potential of nuclear transport proteins as cervical and oesophageal cancer diagnostic biomarkers was investigated. Normal, transformed and cancer cell lines were cultured *in vitro*. The cells were grown to ~70% confluency and were serum-starved for 24 hours; then intracellular and secreted proteins were harvested from the same population of cells. The cells were serum-starved to avoid contamination of the cell secretome by FCS. Harvesting secreted proteins from serum-supplemented cell culture medium would mean the protein sample would be enriched with highly abundant serum-proteins (such as albumin), such that the target proteins may be masked and undetected. Even a serum concentration as low as 0.5% has been reported to affect the detection of secreted target proteins[64]. According to Mbeunkui *et al.* (2006), cell autolysis and contamination of the cell secretome by cytosolic proteins are minimized when the incubation time and cell confluency for serum-starved cells were 24 hours and 60-70% respectively[74]. Those authors reported that the presence of β-actin and/or β-tubulin in the cell secretome could serve as an indication of cytosolic contamination since β-actin and β-tubulin are not secreted by cells[74]. We, therefore, modified the protocol for harvesting secreted proteins from conditioned media *in vitro* as described by Hua Xue (2008)[63] and monitored the level of β-tubulin during WB analysis of the secreted proteins to ensure that the secretome was devoid of contamination.

In the present study, the expression and secretion of 8 members of the nuclear transport protein family were investigated across normal, transformed, cervical cancer and oesophageal cancer cell lines using WB analysis. The nuclear transport proteins included 4 importins (Kpnβ1, IPO5, IPO7, TNPO1), 2 exportins (CRM1, CAS), 1 adaptor protein (Kpnα2) and 1 energy-providing protein (Ran). These nuclear transport proteins were selected because there are reports suggesting that many of these proteins are overexpressed in cancer cells and/or tissue biopsies[169]. Additionally, based on a previous MS study done in our laboratory, these proteins

were shown to be more abundant in the secretomes of cervical and oesophageal cancer cell lines compared to that of a normal cell line (A. Wishart, MSc dissertation, 2017[††]).

It has been reported that Kpnα2 acts as an adaptor protein which forms a trimeric complex with the cargo protein and Kpnβ1 in the classical import pathway[103]. Therefore, Kpnα2 is very essential in the classical nuclear import of cargo proteins like checkpoint kinase 2 (chk2)[170], breast cancer 1 (BRCA1)[171], Nijmegen breakage syndrome 1 (NSB1)[172], Ras-related C3 botulinum toxin substrate 1 (RAC-1)[173], c-Jun[174], HPV16 E6 oncoprotein[175], c-myc and tumour suppressor protein p53[176]. In the non-classical nuclear import pathway, Kpnβ1 has been reported to mediate the nuclear import of nuclear factor kappa-light-chain-enhancer of activated B cells (NF-kB)[177,178], cAMP response element binding protein (CREB) and activator protein 1 (AP-1) transcription factors[179]. Ran is a small Ras-like GTPase which basically supplies the energy required for the facilitated transport of cargo proteins and RNAs across the NPC[102]. CRM1 is the primary nuclear exporter which mediates the translocation of most leucine-rich NES cargo proteins and HIV genomic RNA from the nucleus into the cytoplasm[104,180,181], while CAS mediates the nuclear export of Kpnα2 from the nucleus into the cytoplasm for another round of nuclear import[91,182]. Kang *et al.* (2013) reported that IPO7 mediates the nuclear import of early growth response protein 1 (EGR1) in prostate cancer cells treated with a cinnamaldehyde derivative, hence activating apoptosis[183]. In addition to that, IPO7 has been reported to mediate the nuclear import of c-Jun[174], Histone H1[184], and Smad3[185]. TNPO1, just like Kpnβ1, has been reported to mediate the nuclear import of the high risk HPV16 E6 oncoprotein[175]. Finally, IPO5 has been implicated in the nuclear import of c-Jun[174]. Not only have elevated nuclear transport proteins been shown to associate with cancer, but the

[††] A Wishart. "Investigating secreted biomarkers for cancer: the potential of the nuclear transport proteins." University of Cape Town, 2017.

activities of their cargo proteins, for example NF-kB and AP-1, are often elevated in cancer cells[186–188].

Our results showed that the nuclear transport proteins investigated were expressed by all the cell lines, albeit at varying levels. It was interesting to see that Ran protein (which supplies the energy required for nuclear import and export) was expressed at relatively higher levels in the transformed and cancer cell lines compared to the normal cell line. Our result is in line with the findings of Xia *et al.* (2008) who reported that Ran was overexpressed in prostate adenocarcinoma, β-lymphoblastoid, breast adenocarcinoma, colon adenocarcinoma and cervical carcinoma[189].

As this study is focused on biomarkers discovery, the secretion of these 8 nuclear transport proteins into the extracellular environment of the cell lines was investigated via WB analysis. Our results showed that Kpnβ1, CRM1 and TNPO1 were detected in the secretome of the normal cell line, although at very low levels, and IPO5, IPO7, CAS, Kpnα2, and Ran were not detected in the secretome of the normal cell line using WB analysis. All the nuclear transport proteins under investigation were detected at a higher level in the secretomes of the transformed, cervical cancer and oesophageal cancer cell lines compared to the normal cell line. Vimentin was present in the secretome of the normal cell line at a higher level than the cancer cell lines, highlighting the fact that not all secreted proteins were present at elevated levels in the cancer cells secretomes. We selected Vimentin because previous MS analysis done in our laboratory revealed that Vimentin was overexpressed by normal epithelial cell lines compared to cancer cell lines (unpublished observations). Vimentin has been reported to be an extracellular protein, hence we anticipated that it should be detected in the secretome of the normal cell line[190,191].

Our results corroborate the MS findings of Wu *et al.* (2010) who listed all 8 of the nuclear transport proteins in their supplemental data showing proteins present in the secretomes of several cancer cell lines (of different tissue origins)[192]. In addition to that, our results are independent validation of the MS analysis done previously in our laboratory (A. Wishart, MSc dissertation, 2017‡‡). In that study, an analysis of the secretomes of normal, transformed and cancer cells showed an increase in the abundance of 13 members of the nuclear transport protein family from normal to transformed to cancer cell lines. Those results indicated that members of the nuclear transport protein family could be present at an elevated level in body fluids of cervical and oesophageal cancer patients and could be potential biomarkers for the diagnosis of cervical and oesophageal cancers. To the best of our knowledge, our study is the first to show by antibody-based techniques that multiple nuclear transport proteins (Kpnβ1, IPO5, IPO7, TNPO1, CRM1, CAS, Kpnα2 and Ran) are present in the secretomes of cervical and oesophageal cancer cells at elevated levels.

In this study, we selected blood serum as the source of secreted protein biomarkers because it encounters virtually all cells in the body during its circulation. Thus, cells and tissues secrete some proteins into the blood during its circulation in the body[37]. Furthermore, blood is easily accessible and its collection is minimally invasive, low risk and inexpensive[40]. The concentration of Kpnβ1, CRM1, Kpnα2 and CAS in serum samples from a cohort of non-cancer subjects, cervical cancer and oesophageal cancer patients was measured using ELISA. Amongst the four nuclear transport proteins investigated in this study using ELISA, Kpnβ1, CRM1 and CAS were found to be present at significantly elevated levels in cervical cancer patients compared to the non-cancer control subjects. Interestingly, all four candidate biomarkers were significantly elevated in oesophageal cancer patients compared to the non-

‡‡ A Wishart. "Investigating secreted biomarkers for cancer: the potential of the nuclear transport proteins." University of Cape Town, 2017.

cancer control subjects. These *ex vivo* human serum ELISA results corroborate our findings of the *in vitro* WB analysis of the secretomes of normal and cancer cell lines. Kpnα2 was the only protein which was secreted at an elevated level by cervical cancer cell lines *in vitro* but was not significantly elevated in the serum samples of cervical cancer patients compared to non-cancer subjects. Our data on the serum level of Kpnα2 in oesophageal cancer patients is in line with a study done by Ma and Zhao (2014) who reported that the level of serum Kpnα2 was significantly higher in OSCC patients compared to the non-cancer controls[115]. Together, our findings suggest that Kpnβ1, CRM1 and CAS are potential biomarkers for cervical cancer while Kpnβ1, CRM1, Kpnα2 and CAS have potential as biomarkers for oesophageal cancer.

A comparison between cervical cancer cases and non-cancer controls for candidate biomarkers according to stage indicated that Kpnβ1, CRM1 and CAS have the potential to be biomarkers for the early detection of cervical cancer. We could not do a similar comparison between oesophageal cancer cases and non-cancer controls because of insufficient clinical information for oesophageal cancer patients.

One of the qualities of an ideal biomarker is the ability of the biomarker to minimize false-positive and false-negative values when the disease is tested for[33–36]. We performed a logistics regression analysis by plotting ROC curves and calculating the AUC to determine the sensitivity and specificity of the candidate biomarkers and analyse their ability to discriminate between cancer cases and non-cancer controls. The AUC is a single index for measuring the performance of a diagnostic test. Any outcome from a diagnostic test whose AUC is 0.5 or less is said to have occurred by chance, hence, the closer the AUC is to 1, the better the overall performance of the diagnostic test to correctly identify diseased and non-diseased subjects[166–168]. In this study, CAS was the best performing individual candidate biomarker in discriminating between cervical cancer cases and non-cancer controls. It had the highest

individual AUC (0.85±0.03) and highest sensitivity (55%) at 95% specificity which were better than those of Kpnβ1 (AUC=0.77±0.04 with 35% sensitivity at 95% specificity), CRM1 (AUC=0.64±0.05 with 20% sensitivity at 95% specificity) and Kpnα2 (AUC=0.51±0.05 with <10% sensitivity at 95% specificity). A combination of the four candidate biomarkers gave the highest AUC of 0.89 with a sensitivity of 100% at 60% specificity. In a similar study done by Xu *et. al.* (2018), they identified CTHRC1 as a novel potential diagnostic biomarker for cervical cancer with an AUC of 0.665±0.034 and they also reported an AUC of 0.878±0.027 for SCC-Ag as an individual biomarker for cervical cancer. When they combined CTHRC1 and SCC-Ag as multiple biomarkers for cervical cancer, they reported an AUC of 0.879±0.027[77].

In discriminating oesophageal cancer cases from the non-cancer controls, CAS (AUC=0.86±0.03 with 56% sensitivity at 95% specificity) performed better than Kpnβ1 (AUC=0.62±0.05 with 15% sensitivity at 95% specificity), CRM1 (AUC=0.75±0.04 with 32% sensitivity at 95% specificity) and Kpnα2 (AUC=0.73±0.04 with 21% sensitivity at 95% specificity). The highest diagnostic capacity was achieved when the four candidate biomarkers were combined, with an AUC of 0.90 and 84% sensitivity at 86% specificity. Although Ma and Zhao (2014) previously reported that Kpnα2 may be a potential biomarker for OSCC[115], our study showed that CAS outperformed Kpnα2 as a potential biomarker for oesophageal cancer, and had an improved performance when combined with Kpnβ1, CRM1, and Kpnα2. Their study, however, did not investigate CAS.

Taken together, these findings suggest that members of the nuclear transport protein family are present in the extracellular microenvironment of cancer cells at a higher level compared to normal cells. Hence, measuring their levels (especially as a panel of biomarkers for cervical and oesophageal cancers) in blood could serve as a diagnostic tool for detecting these cancers.

It will, however, be important to further validate these findings by carrying out a similar study using a validation set of serum samples from a different group of cervical and oesophageal cancer patients.

3.4. Summary of key findings

- WB analysis supported by densitometry quantification revealed that the 8 nuclear transport proteins investigated were expressed in the normal, transformed, cervical cancer and oesophageal cancer cell lines but at differential levels.

- WB analysis followed by densitometry quantification showed that the 8 nuclear transport proteins investigated in this study were secreted at a higher level by the transformed, cervical cancer and oesophageal cancer cell lines compared to the normal cell line.

- ELISA analysis of human serum samples showed that Kpnβ1, CRM1 and CAS were present at an elevated level in serum samples from cervical cancer patients compared to serum samples from non-cancer controls.

- ELISA analysis of human serum samples revealed that Kpnβ1, CRM1, Kpnα2 and CAS were elevated in oesophageal cancer serum samples compared to serum samples from non-cancer controls.

- Kpnβ1, CRM1 and CAS were elevated in the serum of patients with early-stage cervical cancer, suggesting that they might be able to detect cervical cancer at an early stage.

- CAS was the best single candidate biomarker for discriminating cervical and oesophageal cancer cases from non-cancer controls. However, combining CAS with

Kpnβ1, CRM1, and Kpnα2 gave the highest diagnostic capacity to discriminate cervical and oesophageal cancer cases from non-cancer controls.

CHAPTER 4

IDENTIFICATION OF THE BINDING PARTNERS OF INTRACELLULAR KPNB1 IN NORMAL AND CANCER CELL LINES USING IMMUNOPRECIPITATION MASS SPECTROMETRY

4.1. Introduction

Proteins are the principal biomolecules in cells because they are involved in most biological processes. Their involvement in numerous biological processes is mostly due to their direct or indirect interactions with one another in a complex or pathway. Consequently, investigating protein-protein interactions is key to understanding the biological roles and processes a target protein is involved in.

Human Kpnβ1 is an important member of the superfamily of nuclear transport proteins responsible for shuttling cargoes into the nucleus. Kpnβ1 is a 97 kDa protein with a flexible super-helical structure composed of 19 tandem HEAT repeat units. It carries out its nuclear import function by binding to the NPC and cargo proteins at its central and C-terminals (HEAT repeats 4-19) and binds RanGTP at its N-terminus (HEAT repeats 1-8)[193–195]. Apart from its principal function as the major nuclear importer of cargo proteins, Kpnβ1 has been implicated in other important biological/cellular functions including the negative regulation of spindle assembly during mitosis[130–133], regulation of the actin cytoskeleton[134], ER-associated degradation of misfolded proteins[135], permeability of NPCs[136], RNA binding/processing[137] and restructuring of the nuclear envelope and NPCs[138,139]. The various roles which Kpnβ1 plays suggest that numerous proteins might be interacting with Kpnβ1 as binding partners. Identifying the binding partners of Kpnβ1 in normal and cancer cells would assist in

understanding the role of deregulated expression of Kpnβ1 in cancer. Furthermore, the binding partners of Kpnβ1 which are enriched in cancer cells can be investigated as potential anti-cancer therapeutic targets or biomarkers.

In this chapter, we performed IP-WB to determine whether proteins identified in the literature to be binding partners of Kpnβ1 could be co-immunoprecipitated with Kpnβ1. Then we aimed to identify further proteins which interact with intracellular Kpnβ1 using IP-MS. IP coupled to MS is a very powerful and sensitive technique for discovering and identifying binding partners of a target protein with the ability to identify hundreds of binding partners at once in a single sample[118,196–198]. During IP-MS, a target protein is precipitated from the proteome of a cell, tissue or an organism using antibody-bound beads which are specific for the target protein. Then the target protein with its binding partners are eluted from the beads for subsequent MS analysis to identify the binding partners of the target protein. IP-MS proteomic technology has seen much improvement over the last decade and can generate ample data.

4.2. Results

4.2.1. Optimization of Kpnβ1 immunoprecipitation conditions

Before co-immunoprecipitation (co-IP) and IP-MS experiments could commence, optimising the ideal conditions for immunoprecipitating Kpnβ1 was necessary. HeLa cells were selected as the source of intracellular protein for optimising the IP conditions because, based on the results shown in section 3.2.1., HeLa cells had the most abundant Kpnβ1 levels. HeLa cells were grown to ~80% confluency and intracellular protein was harvested from the cells as described in section 2.2.5.1. using a non-denaturing lysis buffer to retain the interactions between Kpnβ1 and its binding partners. In two pull-down experiments performed, 25 µg and 50 µg of Anti-Karyopherin β1 (H-7) AC agarose conjugated antibody at 500 µg/ml, 25% agarose (Santa Cruz Biotechnology, Catalogue number: sc-137016 AC) were used to pull-down Kpnβ1 from 500 µg of intracellular protein as described in sections 2.2.7. and 2.2.7.2.

The result showed that immunoprecipitating Kpnβ1 using 50 µg of Anti-Karyopherin β1 (H-7) AC agarose conjugated antibody pulled down substantially more Kpnβ1 than using 25 µg of Anti-Karyopherin β1 (H-7) AC agarose conjugated antibody (Figure 4.1A and B). All further pull-down assays were thus carried out using 50 µg of Anti-Karyopherin β1 (H-7) AC agarose conjugated antibody. A rabbit mAb IgG isotype control that is not directed against any known antigen was included, together with protein A agarose beads, to account for proteins non-specifically binding the antibody or beads. Only minor traces of Kpnβ1 was pulled down using the control.

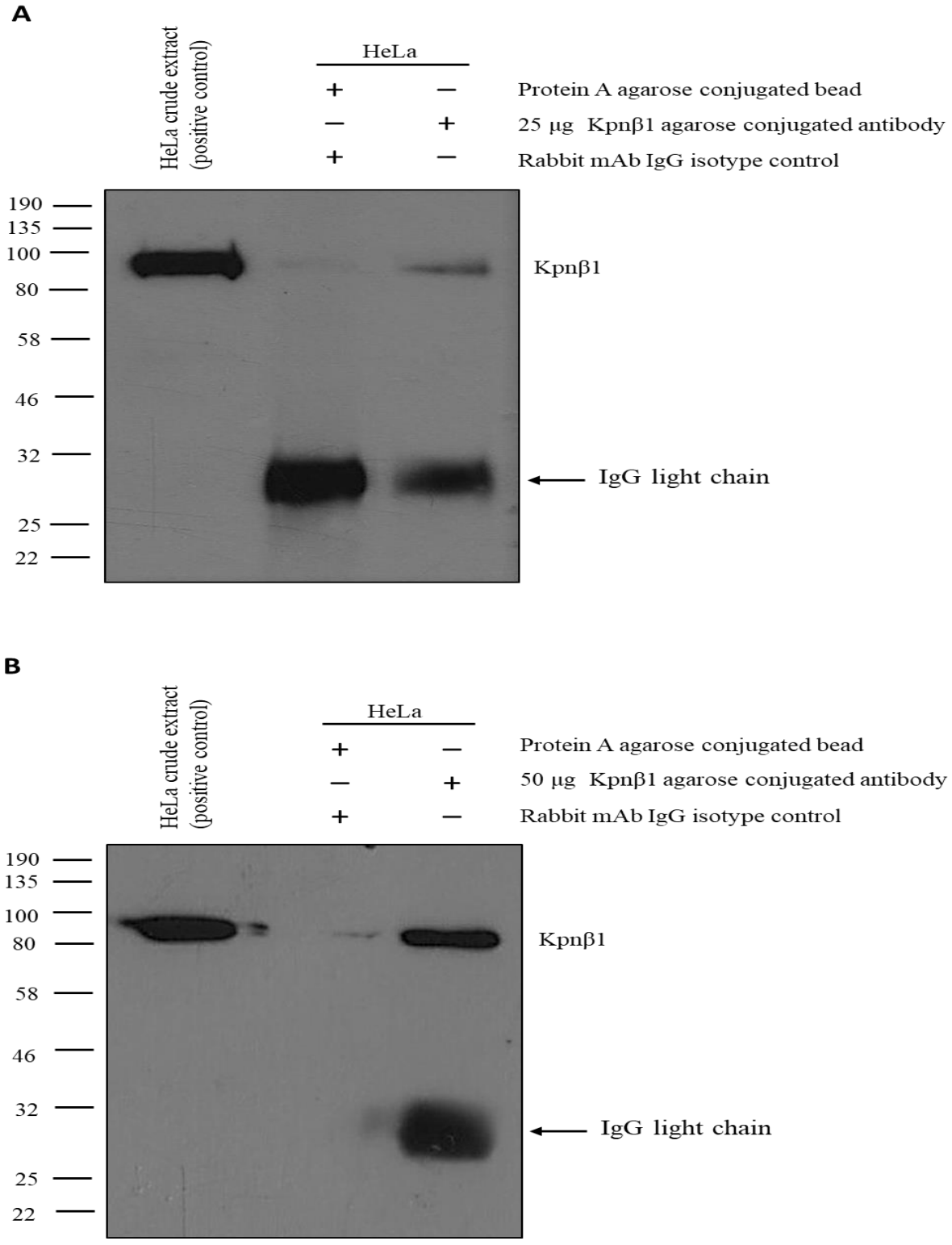

Figure 4.1. Optimization of Kpnβ1 immunoprecipitation. A) 25 µg and **B)** 50 µg of Anti-Karyopherin β1 (H-7) AC agarose conjugated antibody at 500 µg/ml, 25% agarose were used to pull-down Kpnβ1 from 500 µg of HeLa cell extracts. Lane 1 contained 15 µg of HeLa crude extracts as "non-treated" positive control. Lane 2 contained 25 µl of "IgG isotype" eluates as negative control. Lane 3 contained 25 µl of pull-down eluates. The blots were subjected to the same WB protocol.

4.2.2. Co-immunoprecipitation of Kpnβ1 binding partners using immunoprecipitation Western blot

Having established that Kpnβ1 was immunoprecipitated using 50 μg of Anti-Karyopherin β1 (H-7) AC agarose conjugated antibody in the pull-down experiments, we sought to validate the interaction of other nuclear transport proteins and cargo proteins with Kpnβ1 using IP-WB. hTERT-RPE1, HeLa, WHCO5 and KYSE30 cell lines were grown to ~80% confluency and intracellular protein was harvested from the cells using non-denaturing lysis buffer to retain the interactions between Kpnβ1 and its binding partners. For IP-WB and co-IP analysis, the "IgG isotype" control samples and the pull-down samples were prepared as described in sections 2.2.7., and 2.2.7.2.

There is evidence in the literature which suggests that some members of the nuclear transport protein family are potential binding partners of Kpnβ1[137]. Using IP-WB, we were able to show the co-IP of four binding partners of Kpnβ1 which are involved in the nuclear-cytoplasmic transport of cargo proteins in cells: Kpnα2, Ran, CRM1 and IPO7 (Figure 4.2). Our results showed that Kpnβ1 was immunoprecipitated from the normal and cancer cells extracts, albeit at varying levels, with greater pull-down amounts detected in the cancer cell lines. Higher amounts of Kpnβ1, CRM1, and Kpnα2 in the cancer cell lines are in line with previous findings in our laboratory reporting elevated expression of these nuclear transport proteins in cancer cell lines and patient tissue[80]. GAPDH was included as a negative control since it is not reported to bind Kpnβ1.

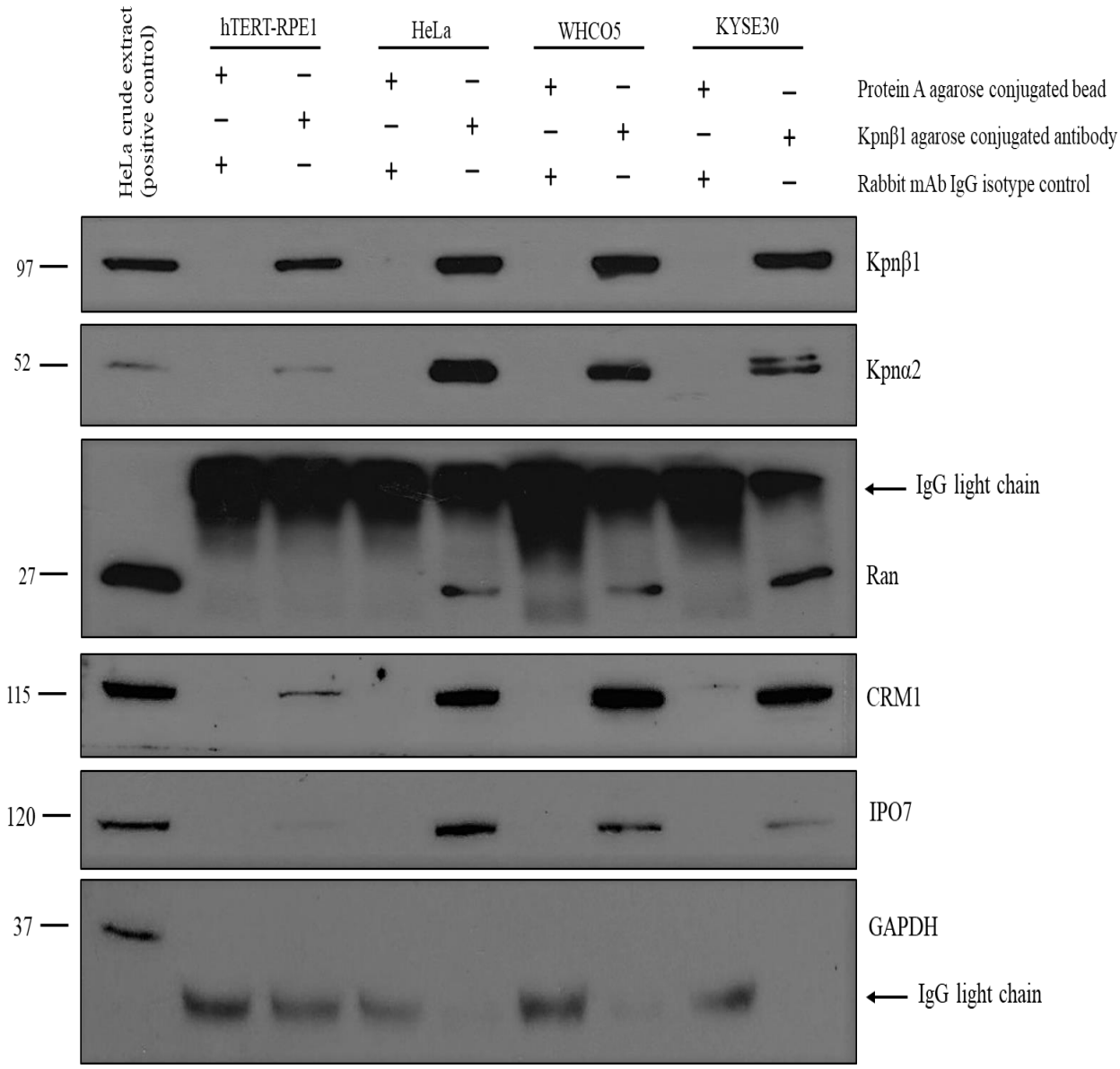

Figure 4.2. Co-immunoprecipitation of Kpnβ1 binding partners involved in nuclear-cytoplasmic transport. 50 µg of Anti-Karyopherin β1 (H-7) AC agarose conjugated antibody at 500µg/ml, 25% agarose was used to pull-down Kpnβ1 from 500 µg of hTERT-RPE1, HeLa, WHCO5 and KYSE30 cells extracts. Lane 1 contained 10 µg of HeLa crude extract as "non-treated" positive control. Lanes 2, 4, 6 and 8 contained 35 µl of "IgG isotype" eluates as a negative control for hTERT-RPE1, HeLa, WHCO5 and KYSE30 cells extracts, respectively. Lanes 3, 5, 7 and 9 contained 35 µl of pull-down eluates for hTERT-RPE1, HeLa, WHCO5 and KYSE30 cells extracts, respectively. The resulting immunoblots were probed for Kpnβ1 and four nuclear transport proteins suggested to be potential binding partners of Kpnβ1. GAPDH was used as a negative control for all samples.

We also searched in the literature to find known cargo proteins of Kpnβ1 which have been associated with tumorigenesis. NF-kB and c-Jun were selected for further investigation because of the role which their nuclear import plays in cancer cells progression, proliferation and survival[178]. Our group has previously reported that the transcription factor, NF-kB, is transported into the nucleus by Kpnβ1[177]. In a different study, Waldmann and Kehlenbach (2015) implicated Kpnβ1 as one of the nuclear transport receptors for c-Jun[174]. We, therefore, probed for NF-kB and c-Jun from the same blot used for immunoprecipitating Kpnβ1 in hTERT-RPE1, HeLa, WHCO5 and KYSE30 cells extracts.

The results showed that NF-kB was co-immunoprecipitated with Kpnβ1 in HeLa and WHCO5 cancer cell lines but with little or none detected in the normal hTERT-RPE1 cell line and KYSE30 oesophageal cancer cell line. The faint band seen in the co-immunoprecipitation of NF-kB with Kpnβ1 in KYSE30 cell extracts could be due to a low expression or activity of NF-kB in KYSE30 cell line. Also, c-Jun was co-immunoprecipitated with Kpnβ1 in all the cancer cells extracts but with little or none detected in the normal hTERT-RPE1 cell line (Figure 4.3). This could be an indication that the increased proliferative activities of cancer cells may be associated with the increased nuclear import of transcription factors like NF-kB and c-Jun, which promote cell proliferation and downregulate apoptosis in cancer cells.

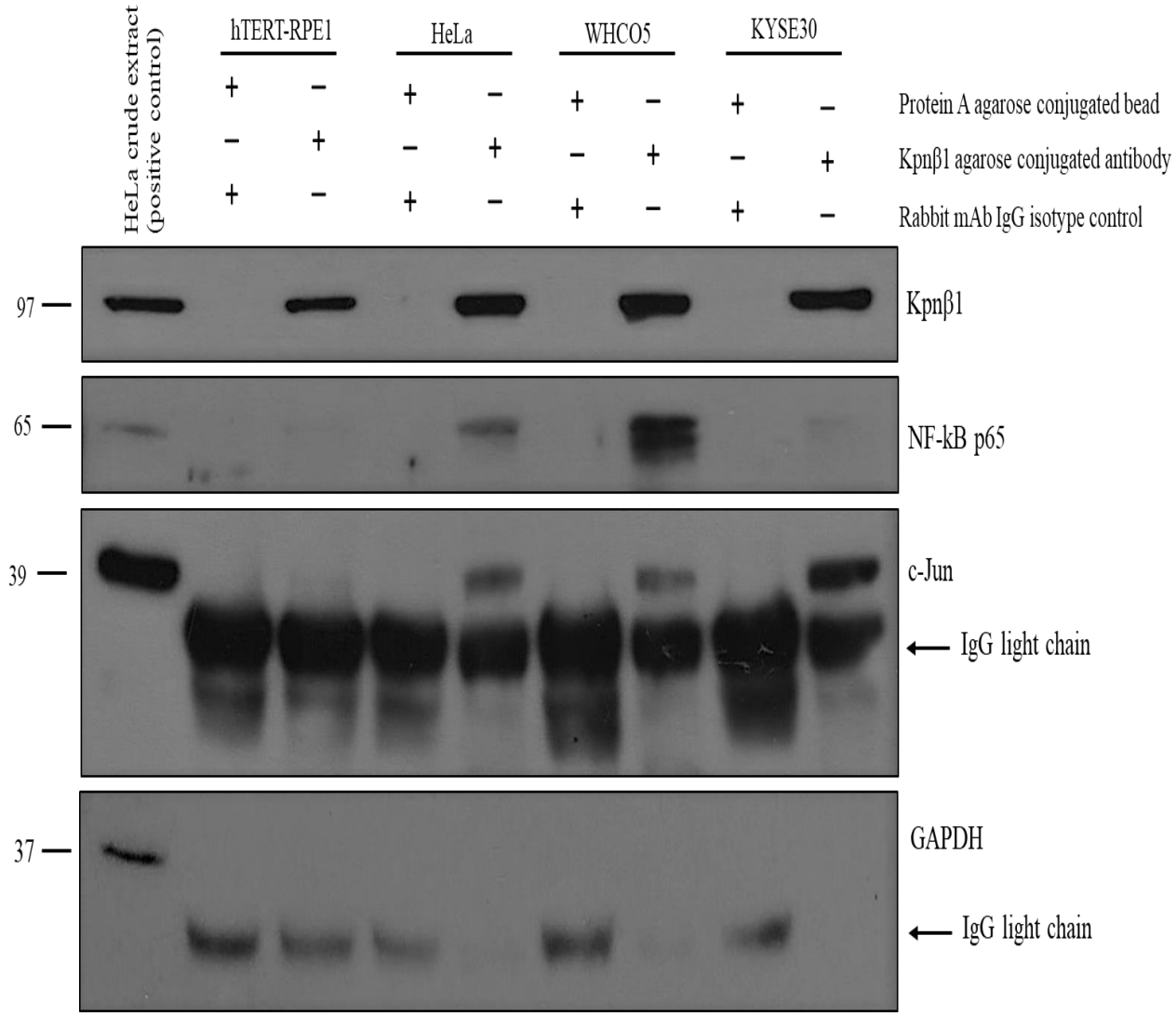

Figure 4.3. Co-immunoprecipitation of Kpnβ1 cargo proteins. 50 µg of Anti-Karyopherin β1 (H-7) AC agarose conjugated antibody at 500µg/ml, 25% agarose was used to pull-down Kpnβ1 from 500 µg of hTERT-RPE1, HeLa, WHCO5 and KYSE30 cells extracts. Lane 1 contained 10 µg of HeLa crude extract as "non-treated" positive control. Lanes 2, 4, 6 and 8 contained 35 µl of "IgG isotype" control eluates as a negative control for hTERT-RPE1, HeLa, WHCO5 and KYSE30 cells extracts respectively. Lanes 3, 5, 7 and 9 contained 35 µl of pull-down eluates for hTERT-RPE1, HeLa, WHCO5 and KYSE30 cells extracts respectively. The resulting immunoblots were probed for Kpnβ1, NF-kB and c-Jun. GAPDH was used as a negative control for all samples.

4.2.3. Identifying the binding partners of Kpnβ1 in normal and cancer cells using IP-MS

Having established that Kpnβ1 was immunoprecipitated from the normal and cancer cells extracts, we sought to identify further binding partners of Kpnβ1 in normal, cervical cancer and oesophageal cancer cell lines using IP-MS. hTERT-RPE1, HeLa, WHCO5 and KYSE30 cell lines were grown to ~80% confluency and intracellular protein was harvested from the cells using non-denaturing lysis buffer to retain the interactions between Kpnβ1 and its binding partners. For IP-MS analysis, the "IgG isotype" control samples and the pull-down samples were prepared in triplicates for each cell line. Three mg of protein sample from each cell line was divided into 6 Eppendorf tubes at 500 ug per Eppendorf tube. Three samples were used as "IgG isotype" controls while the other three were used in the Kpnβ1 pull-down. Both "IgG isotype" and pull-down samples were subjected to the IP-MS protocol as described in sections 2.2.7., 2.2.7.1., 2.2.7.1.1. and 2.2.7.1.2.

The "IgG isotype" and pull-down samples were analysed on an Orbitrap Q Exactive mass spectrometer (Thermo Fisher, San Jose, CA, USA) and the raw Xcalibur files generated were processed using MaxQuant (version 1.5.4.1.). The MaxQuant generated text output files which were then imported into Perseus statistical software package (version 1.5.5.3.) for further data processing[199]. The data were subjected to stringent clean-up to remove all reverse hits, possible contaminants, protein groups that were only identified by one modification site, protein groups with Q-values greater than 0.01 and protein groups with less than 2 unique peptides.

Using the Perseus statistical software package, the reproducibility of experiments was tested by plotting a multi scatterplot of the log2 transformed intensity-based absolute quantification (iBAQ). The reproducibility of the "IgG isotype" control samples prepared in triplicate against each other are shown in Figure 4.4 and that of the Kpnβ1 pull-down samples prepared in triplicate against each other are shown in Figure 4.5.

The Pearson correlation coefficients within replicates for the “IgG isotype” control samples in the same cell line varied between 0.63–0.91 (Figure 4.4). The relatively low correlation coefficients within this group are likely due to the non-specificity of interactions with the Rabbit (DA1E) mAb IgG isotype control and protein A agarose beads used. As a result, different proteins would bind non-specifically to the Rabbit (DA1E) mAb IgG isotype control and beads in each replicate experiment, therefore, introducing some level of variability in the protein groups identified. The Pearson correlation coefficients within replicates for the Kpnβ1 pull-down samples were very high amongst the same cell line with Pearson correlation coefficients greater than 0.93 (Figure 4.5). This is an indication that reproducibility within the pull-down replicates was very high; and as such, provided a level of confidence that the co-immunoprecipitants of Kpnβ1 for the replicates of the same cell line are very similar.

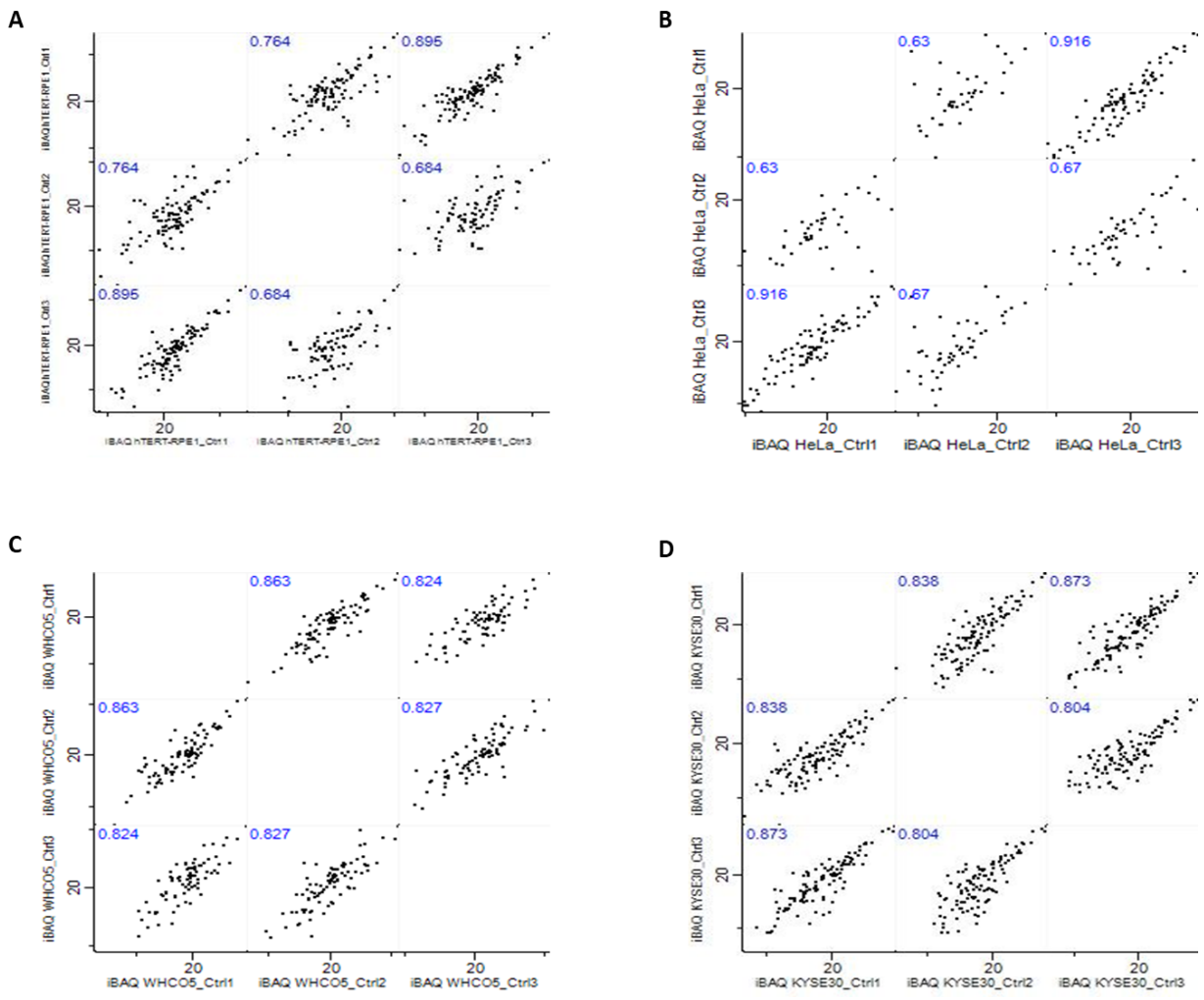

Figure 4.4. Multi scatter-plot of the "IgG isotype" control samples. Scatterplots with Pearson correlations of the log2 transformed iBAQ of the "IgG isotype" control samples of **A)** hTERT-RPE1 **B)** HeLa **C)** WHCO5 and **D)** KYSE30 prepared in triplicate, with the Pearson correlation coefficients varying between 0.63–0.91.

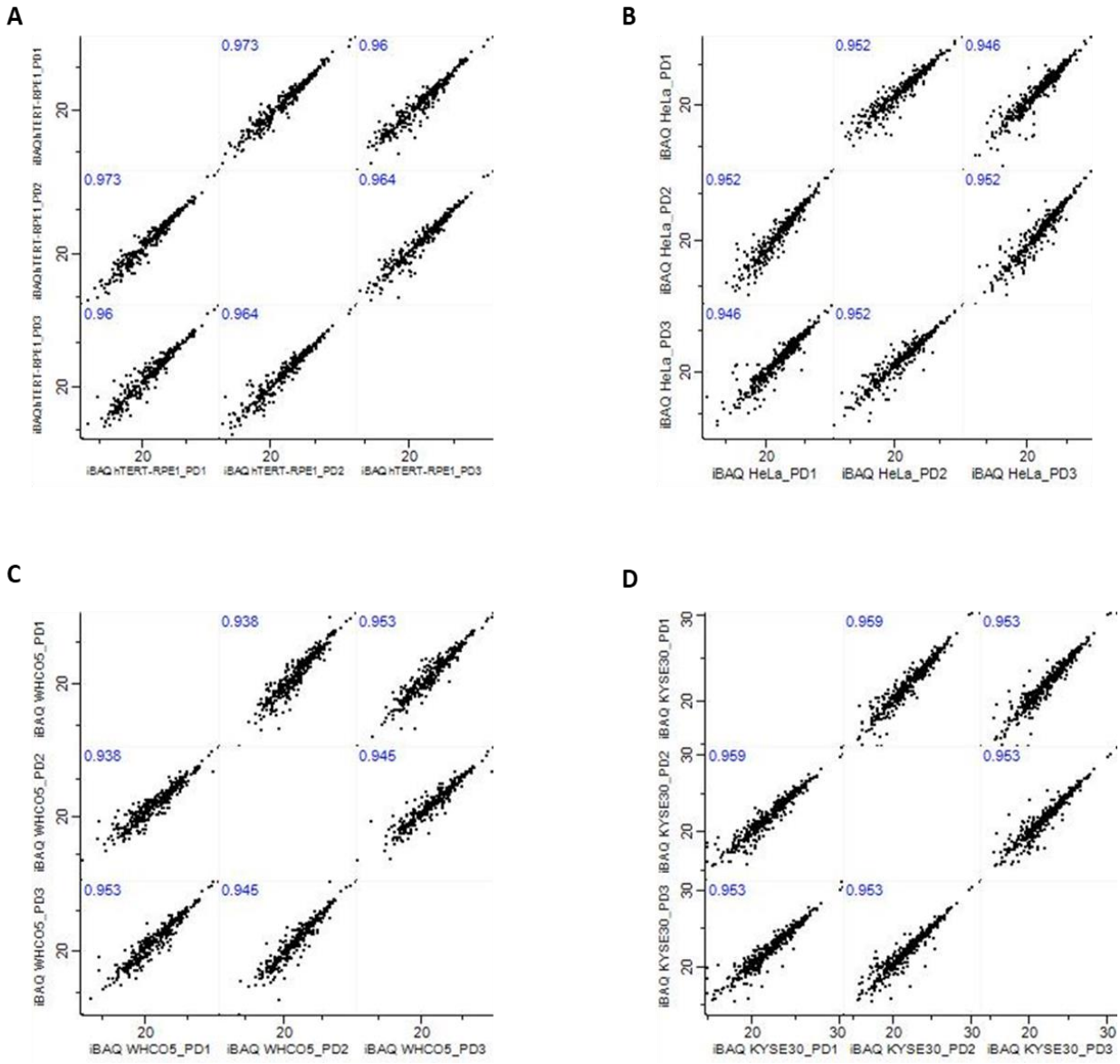

Figure 4.5. Multi scatter-plot of the pull-down samples. Scatterplots with Pearson correlations of the log2 transformed iBAQ of the pull-down samples of **A)** hTERT-RPE1 **B)** HeLa **C)** WHCO5 and **D)** KYSE30 prepared in triplicate, with the Pearson correlation coefficients greater than 0.93.

To further tighten the Kpnβ1 pull-down data, protein groups detected in the "IgG isotype" control samples were removed from the protein groups identified in the Kpnβ1 pull-down samples. As expected, Kpnβ1 was not identified in any of the "IgG isotype" control samples indicating that Kpnβ1 was specifically immunoprecipitated in the pull-down assay.

There were more Kpnβ1 binding partners identified in the cancer cells extracts compared to the normal cell extracts. Our results revealed that 100 proteins were identified as potential binding partners of Kpnβ1 in normal hTERT-RPE1 cell extracts. For the HeLa cervical cancer cell extracts, 179 proteins were pulled down with Kpnβ1. Furthermore, 147 and 176 proteins were pulled down with Kpnβ1 in WHCO5 and KYSE30 oesophageal cancer cells extracts, respectively. The full lists of proteins identified as potential binding partners of Kpnβ1 in hTERT-RPE1, HeLa, WHCO5 and KYSE30 cells extracts are shown in Appendix IA, IB, IC and ID, respectively. These results indicate an approximately 1.5 to 2-fold greater interaction of Kpnβ1 with other proteins in the cancer cell lines than in the normal cell line.

4.2.3.1. Venn diagrams showing common and unique Kpnβ1 binding partners in normal and cancer cell lines

A comparison of the list of identified binding partners of Kpnβ1 in each cell line revealed that multiple binding partners were common to two or more cell lines. The VennDis JavaFX-based Venn and Euler diagram software created by Ignatchenko *et al.*[152] was used to overlap the lists of binding partners of Kpnβ1 in the normal and cancer cell lines. Then the common and unique binding partners were identified. Only protein groups identified in all triplicate samples for each cell line were used for the Venn diagram analysis.

For each Venn diagram in Figure 4.6, the number in the region of intersection for two or more cell lines is the number of common binding partners of Kpnβ1 identified for the cell lines.

Since Kpnβ1 is the target protein for this IP-MS study, it was not counted as a common binding partner. Therefore, 77 proteins were identified as the common binding partners of Kpnβ1 in normal hTERT-RPE1 and HeLa cervical cancer cells (Figure 4.6A). An overlap of the lists of binding partners of Kpnβ1 in hTERT-RPE1, WHCO5 and KYSE30 oesophageal cancer cell lines revealed 41 common proteins (Figure 4.6B). There were 56 proteins identified as the common binding partners of Kpnβ1 in HeLa, WHCO5 and KYSE30 cancer cells extracts (Figure 4.6C). An overlap of the pull-down data for all four cell lines revealed that 38 proteins were common binding partners of Kpnβ1 in the four cell lines (Figure 4.6D). This group of 38 binding partners of Kpnβ1 was viewed as having the highest probability of being true Kpnβ1 binding partners, as they were consistently co-immunoprecipitated with Kpnβ1 in all the cell lines. Amongst the identified common binding partners of Kpnβ1 in the four cell lines are proteins involved in spliceosome formation, RNA binding/processing, RNA metabolism, cleavage of newly synthesized pre-mRNA molecule, translation of mRNA transcripts and nuclear-cytoplasmic translocation of biomolecules. (See Table 4.1 for the list of the binding partners of Kpnβ1 which were common to the normal and cancer cell lines). Overlapping the lists of Kpnβ1 binding partners for the normal and cancer cell lines revealed that 18 proteins which were co-immunoprecipitated with Kpnβ1 were unique to the cancer cell lines (Figure 4.6D. See Table 4.2 for the list of the binding partners of Kpnβ1 which were unique to the cancer cell lines).

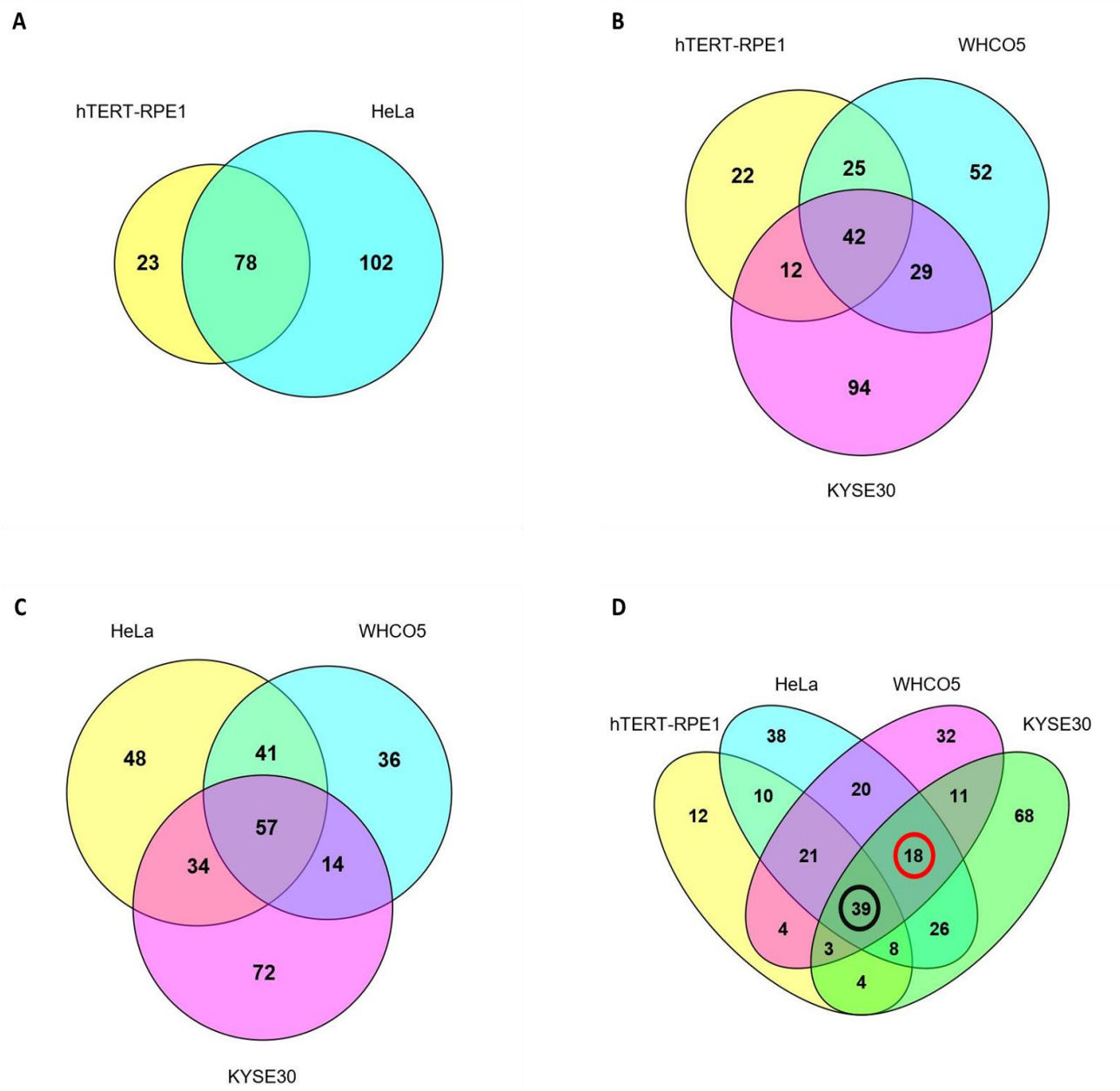

Figure 4.6. Venn diagrams of identified binding partners of Kpnβ1 in the IP-MS assays. The protein identifier numbers of the identified binding partners of Kpnβ1 were input into VennDis JavaFX-based Venn and Euler diagram generator[152] to generate Venn diagrams representing overlaps of the lists of binding partners of Kpnβ1 in: **A)** hTERT-RPE1 and HeLa cell lines **B)** hTERT-RPE1, WHCO5 and KYSE30 cell lines **C)** HeLa, WHCO5 and KYSE30 cell lines and **D)** hTERT-RPE1, HeLa, WHCO5 and KYSE30 cell lines. The number of Kpnβ1 binding partners that are common to the normal and cancer cell lines is in the black ring and the number of Kpnβ1 binding partners which are unique to the cancer cell lines is in the red ring.

Table 4.1. List of common protein hits identified by IP-MS in the Kpnβ1 co-IP experiments from human normal, cervical cancer and oesophageal cancer cells extracts

Group/pathway/ function	Protein IDs[a]	Protein name[b]	Gene name[c]	Molecular weight (kDa)[d]
Nuclear import	Q14974	Importin subunit beta-1	KPNB1	97.169
Spliceosomal component	J3QLE5	Small nuclear ribonucleoprotein-associated protein N	SNRPN	17.546
	P08621	U1 small nuclear ribonucleoprotein 70 kDa	SNRNP70	51.556
	P09012	U1 small nuclear ribonucleoprotein A	SNRPA	31.279
	P62316	Small nuclear ribonucleoprotein Sm D2	SNRPD2	13.527
	P62318	Small nuclear ribonucleoprotein Sm D3	SNRPD3	13.916
	Q13435	Splicing factor 3B subunit 2	SF3B2	100.23
	Q15637	Splicing factor 1	SF1	68.329
Heterogeneous nuclear ribonucleoproteins	A0A087WUK2	Heterogeneous nuclear ribonucleoprotein D-like	HNRNPDL	40.04
	A0A0A0MRA5	Heterogeneous nuclear ribonucleoprotein U-like protein 1	HNRNPUL1	85.939
	D6R9P3	Heterogeneous nuclear ribonucleoprotein A/B	HNRNPAB	30.302
	O43390	Heterogeneous nuclear ribonucleoprotein R	HNRNPR	70.942
	Q13151	Heterogeneous nuclear ribonucleoprotein A0	HNRNPA0	30.84
RNA binding/processing	B0QYK0	RNA-binding protein EWS	EWSR1	64.929
	P35637	RNA-binding protein FUS	FUS	53.425
	Q15717	ELAV-like protein 1	ELAVL1	36.091
	Q9Y224	UPF0568 protein C14orf166	C14orf166	28.068
RNA Helicases	A0A0D9SFB3	ATP-dependent RNA helicase DDX3X	DDX3X	70.839
	A0A1X7SBZ2	Probable ATP-dependent RNA helicase DDX17	DDX17	80.253
	P26196	Probable ATP-dependent RNA helicase DDX6	DDX6	54.416
	J3KTA4	Probable ATP-dependent RNA helicase DDX5	DDX5	69.086
Cleavage and polyadenylation	F8WJN3	Cleavage and polyadenylation specificity factor subunit 6	CPSF6	52.269
	Q05048	Cleavage stimulation factor subunit 1	CSTF1	48.357
	O43809	Cleavage and polyadenylation specificity factor subunit 5	NUDT21	26.227
Ribosomal proteins	M0R3D6	60S ribosomal protein L18a	RPL18A	16.714
	P62277	40S ribosomal protein S13	RPS13	17.222
	P62899	60S ribosomal protein L31	RPL31	14.463
NPC component	Q8N1F7	Nuclear pore complex protein Nup93	NUP93	93.487
	F5H365	Protein transport protein Sec23A	SEC23A	82.968
	P55735	Protein SEC13 homolog	SEC13	35.54
ssDNA binding/ stabilization	Q96I24	Far upstream element-binding protein 3	FUBP3	61.64
	P27694	Replication protein A 70 kDa DNA-binding subunit	RPA1	68.137
SWItch/Sucrose Non-Fermentable (SWI/SNF) component	Q8TAQ2	SWI/SNF complex subunit SMARCC2	SMARCC2	132.88
	O96019	Actin-like protein 6A	ACTL6A	47.46
Vesicle transport	Q92734	Protein TFG	TFG	43.447

Regulation of gene expression	A5YKK6	CCR4-NOT transcription complex subunit 1	CNOT1	266.94
Microtubule organization	P23258	Tubulin gamma-1 chain	TUBG1	51.169
Methylation of arginyl residues	Q86X55	Histone-arginine methyltransferase CARM1	CARM1	65.853
Regulation of circadian clock	Q8WXF1	Paraspeckle component 1	PSPC1	58.743

The definitions and parameters for each column are given in MaxQuant (version 1.5.4.1)
[a] Identifier(s) of major proteins possessing at least 50% of the peptides ascribed to a protein group.
[b] Name(s) of protein(s) contained within the protein group.
[c] Name(s) of the gene(s) associated to the proteins contained within the protein group.
[d] Total number of peptide sequences associated with all the proteins in the protein group. Only protein identifications made from at least 2 peptides were selected from the original data set.

Table 4.2. List of 18 common protein hits identified by IP-MS in the Kpnβ1 co-IP experiments unique to human cervical and oesophageal cancer cells extracts

Group/pathway/ function	Protein IDs[a]	Protein name[b]	Gene name[c]	Molecular weight (kDa)[d]
Nuclear transport	P62826	GTP-binding nuclear protein Ran	RAN	26.224
Ribosomal proteins	P18124	60S ribosomal protein L7	RPL7	29.225
	P62753	40S ribosomal protein S6	RPS6	28.68
	P27635	60S ribosomal protein L10	RPL10	18.565
	G3V203	60S ribosomal protein L18	RPL18	18.756
	P62701	40S ribosomal protein S4, X isoform	RPS4X	29.597
	M0QZC5	40S ribosomal protein S11	RPS11	13.997
	P40429	60S ribosomal protein L13A	RPL13A	23.577
Heterogeneous nuclear ribonucleoproteins	Q1KMD3	Heterogeneous nuclear ribonucleoprotein U-like protein 2	HNRNPUL2	84.69
	P31942	Heterogeneous nuclear ribonucleoprotein H3	HNRNPH3	36.926
RNA binding/processing	Q6UN15	Pre-mRNA 3-end-processing factor FIP1	FIP1L1	66.526
Cleavage and polyadenylation	Q8N684	Cleavage and polyadenylation specificity factor subunit 7	CPSF7	41.265
Spliceosomal component	J3KTL2	Serine/arginine-rich splicing factor 1	SRSF1	28.329
	A0A087X2D0	Serine/arginine-rich splicing factor 3	SRSF3	10.32
NPC component	P35658	Nuclear pore complex protein Nup214	NUP214	213.62
ssDNA binding/ stabilization	Q96AE4	Far upstream element-binding protein 1	FUBP1	67.56
Motor protein	F8W1R7	Myosin light polypeptide 6	MYL6	14.436
Regulation of cell growth	Q8IX12	Cell division cycle and apoptosis regulator protein 1	CCAR1	132.82

The definitions and parameters for each column are given in MaxQuant (version 1.5.4.1)
[a] Identifier(s) of major proteins possessing at least 50% of the peptides ascribed to a protein group.
[b] Name(s) of protein(s) contained within the protein group.
[c] Name(s) of the gene(s) associated to the proteins contained within the protein group.
[d] Total number of peptide sequences associated with all the proteins in the protein group. Only protein identifications made from at least 2 peptides were selected from the original data set.

4.2.3.2. STRING interaction networks for identified binding partners of Kpnβ1

Next, we sought to understand how the common binding partners of Kpnβ1 interact with Kpnβ1 in protein interaction networks. STRING protein-protein interaction mapping was used to generate Kpnβ1 binding partner networks. The protein identifier/accession numbers of Kpnβ1 and its binding partners were input into the STRING website (www.string-db.org)[153] and *Homo sapiens* was selected as the organism since the cell lines were of human origin. All active interaction sources – including database imports, high throughput experiments, conserved genomic neighbourhoods, gene fusion, gene co-occurrence, literature/text mining co-occurrence, co-expression and phylogenetic co-occurrence – were selected. The minimum required interaction score was set at 90% confidence level.

In STRING interaction network mapping, the interaction edges connecting the protein nodes indicate that the proteins share some functions and the colour(s) of the interaction edges indicate the interaction source(s). The number of proteins shown in the STRING interaction networks are fewer than the number of proteins in the Venn diagrams because 1) the STRING database does not contain every protein identifier/accession number obtained from the IP-MS data analysis using MaxQuant (version 1.5.4.1.), 2) the minimum required interaction score was set at the highest confidence level of 90% to get the highest confidence in the interactions. The STRING interaction networks for the binding partners of Kpnβ1 in individual hTERT-RPE1, HeLa, WHCO5 and KYSE30 cells extracts are shown in Appendix II, Figures A.1, A.2, A.3 and A.4 respectively.

To make a comparison between the binding partners of Kpnβ1 in normal and cancer cell lines, we generated two interaction networks using STRING. The first was the interaction network of Kpnβ1 with its binding partners that are common to the normal and cancer cell lines (Figure 4.7A). The second was the interaction network of Kpnβ1 with its binding partners that are

common to only the cancer cell lines (Figure 4.7B). Comparing the STRING interaction networks by applying a presence/absence approach, we identified 10 proteins that were co-immunoprecipitated as binding partners of Kpnβ1 in the cancer cell lines but were absent in the pull-down from the normal cell line. The 10 proteins included nucleoporin 214 (Nup214), Pre-mRNA 3'-end-processing factor FIP1 (FIP1L1), cell division cycle and apoptosis regulator 1 (CCAR1), cleavage and polyadenylation specific factor 7 (CPSF7), ribosomal protein L7 (RPL7), ribosomal protein L10 (RPL10), ribosomal protein L13A (RPL13A), ribosomal protein S6 (RPS6), ribosomal protein S4, X isoform (RPS4X) and Ras-related nuclear protein (Ran). Interestingly, 5 of these 10 Kpnβ1 binding partners are ribosomal proteins.

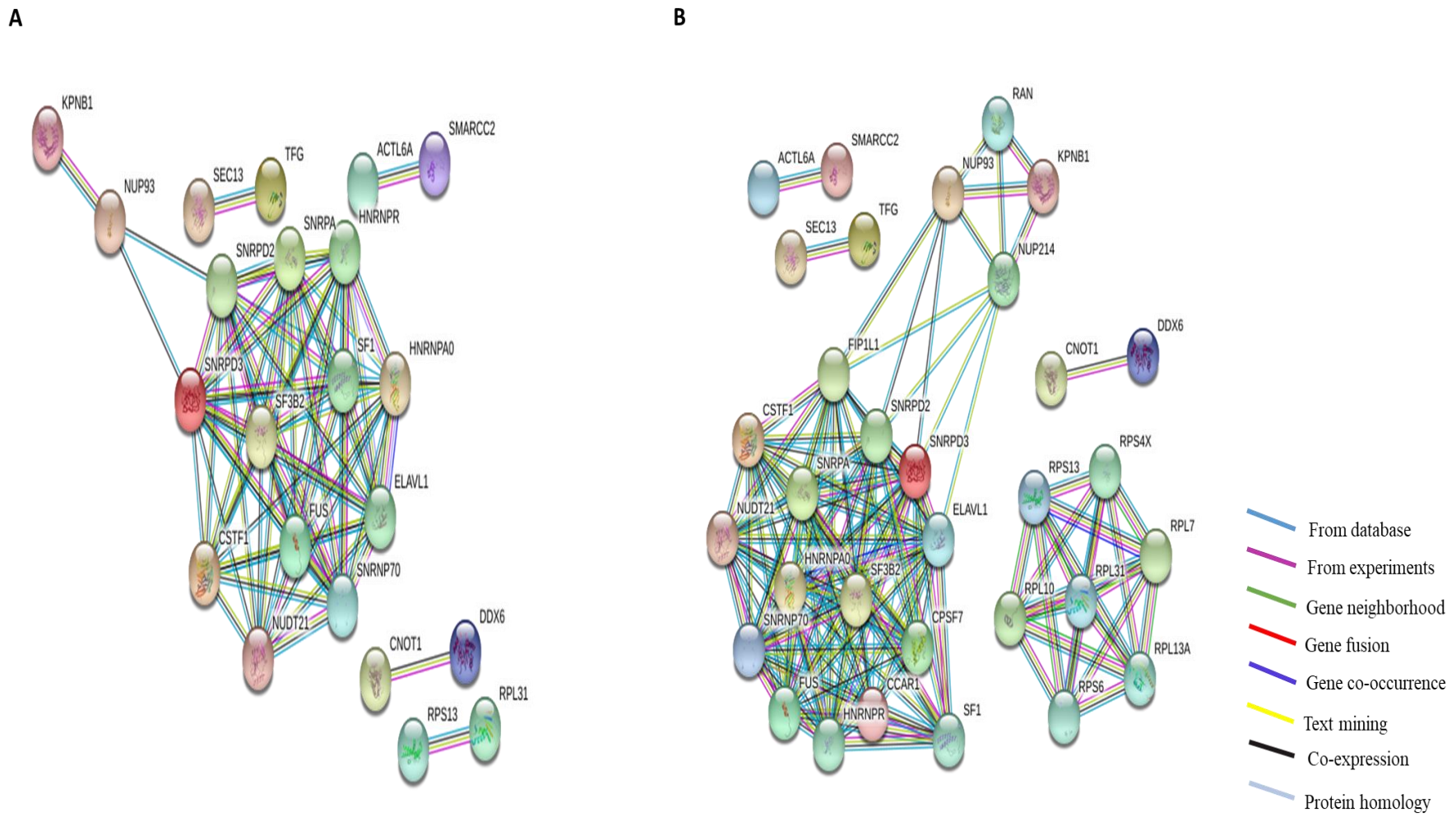

Figure 4.7. STRING protein-protein interaction mapping for the binding partners of Kpnβ1. The protein identifiers of the common binding partners of Kpnβ1 in: **A)** normal and cancer cells extracts and **B)** cancer cells extracts were input into www.string-db.org[153] and *Homo sapiens* was chosen as species. All active interaction sources were selected, and the minimum interaction score was set at 90% confidence level. The network edges do not necessarily imply a physical interaction between the proteins but that the associated proteins are responsible for a shared function.

To confirm the 10 proteins identified through the presence/absence approach and visualize how they interact with Kpnβ1, a STRING interaction network of Kpnβ1 and the 18 proteins identified in Figure 4.6D as Kpnβ1 binding partners which are unique to cancer cell lines was generated. The STRING interaction network confirmed the 10 proteins which were identified through the presence/absence approach and showed how they associated with Kpnβ1 (Figure 4.8). The reduction in the number of Kpnβ1 binding partners from 18 proteins in the Venn diagram (Figure 4.6D) to 10 proteins in the STRING interaction network (Figure 4.8) is because 1) the STRING database does not contain every protein identifier/accession number obtained from the IP-MS data analysis using MaxQuant (version 1.5.4.1.), 2) the minimum required interaction score was set at the highest confidence level of 90% to get the highest confidence in the interactions.

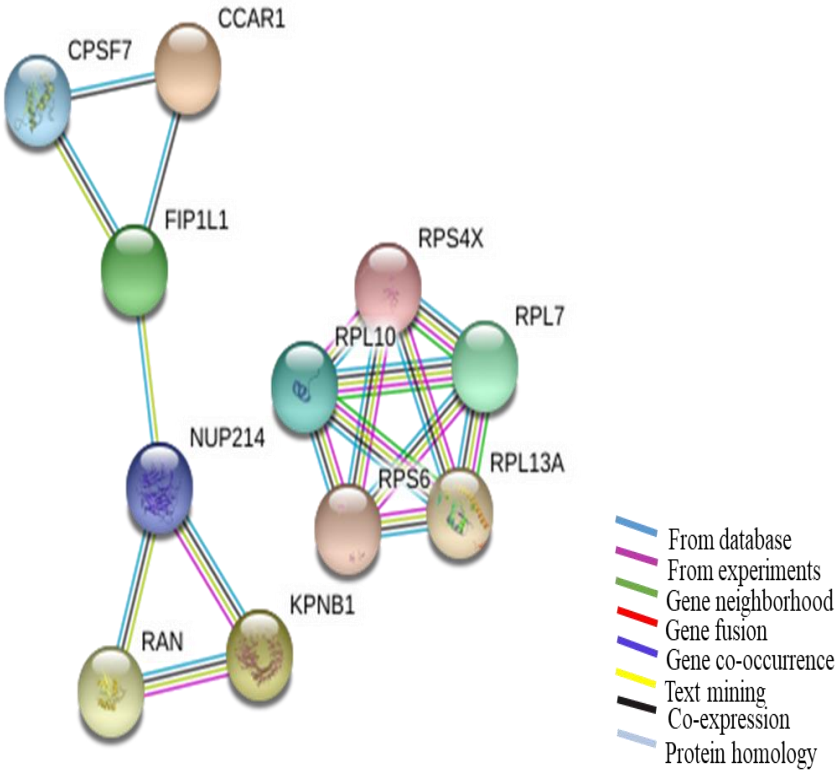

Figure 4.8. STRING protein-protein interaction mapping for the binding partners of Kpnβ1 unique to the cancer cell lines. The protein identifiers of the binding partners of Kpnβ1 unique to the cancer cell lines were input into www.string-db.org[153] and *Homo sapiens* was chosen as species. All active interaction sources were selected, and the minimum interaction score was set at 90% confidence level. The network edges do not necessarily imply a physical interaction between the proteins but that the associated proteins are responsible for a shared function.

4.3. Discussion

The use of IP-MS to identify the binding partners of a target protein is a very useful technique in cell biology in that it can reveal how a target protein interacts with other proteins and carryout shared functions as a complex. The technique has seen much improvements in the last decade and can identify ~70 to 600 binding partners in a single sample[197].

However, there are still some grey areas that need more improvements. For instance, it is difficult to strike a balance between co-immunoprecipitating low abundance proteins while also trying to minimize non-specific binding of some proteins to the beads. Applying very stringent lysis and wash steps minimize non-specific binding of proteins to the beads. But at the same time, can lead to loss of many low abundance proteins which are true binding partners[197,200]. In this study, we utilized a salt concentration of 120 millimolar (mM) in the wash buffer to maintain a balance between minimizing non-specific binding of proteins to the beads and the loss of low abundance binding proteins[197]. We avoided the use of ionic detergents because they could denature the protein extracts or even lead to loss of interactions between the target protein and its binding partners. Moreover, ionic detergents have been reported to interfere with MS experiments[201,202].

Kpnβ1 is a nuclear import protein responsible for the transport of cargo proteins and RNAs from the cytoplasm into the nucleus[82,85]. As a result, Kpnβ1 is expected to interact – directly or indirectly – with many other proteins. In this study, Kpnβ1 was successfully pulled down from hTERT-RPE1, HeLa, WHCO5 and KYSE30 cells extracts using an IP-WB technique. Then four members of the nuclear transport protein family (Kpnα2, Ran, CRM1 and IPO7) that have been previously described as potential interactors of Kpnβ1 were identified using co-IP[137]. We also co-immunoprecipitated NF-kB and c-Jun with Kpnβ1. NF-kB and c-Jun are cargo proteins for Kpnβ1 during its nuclear import function[174,177]. These co-immunoprecipitants of

Kpnβ1, especially c-Jun, were detected at higher levels in the cancer cells extracts with little to none detected in the normal cell extracts. There are studies which suggest that increased activities of NF-kB and c-Jun are associated with cancer cells proliferation and progression[203,204]. Hence, it was interesting to find that NF-kB and c-Jun were co-immunoprecipitated with Kpnβ1 in the cancer cell lines with little to none detected in the normal cell line.

We used IP-MS techniques to identify further potential binding partners of Kpnβ1 in normal and cancer cell lines. After careful removal of reverse hits, possible contaminants, protein groups that were only identified by one modification site, protein groups with Q-values greater than 0.01, protein groups with less than 2 unique peptides and all protein groups identified in the "IgG isotype" control samples, a list of protein hits was identified containing binding partners of Kpnβ1 in hTERT-RPE1, HeLa, WHCO5 and KYSE30 cells extracts. Our results showed that Kpnβ1 associated with more proteins in cancer cells than in normal cells, with 100 proteins in the normal cell line and between 147 and 179 in the cancer cell lines. A recent IP-MS study identified 272 proteins as potential binding partners of Kpnβ1 in synchronized mitotic HeLa cells[137]. 65 of the 272 proteins identified in that study were also co-immunoprecipitated with Kpnβ1 from the HeLa cell extracts in our study.

Our study had interest in Kpnβ1 binding partners in cancer cells of different tissue origins, including cervical and oesophageal cancer. Using the VennDis JavaFX-based Venn and Euler diagram software created by Ignatchenko *et al.*[152], 38 proteins were identified as common co-immunoprecipitants of Kpnβ1 in hTERT-RPE1, HeLa, WHCO5 and KYSE30 cells extracts. 56 proteins were consistently co-immunoprecipitated with Kpnβ1 in the cancer cells extracts. The difference in the number of proteins identified suggests that there are some proteins which were specifically co-immunoprecipitated with Kpnβ1 in the cancer cells extracts but not in

normal cells extracts. NF-kB and c-Jun were co-immunoprecipitated with Kpnβ1 using IP-WB but were not among the 18 proteins which were specifically co-immunoprecipitated with Kpnβ1 in the cancer cells extracts using IP-MS technique. This could be because of the stringent clean-up steps that the IP-MS data were subjected to. They include careful removal of reverse hits, possible contaminants, protein groups that were only identified by one modification site, protein groups with Q-values greater than 0.01, protein groups with less than 2 unique peptides and all protein groups identified in the "IgG isotype" control samples.

To properly understand how the cancer-specific binding partners of Kpnβ1 interact with Kpnβ1, STRING protein-protein interaction mapping was used to create interaction networks of Kpnβ1 and its common binding partners in all the cell lines and in only the cancer cell lines. With the minimum required interaction score set at 90% confidence level and all active interaction sources selected, we applied a presence/absence approach and identified 10 binding partners of Kpnβ1 which were enriched in the cancer cell lines compared to the normal cell line. These proteins were seen in the STRING interaction network for common proteins pulled down with Kpnβ1 in only the cancer cell lines but were absent in the STRING interaction network for the common proteins pulled down with Kpnβ1 in all the cell lines. They include Nup214, FIP1L1, CCAR1, CPSF7, RPL7, RPL10, RPL13A, RPS6, RPS4X and Ran. While it is possible that these proteins only bind Kpnβ1 when cells are in the cancer state, we propose that the presence of these proteins in the cancer only group could also be due to their 1) increased expression, 2) higher affinity binding to Kpnβ1, or 3) increased duration of interaction with Kpnβ1 in the cancer cell lines. Thus, their interaction with Kpnβ1 is enriched in the cancer cells, rather than not binding Kpnβ1 at all in the normal cells.

Our IP-MS and IP-WB data both showed that Ran was one of the binding partners of Kpnβ1 in the cancer cells extracts with little/none detected in the normal cell extracts. Ran is a small

Ras-like GTPase and a member of the RAS oncogene superfamily[102]. Ran has been previously reported to provide the energy required by nuclear import proteins, like Kpnβ1, to carry out the facilitated nuclear import of cargo proteins[205–208]. Results from the previous chapter in this study revealed that Ran is overexpressed in actively proliferating cells and present at an elevated level in the extracellular microenvironment of cervical and oesophageal cancer cells. There is evidence to show that Ran is also overexpressed in prostate adenocarcinoma, β-lymphoblastoid, breast adenocarcinoma, colon adenocarcinoma and cervical carcinoma[189]. This could probably be because the cells have been transformed from normal to actively proliferating cells; and therefore, require more Ran to supply the energy needed to carry out some enhanced cellular/biological functions. These findings also suggest that the rate of nuclear-cytoplasmic transport of cargo proteins could be higher in cancer cells than in normal cells. Hence, Ran, which forms a complex with Kpnβ1 during nuclear import of cargo proteins was co-immunoprecipitated with Kpnβ1 in cancer cell extracts as revealed by the IP-MS and IP-WB data. Ran has also been reported to perform an important role in mitosis which is regulated by Kpnβ1. Nachury *et al.* (2001) reported that the organization and stabilization of microtubules during mitotic assembly is achieved by an inhibitory effect of the interaction of Kpnβ1 with Ran[132].

Nup214 is another interesting binding partner of Kpnβ1 identified in cancer cells extracts with little or none co-immunoprecipitated in normal cell extracts. Nup214 is of interest because it plays a very important role in nuclear-cytoplasmic trafficking of cargo proteins in cells. Nup214 is one of the major FG-repeat-containing Nups that form the NPC in eukaryotic cells[100,101]. Nup214 has been implicated as an important protein in nuclear import and export processes[209,210]. It contributes to nuclear-cytoplasmic transport of cargo proteins by serving as a docking site for nuclear import substrates. It has been shown through crystal structure evidence that Nup214 FxFG repeats (where x represents a small amino acid with a polar side

chain) bind to Kpnβ1 to form a complex which is essential in the nuclear trafficking of transcription factors like Smad2[209,211]. Apart from its important role in nuclear-cytoplasmic shuttling of transcription factors like Smad2, Nup214 could form a complex with Nup88 and is very essential in CRM1-dependent nuclear export of cargo proteins possessing NES[210].

Apart from Ran and Nup214 which were specifically co-immunoprecipitated with Kpnβ1 in the cancer cells extracts, proteins which are not directly involved in nuclear-cytoplasmic trafficking were also identified. They are CCAR1, CPSF7, FIP1L1, RPL7, RPL10, RPL13A, RPS6, RPS4X.

CCAR1 protein, also known as cell cycle- and apoptosis-regulatory protein-1 (CARP-1) is a perinuclear phosphoprotein which has biphasic roles in the regulation of apoptosis and cell growth[212]. In its role as a promoter of apoptosis, CCAR1 promotes apoptosis by activating p38 mitogen-activated protein kinase (MAPK) and caspase-9[213]. In cells treated with epidermal growth factor (EGF) receptor-related protein (ERRP), the level of CCAR1 in the cells was elevated; and associates with activation of intrinsic apoptosis[213]. In a different study, Kim *et al.* (2008) reported that CCAR1, in conjunction with coiled-coil co-activator (CoCoA), regulates the growth of cells by acting as a co-activator of tumour suppressor gene p53[212], thereby ensuring that cells with damaged DNA undergo apoptosis. Our study is the first to report that CCAR1 interacts with Kpnβ1. Its role with Kpnβ1 in apoptosis is yet to be explored.

Other proteins of interest co-immunoprecipitated with Kpnβ1 in all cancer cells extracts include CPSF7 and FIP1L1. These proteins have an essential role in the processing of precursor mRNA (pre-mRNA) during protein synthesis. CPSF7, also known as Cleavage factor Im (CFIm) 59, is a subunit of the CFIm heterotetrameric complex. It forms a tetrameric complex with a dimer of CFIm28 (also known as CPSF5 or NUDT21) and a monomer of CFIm68 (also referred to as CPSF6). Collectively, they play an essential role in pre-mRNA 3'-processing

through cleavage and polyadenylation reactions[214]. During the transcriptional process of converting most primary pre-mRNA transcripts into matured mRNA, the complex promotes the cleavage of the 3' untranslated region (UTR) of the pre-mRNA transcripts by binding preferentially to a UGUA motif on the pre-mRNA transcripts[215], followed immediately by polyadenylation of the pre-mRNA transcripts[216,217]. Although the characterization of the factors involved in pre-mRNA cleavage and polyadenylation have been successfully achieved, it will be interesting to further explore the mechanisms through which each factor contributes to the cleavage and polyadenylation process. The 3'-processing of pre-mRNAs to matured mRNAs is a very important process because it makes the mRNA more stable by preventing the degradation of mRNAs from the 3'-ends. It also promotes the nuclear export of mRNAs and improves the translational process in the cytoplasm[218–220].

FIP1L1 was another co-immunoprecipitant of Kpnβ1 identified specifically in all the cancer cells extracts. FIP1L1 is one of the two subunits of CPSF involved in RNA binding and it possesses an arginine-rich C-terminal domain which selectively binds to poly(U) sequences on RNAs[221]. As an integral part of the CPSF complex, FIP1L1 plays an essential role in pre-mRNA 3'-end formation. During this process, CPSF recognizes an AAUAAA sequence on the RNA, then interacts with poly(A) polymerase and some other factors to stimulate cleavage and polyadenylation of the pre-mRNA transcripts[219]. As no study has previously reported CCAR1, CPSF7 and FIP1L1 as binding partners of Kpnβ1, it will be interesting to investigate – using other biochemical assays – the functions which Kpnβ1 shares with these proteins or whether they are nuclear import cargoes of Kpnβ1.

A group of 5 ribosomal proteins were identified as co-immunoprecipitants of Kpnβ1 in the cancer cells extracts. They include RPL7, RPL10, RPL13A RPS6, RPS4X. Ribosomal proteins play important roles in ribosome assembly and in ensuring the stability of ribosomal

ribonucleic acid (rRNA) structure in the ribosome, thus promoting efficient protein synthesis[222]. To perform this basic function, ribosomal proteins – which are synthesized in the cytoplasm – must be transported into the nucleus. There are reports which suggest that Kpnβ1 and other nuclear transport proteins are responsible for the nuclear import of ribosomal proteins and that Ran protein is required by the nuclear import receptors during the facilitated nuclear import of ribosomal proteins[85,100]. These reports further strengthen our identification of Ran and ribosomal proteins as binding partners of Kpnβ1. Identifying this group of ribosomal proteins with Ran protein as co-immunoprecipitants of Kpnβ1 in cancer cells suggests that there may be elevated protein synthesis in cancer cells compared to normal cells[223,224]. This is supported by the elevated levels of multiple proteins in cancer cells.

In conclusion, this study identified potential binding partners of Kpnβ1 in normal and cancer cell lines. Comparing the identified binding partners of Kpnβ1 in normal and cancer cell lines using Venn diagrams and STRING interaction network mapping revealed 10 proteins as binding partners of Kpnβ1 which were enriched in the cancer cell lines compared to the normal cell line. These proteins can be investigated further as potential anti-cancer therapeutic targets or biomarkers. Lastly, this study identified CCAR1, FIP1L1 and CPSF7 as proteins that have not been previously reported to interact with Kpnβ1. To the best of our knowledge, this study is the first to investigate and compare the binding partners of Kpnβ1 in normal, cervical cancer and oesophageal cancer cell lines.

4.4. Summary of key findings

- 50 μg of Anti-Karyopherin β1 (H-7) AC agarose conjugated antibody was used to pull-down Kpnβ1 from 500 μg of whole cell extracts.
- IP-WB experiments revealed that more Kpnβ1 was pulled down from the cancer cells extracts than the normal cell extracts. This was reflected in the levels of Kpnα2, Ran,

CRM1, IPO7, NF-kB and c-Jun co-immunoprecipitated with Kpnβ1 in the cancer and normal cells extracts.

- IP-MS revealed that more proteins were co-immunoprecipitated with Kpnβ1 in cancer cells extracts than in the normal cell extracts. 100, 179, 147 and 176 proteins were identified as potential binding partners of Kpnβ1 in hTERT-RPE1, HeLa, WHCO5 and KYSE30 cells extracts, respectively.
- Venn diagram overlap of Kpnβ1 binding partners revealed 77 proteins as common binding partners of Kpnβ1 in hTERT-RPE1 and HeLa cell lines. 41 proteins were identified as common binding partners of Kpnβ1 in hTERT-RPE1, WHCO5 and KYSE30 cell lines. 56 proteins were common binding partners of Kpnβ1 in HeLa, WHCO5 and KYSE30 cells extracts. 38 proteins were common binding partners of Kpnβ1 in all the four cell lines. 18 binding partners of Kpnβ1 were unique to the cancer cell lines.
- The 38 proteins which were consistently co-immunoprecipitated with Kpnβ1 in all the cell lines gave the highest confidence as potential binding partners of Kpnβ1.
- STRING interaction network mapping revealed 10 binding partners of Kpnβ1 which were enriched in the cancer cell lines compared to the normal cell line. They include Nup214, FIP1L1, CCAR1, CPSF7, RPL7, RPL10, RPL13A RPS6, RPS4X and Ran. Among these, FIP1L1, CCAR1 and CPSF7 have not been previously described as binding partners of Kpnβ1.

CHAPTER 5

CONCLUSION

Cervical and oesophageal cancers are mostly diagnosed in their late stages, thereby reducing the patient's chance of responding positively to chemotherapy. In this study, we set out to identify protein biomarkers which may in future assist with the diagnosis of cervical and oesophageal cancers.

With the use of microarray technologies, our group previously reported that members of the nuclear transport protein family (Kpnβ1, CRM1 and Kpnα2) were upregulated at the mRNA and protein levels in cervical cancer biopsies compared to normal cervix tissues[80]. The members of this protein family have been reported to be secreted into the extracellular microenvironment by cancer cells[192]. A study performed in our laboratory using MS analysis of the secretomes of normal, transformed and cancer cells showed that there was a general increase in the abundance of 13 members of the nuclear transport protein family from normal to transformed to cancer cell lines (A. Wishart, MSc dissertation, 2017[§§]). We, therefore, hypothesized that these nuclear transport proteins may be elevated in the extracellular microenvironment of cancer cells and in cancer patient material. Thus, they may be measurable in body fluids for the detection of cervical and oesophageal cancers.

The focus of this study was to validate MS data obtained using cancer cell lines by 1) measuring nuclear transport protein levels in the secretomes of cancer cell lines by WB analysis and 2) measuring nuclear transport protein levels in cervical and oesophageal cancer patient serum

[§§] A Wishart. "Investigating secreted biomarkers for cancer: the potential of the nuclear transport proteins." University of Cape Town, 2017.

samples. In addition, we identified the binding partners of Kpnβ1 in normal and cancer cell lines.

WB analysis of intracellular proteins from normal, transformed, cervical cancer and oesophageal cancer cell lines revealed that the nuclear transport proteins (Kpnβ1, IPO5, IPO7, TNPO1, CRM1, CAS, Kpnα2 and Ran) were expressed by all the cell lines, albeit, at differential levels. However, WB analysis of the normal, transformed, cervical cancer and oesophageal cancer cells secretomes revealed that all the 8 nuclear transport proteins investigated were elevated in the secretomes of the transformed and cancer cell lines compared to the normal cell line. These *in vitro* results were validated in an *ex vivo* ELISA analysis of patient serum samples. Kpnβ1, CRM1 and CAS were elevated in cervical and oesophageal cancer patients while Kpnα2 was elevated in only oesophageal cancer patients. To ascertain the efficacy of Kpnβ1, CRM1 and CAS for the early detection of cervical cancer, a control versus early-stage comparison was made. Our data showed that the levels of Kpnβ1, CRM1 and CAS were elevated in early-stage cervical cancer patient serum samples compared to the non-cancer control subjects. The unavailability of cancer stage information for approximately half of the oesophageal cancer cases meant we could not do a control versus early-stage comparison for the oesophageal cancer cases.

Having seen that these nuclear transport proteins possess some diagnostic potential, we then tested their abilities to minimize false-positive and false-negative results by carrying out some logistics regression analyses. In this study, CAS was the best performing individual candidate biomarker in discriminating between cervical cancer cases and non-cancer controls. It had the highest AUC (0.85±0.03) and highest sensitivity (55%) at 95% specificity. A cut-off concentration >0.67 ng/ml was obtained for CAS as an individual diagnostic marker for cervical cancer by evaluating the Youden's index (J) for each patient's CAS serum

concentration. An improved AUC of 0.89 and 100% sensitivity at 60% specificity were attained when CAS was combined with Kpnβ1, CRM1, and Kpnα2.

For oesophageal cancer cases, CAS (AUC=0.86±0.03 with 56% sensitivity at 95% specificity) outperformed other candidate biomarkers as an individual biomarker in discriminating between oesophageal cancer cases and non-cancer controls. The cut-off concentration of CAS as a diagnostic biomarker for oesophageal cancer was >0.46 ng/ml. A combination of Kpnβ1, CRM1, Kpnα2 and CAS displayed the highest diagnostic capacity for oesophageal cancer with a combined AUC of 0.90 and 84% sensitivity at 86% specificity. These results suggest that some members of the nuclear transport protein family are potential diagnostic biomarkers for cervical and oesophageal cancers with a combination of Kpnβ1, CRM1, Kpnα2 and CAS being the best multiple candidate biomarkers.

Kpnβ1 is known to be involved in several biological/cellular processes among which are the nuclear import of cargo proteins[103], negative regulation of spindle assembly during mitosis[130–133], regulation of actin cytoskeleton[134], ER-associated degradation of misfolded proteins[135], permeability of NPCs[136], and restructuring of the nuclear envelope and NPCs[138,139]. These functions attributed to Kpnβ1 suggest that it has multiple binding partners.

To explore the protein-protein interactions of Kpnβ1, we used IP-MS technology to identify the binding partners of Kpnβ1 in normal and cancer cells extracts. This study revealed that Kpnβ1 interacted with more proteins in cancer cells than in normal cells. To compare Kpnβ1 binding partners identified in cancer cells to those in normal cells, VennDis JavaFX-based Venn and Euler diagram software created by Ignatchenko *et al.*[152] was used to generate different Venn diagrams. 56 proteins were identified as common binding partners of Kpnβ1 in the three cancer cell lines while 38 proteins were identified as common interactors of Kpnβ1 in the normal and cancer cell lines. With the minimum required interaction score set at 90%

confidence level and all active interaction sources selected, the STRING protein-protein interaction mapping identified 10 co-immunoprecipitants of Kpnβ1 which interacted with Kpnβ1 in the cancer cell lines but were not detected as Kpnβ1 binding partners in the normal cell line. They include Nup214, FIP1L1, CCAR1, CPSF7, RPL7, RPL10, RPL13A, RPS6, RPS4X and Ran.

Previous studies have described how the FxFG repeats of Nup214 bind to Kpnβ1 to form a complex which is essential in the nuclear-cytoplasmic shuttling of cargo proteins[209,211]. The energy required for the facilitated nuclear import of cargo proteins by Kpnβ1 is provided by Ran[205–208], and ribosomal proteins are among the numerous proteins transported into the nucleus by Kpnβ1[85,100]. CPSF7 and FIP1L1 are involved in the processing of pre-mRNA transcripts during protein synthesis[215–217,219], while CCAR1 functions as a co-activator of p53 and activates p38 MAPK and caspase-9 to promote apoptosis[212,213]. The role which Kpnβ1 plays with CPSF7, FIP1L1 and CCAR1 in their respective biological/cellular functions is yet to be determined. We, therefore, report that CPSF7, FIP1L1 and CCAR1 are novel binding partners of Kpnβ1 as they have not been previously reported to interact with Kpnβ1. They should be investigated further to understand fully the roles they play with Kpnβ1 in mediating cancer biology and their potential as anti-cancer therapeutic targets and cancer biomarkers.

Conclusively, the elevated levels of nuclear transport proteins in the cancer cells secretomes and in cancer patient serum suggest that members of the nuclear transport protein family have potential as biomarkers for cervical and oesophageal cancers, with a combination of Kpnβ1, CRM1, Kpnα2 and CAS being the strongest predictor. Also, Kpnβ1 interacts with more proteins in cancer cells than normal cells. As a result, we identified 10 binding partners of Kpnβ1 which were specifically enriched in the cancer cell lines and could be potential anti-cancer therapeutic targets and biomarkers.

5.1. Limitations and future perspectives

There were a few challenges that this research project was faced with – especially with regards to investigating nuclear transport proteins as potential biomarkers for cervical and oesophageal cancers. It must be stated here that *in vitro* cell culture models used in most studies are not a perfect representation of what is obtainable *in vivo* in a living organism[64]. In this study, cells were serum-starved for 24 hours and the possibility that the cell secretome could have been contaminated with autolysed cells cannot be completely ruled out. Although, as a control measure, we used β-tubulin to monitor cytosolic contamination of the cell secretome[74]. Another challenge with studies involving secreted proteins in conditioned media is the very low concentration of proteins secreted by cells into the conditioned media. The conditioned media can be subjected to step-wise centrifugation using commercially available ultra-centrifugal filter units to concentrate the secreted proteins. These ultra-centrifugal units have designated molecular weight cut-offs and could lead to a partial loss of secreted proteins during centrifugation, as well as loss of the proteins with low molecular weight under the cut-off.

During the *ex vivo* analysis of patient serum samples, it was imperative to prepare dilutions of the serum samples. As a result, the frozen serum samples were thawed, and this could have led to protein degradation, thereby affecting the integrity of the potential biomarkers in the serum samples[225]. We could only strive to reduce the freeze-thaw cycles of the serum samples to a maximum of 2 cycles since it was practically impossible to assay the serum samples immediately after they were obtained from the patients.

We set out at the beginning of this study to first analyse the samples made available to us before requesting for the demographic and clinicopathological information of the non-cancer subjects and cancer patients. This was to ensure that we eliminated all forms of bias in the study. The unavailability of some patient information meant we could not perform non-cancer control

versus oesophageal cancer case comparisons based on cancer stage. Out of the 73 oesophageal cancer cases tested in this study, 32 cases were recorded as “not staged" in the database, with only 1 case recorded as early-stage oesophageal cancer and 40 cases designated as late-stage oesophageal cancer cases. Therefore, we could not perform a control versus early-stage or an early-stage versus late-stage comparison for oesophageal cancer cases.

To validate our findings on nuclear transport proteins as biomarkers for cervical and oesophageal cancers, it will be important to repeat this study using a validation set of serum samples from a different group of cervical and oesophageal cancer patients. In addition, serum samples from non-cancer subjects suffering from cervicitis and oesophagitis should be assayed for the level of Kpnβ1, CRM1, Kpnα2 and CAS using ELISA. Then a comparison could be made with serum samples from healthy subjects to ascertain if the elevated level of Kpnβ1, CRM1, Kpnα2 and CAS in cancer patients was due to inflammation or because of the cancer state.

As a result of time constraints, we could not perform IP-WB experiments to validate the co-IP results of the binding partners of Kpnβ1 – CPSF7, FIP1L1 and CCAR1 – which are yet to be reported in the literature. We, therefore, recommend that future work on this study should seek to validate CPSF7, FIP1L1 and CCAR1 as binding partners of Kpnβ1.

References

1. World Health Organization. http://www.who.int/topics/cancer/en/. (2017). Available at: http://www.who.int/topics/cancer/en/.

2. Sener, S. F. & Grey, N. The global burden of cancer. *J. Surg. Oncol.* **92,** 1–3 (2005).

3. Kumar, M. & Sarin, S. K. Biomarkers of diseases in medicine. *Current Trends in Science* **15,** 403–4017 (2010).

4. Ferlay, J. *et al.* Cancer incidence and mortality worldwide: Sources, methods and major patterns in GLOBOCAN 2012. *Int. J. Cancer* **136,** E359–E386 (2015).

5. Moten, A., Schafer, D., Farmer, P., Kim, J. & Ferrari, M. Redefining global health priorities: Improving cancer care in developing settings. *J. Glob. Health* **4,** 1–5 (2014).

6. Bray, F., Jemal, A., Grey, N., Ferlay, J. & Forman, D. Global cancer transitions according to the Human Development Index (2008-2030): A population-based study. *Lancet Oncol.* **13,** 790–801 (2012).

7. World Health Organization. *National Cancer Control Programmes: Policies and managerial guidelines. Health (San Francisco)* **1,** (2002).

8. Fitzmaurice, C. *et al.* Global, regional, and national cancer incidence, mortality, years of life lost, years lived with disability, and disability-adjusted life-years for 32 cancer groups, 1990 to 2015: A Systematic Analysis for the Global Burden of Disease Study Global Burden . *JAMA Oncol.* **3,** 524–548 (2017).

9. The American Cancer Society. What is cervical cancer? (2016). Available at: http://www.cancer.org/cancer/cervicalcancer/detailedguide/cervical-cancer-what-is-cervical-cancer.

10. Jefferies, H. Cervical cancer 1: an overview of screening and diagnosis. *Nurs. Times* **104,** 26–27 (2008).

11. Bruni L, Barrionuevo-Rosas L, Albero G, Serrano B, Mena M, Gómez D, Muñoz J, Bosch FX, de S. S. *Human Papillomavirus Related Diseases in South Africa*. (ICO Information Centre on HPV and Cancer (HPV Information Centre), 2017).

12. Muñoz, N., Castellsagué, X., de González, A. B. & Gissmann, L. Chapter 1: HPV in the etiology of human cancer. *Vaccine* **24,** S3/1-S3/10 (2006).

13. Walboomers, J. M. M. *et al.* Human papillomavirus is a necessary cause of invasive cervical cancer worldwide. *J. Pathol.* **189,** 12–19 (1999).

14. Goldie, S. J. *et al.* Projected Clinical Benefits and Cost-effectiveness of a Human Papillomavirus 16/18 Vaccine. *JNCI J. Natl. Cancer Inst.* **96,** 604–615 (2004).

15. Torre, L. A. *et al.* Global Cancer Statistics, 2012. *CA A Cancer J. Clin.* **65,** 87–108 (2015).

16. Duraisamy, K., Jaganathan, K. S. & Bose, J. C. Methods of Detecting Cervical Cancer. *Adv. Biol. Res. (Rennes).* **5,** 226–232 (2011).

17. Key, C. & Meisner, A. L. W. Cancers of the esophagus, stomach, and small intestine. in *Cancer Survival Among Adults: U.S. SEER Program, 1988-2001 Patient and Tumor Characteristics* (eds. Ries, L. A. G. et al.) 23–32 (2006).

18. Kachala, R. Systematic review: epidemiology of oesophageal cancer in Sub-Saharan Africa. *Malawi Med. J.* **22,** 65–70 (2010).

19. Demeester, S. R. Epidemiology and biology of esophageal cancer. *Gastrointest. Cancer Res.* **3,** S2-5 (2009).

20. Simard, E. P., Ward, E. M., Siegel, R. & Jemal, A. Cancers with increasing incidence trends in the United States: 1999 through 2008. *CA. Cancer J. Clin.* **62,** 118–128 (2012).

21. Nasrollahzadeh, D. *et al.* Opium, tobacco, and alcohol use in relation to oesophageal squamous cell carcinoma in a high-risk area of Iran. *Br. J. Cancer* **98,** 1857–1863 (2008).

22. Delima, S. L., McBride, R. K., Preshaw, P. M., Heasman, P. A. & Kumar, P. S. Response of subgingival bacteria to smoking cessation. *J. Clin. Microbiol.* **48,** 2344–2349 (2010).

23. Toh, Y. *et al.* Alcohol drinking, cigarette smoking, and the development of squamous cell carcinoma of the esophagus: Molecular mechanisms of carcinogenesis. *Int. J. Clin. Oncol.* **15,** 135–144 (2010).

24. Pacella-Norman, R. *et al.* Risk factors for oesophageal, lung, oral and laryngeal cancers in black South Africans. *Br. J. Cancer* **86,** 1751–1756 (2002).

25. Layke, J. C. & Lopez, P. P. Esophageal cancer: A review and update. *Am. Fam. Physician* **73,** 2187–2194 (2006).

26. Leeuwenburgh, I. *et al.* Long-term esophageal cancer risk in patients with primary achalasia: A prospective study. *Am. J. Gastroenterol.* **105,** 2144–2149 (2010).

27. Messmann, H. Squamous cell cancer of the oesophagus. *Best Pract. Res. Clin. Gastroenterol.* **15,** 249–265 (2001).

28. Cancer Council Australia. *Understanding Stomach and Oesophageal Cancer*. (SOS Print + Media Group, 2017).

29. National Cancer Institute. NCI Dictionary of Cancer Terms. (2011). Available at: https://www.cancer.gov/publications/dictionaries/cancer-terms/def/biomarker.

30. Kulasingam, V. & Diamandis, E. P. Strategies for discovering novel cancer biomarkers through utilization of emerging technologies. *Nat. Clin. Pract. Oncol.* **5,** 588–599 (2008).

31. Solier, C. & Langen, H. Antibody-based proteomics and biomarker research-current

status and limitations. *Proteomics* **14,** 774–783 (2014).

32. Hanash, S. M., Pitteri, S. J. & Faca, V. M. Mining the plasma proteome for cancer biomarkers. *Nature* **452,** 571–579 (2008).

33. Berrade, L., Garcia, A. E. & Camarero, J. A. Protein microarrays: Novel developments and applications. *Pharm. Res.* **28,** 1480–1499 (2011).

34. Frank, R. & Hargreaves, R. Clinical biomarkers in drug discovery and development. *Nat. Rev. Drug Discov.* **2,** 566–580 (2003).

35. Rifai, N., Gillette, M. A. & Carr, S. A. Protein biomarker discovery and validation: The long and uncertain path to clinical utility. *Nat. Biotechnol.* **24,** 971–983 (2006).

36. Fathi, E., Mesbah-Namin, S. A. & Farahzadi, R. Biomarkers in Medicine: An overview. *Br. J. Med. Med. Res.* **4,** 1701–1718 (2014).

37. Schaaij-Visser, T. B. M., De Wit, M., Lam, S. W. & Jimenez, C. R. The cancer secretome, current status and opportunities in the lung, breast and colorectal cancer context. *Biochim. Biophys. Acta - Proteins Proteomics* **1834,** 2242–2258 (2013).

38. Omenn, G. S. *et al.* Overview of the HUPO Plasma Proteome Project: Results from the pilot phase with 35 collaborating laboratories and multiple analytical groups, generating a core dataset of 3020 proteins and a publicly-available database. *Proteomics* **5,** 3226–3245 (2005).

39. Zhang, H. *et al.* Mass spectrometric detection of tissue proteins in plasma. *Mol Cell Proteomics* **6,** 64–71 (2007).

40. Tambor, V. *et al.* Application of proteomics in biomarker discovery: A primer for the clinician. *Physiol. Res.* **59,** 471–497 (2010).

41. Galasko, D. & Golde, T. E. Biomarkers for Alzheimer's disease in plasma, serum and blood - conceptual and practical problems. *Alzheimers. Res. Ther.* **5,** 10 (2013).

42. Goldknopf, Essam Sheta, Jennifer Bryson, Brian Folsom, Chris Wilson, Jeff Duty, A. Y. and S. A. Blood serum biomarkers for differential diagnosis of Parkinson's Disease. *Faseb J.* **20,** A64–A64 (2006).

43. Allen, R. E., Rogozinska, E., Cleverly, K., Aquilina, J. & Thangaratinam, S. Abnormal blood biomarkers in early pregnancy are associated with preeclampsia: A meta-analysis. *Eur. J. Obstet. Gynecol. Reprod. Biol.* **182,** 194–201 (2014).

44. Jesneck, J. L. *et al.* Do serum biomarkers really measure breast cancer? *BMC Cancer* **9,** 164 (2009).

45. Schalken, J. A. Clinical use of novel urine and blood based prostate cancer biomarkers: a review. *Clin. Biochem.* **47,** 889–896 (2014).

46. Füzéry, A. K., Levin, J., Chan, M. M. & Chan, D. W. Translation of proteomic biomarkers into FDA approved cancer diagnostics: Issues and challenges. *Clin. Proteomics* **10,** 1 (2013).

47. Lodish H, Berk A, Zipursky SL, E. A. *Overview of the Secretory Pathway*. *Molecular Cell Biology.* (W. H. Freeman & co., 2000).

48. Nickel, W. The mystery of nonclassical protein secretion: A current view on cargo proteins and potential export routes. *Eur. J. Biochem.* **270,** 2109–2119 (2003).

49. Mathivanan, S., Fahner, C. J., Reid, G. E. & Simpson, R. J. ExoCarta 2012: Database of exosomal proteins, RNA and lipids. *Nucleic Acids Res.* **40,** 1241–1244 (2012).

50. Skog, J. *et al.* Glioblastoma microvesicles transport RNA and protein that promote tumor growth and provide diagnostic biomarkers. *Nat. Cell Biol.* **10,** 1470–1476 (2008).

51. Rabinowits, G., Gerçel-Taylor, C., Day, J. M., Taylor, D. D. & Kloecker, G. H. Exosomal microRNA: A diagnostic marker for lung cancer. *Clin. Lung Cancer* **10,** 42–46 (2009).

52. Ge, R., Tan, E., Sharghi-Namini, S. & Asada, H. H. Exosomes in cancer microenvironment and beyond: Have we overlooked these extracellular messengers? *Cancer Microenviron.* **5,** 323–332 (2012).

53. Pant, S., Hilton, H. & Burczynski, M. E. The multifaceted exosome: Biogenesis, role in normal and aberrant cellular function, and frontiers for pharmacological and biomarker opportunities. *Biochem. Pharmacol.* **83,** 1484–1494 (2012).

54. Kharaziha, P., Ceder, S., Li, Q. & Panaretakis, T. Tumor cell-derived exosomes: A message in a bottle. *Biochim. Biophys. Acta - Rev. Cancer* **1826,** 103–111 (2012).

55. Mathivananlab. http://mathivananlab.org/images/Protein_Secretion.png. Available at: http://mathivananlab.org/images/Protein_Secretion.png.

56. Pavlou, M. P. & Diamandis, E. P. The cancer cell secretome: A good source for discovering biomarkers? *J. Proteomics* **73,** 1896–1906 (2010).

57. Volmer, M. W. *et al.* Differential proteome analysis of conditioned media to detect Smad4 regulated secreted biomarkers in colon cancer. *Proteomics* **5,** 2587–2601 (2005).

58. Tjalsma, H., Bolhuis, A., Jongbloed, J. D. H. & Dijl, J. M. Van. Signal Peptide-Dependent Protein Transport in Bacillus subtilis : a Genome-Based Survey of the Secretome. *Microbiol. Mol. Biol. Rev.* **64,** 515–547 (2000).

59. Eichelbaum, K., Winter, M., Diaz, M. B., Herzig, S. & Krijgsveld, J. Selective enrichment of newly synthesized proteins for quantitative secretome analysis. *Nat. Biotechnol.* **30,** 984–990 (2012).

60. Stastna, M. & Van Eyk, J. E. Secreted proteins as a fundamental source for biomarker discovery. *Proteomics* **12,** 722–735 (2012).

61. Doroudgar, S. & Glembotski, C. C. The cardiokine story unfolds: Ischemic stress-induced protein secretion in the heart. *Trends Mol. Med.* **17,** 207–214 (2011).

62. Diamandis, E. P. How are we going to discover new cancer biomarkers? A proteomic approach for bladder cancer. *Clin. Chem.* **50,** 793–795 (2004).

63. Xue, H., Lu, B. & Lai, M. The cancer secretome: a reservoir of biomarkers. *J. Transl. Med.* **6,** 52 (2008).

64. Dowling, P. & Clynes, M. Conditioned media from cell lines: A complementary model to clinical specimens for the discovery of disease-specific biomarkers. *Proteomics* **11,** 794–804 (2011).

65. Polisetty, R. V. *et al.* Glioblastoma cell secretome: Analysis of three glioblastoma cell lines reveal 148 non-redundant proteins. *J. Proteomics* **74,** 1918–1925 (2011).

66. Kashat, L. *et al.* Secretome-Based Identification and Characterization of Potential Biomarkers in Thyroid Cancer. *J. Proteome Res.* **9,** 5757–5769 (2010).

67. Álvarez-Chaver, P., Otero-Estévez, O., de la Cadena, M. P., Rodríguez-Berrocal, F. J. & Martínez-Zorzano, V. S. Proteomics for discovery of candidate colorectal cancer biomarkers. *World J. Gastroenterol.* **20,** 3804–3824 (2014).

68. Gromova, I. *et al.* Immunoexpression Analysis and Prognostic Value of BLCAP in Breast Cancer. *PLoS One* **7,** 1–10 (2012).

69. Chang, Y. T. *et al.* Secretome-based identification of ULBP2 as a novel serum marker for pancreatic cancer detection. *PLoS One* **6,** 1–10 (2011).

70. Ralhan, R. *et al.* Identification of proteins secreted by head and neck cancer cell lines using LC-MS/MS: Strategy for discovery of candidate serological biomarkers. *Proteomics* **11,** 2363–2376 (2011).

71. Planque, C. *et al.* Identification of Five Candidate Lung Cancer Biomarkers by Proteomics Analysis of Conditioned Media of Four Lung Cancer Cell Lines. *Mol. Cell. Proteomics* **8,** 2746–2758 (2009).

72. Hood, J. L., San Roman, S. & Wickline, S. A. Exosomes released by melanoma cells prepare sentinel lymph nodes for tumor metastasis. *Cancer Res.* **71,** 3792–3801 (2011).

73. Makridakis, M. & Vlahou, A. Secretome proteomics for discovery of cancer biomarkers. *J. Proteomics* **73,** 2291–2305 (2010).

74. Mbeunkui, F., Fodstad, O. & Pannell, L. K. Secretory protein enrichment and analysis: An optimized approach applied on cancer cell lines using 2D LC-MS/MS. *J. Proteome Res.* **5,** 899–906 (2006).

75. Chevallet, M., Diemer, H., Van Dorssealer, A., Villiers, C. & Rabilloud, T. Toward a better analysis of secreted proteins: The example of the myeloid cells secretome. *Proteomics* **7,** 1757–1770 (2007).

76. Kulasingam, V. & Diamandis, E. P. Proteomics Analysis of Conditioned Media from Three Breast Cancer Cell Lines. *Mol. Cell. Proteomics* **6,** 1997–2011 (2007).

77. Xu, G. *et al.* CTHRC1 as a novel biomarker in the diagnosis of cervical squamous cell carcinoma. *Int. J. Clin. Exp. Pathol.* **11,** 847–854 (2018).

78. Van Raemdonck, G. A. A., Tjalma, W. A. A., Coen, E. P., Depuydt, C. E. & Van Ostade, X. W. M. Identification of Protein Biomarkers for Cervical Cancer Using Human Cervicovaginal Fluid. *PLoS One* **9,** e106488 (2014).

79. Quillien, V., Raoul, J. L., Laurent, J. F., Meunier, B. & Le Prise, E. Comparison of Cyfra 21-1, TPA and SCC tumor markers in esophageal squamous cell carcinoma. *Oncol. Rep.* **5,** 1561–1565 (1998).

80. van der Watt, P. J. *et al.* The karyopherin proteins, Crm1 and Karyopherin β1, are overexpressed in cervical cancer and are critical for cancer cell survival and proliferation. *Int. J. Cancer* **124,** 1829–1840 (2009).

81. Kimura, M. & Imamoto, N. Biological Significance of the Importin-β Family-Dependent Nucleocytoplasmic Transport Pathways. *Traffic* **15,** 727–748 (2014).

82. Tiganis, T., Flint, A. J., Adam, S. A. & Tonks, N. K. Association of the T-cell protein tyrosine phosphatase with nuclear import factor p97. *J. Biol. Chem.* **272,** 21548–21557 (1997).

83. Nakielny, S. *et al.* Transportin: nuclear transport receptor of a novel nuclear protein import pathway. *Exp. Cell Res.* **229,** 261–6 (1996).

84. Guttinger, S., Muhlhausser, P., Koller-Eichhorn, R., Brennecke, J. & Kutay, U. From The Cover: Transportin2 functions as importin and mediates nuclear import of HuR. *Proc. Natl. Acad. Sci.* **101,** 2918–2923 (2004).

85. Jäkel, S. & Görlich, D. Importin β, transportin, RanBP5 and RanBP7 mediate nuclear import of ribosomal proteins in mammalian cells. *EMBO J.* **17,** 4491–4502 (1998).

86. Jakel, S. Importins fulfil a dual function as nuclear import receptors and cytoplasmic chaperones for exposed basic domains. *EMBO J.* **21,** 377–386 (2002).

87. Wei, Y., Li, L., Wang, D., Zhang, C. Y. & Zen, K. Importin 8 regulates the transport of mature microRNAs into the cell nucleus. *J. Biol. Chem.* **289,** 10270–10275 (2014).

88. Plafker, S. M. *et al.* Importin-11, a nuclear import receptor for the ubiquitin-conjugating enzyme, UbcM2. *EMBO J.* **19,** 5502–13 (2000).

89. Kataoka, N., Bachorik, J. L. & Dreyfuss, G. Transportin-SR, a nuclear import receptor for SR proteins. *J. Cell Biol.* **145,** 1145–1152 (1999).

90. Ossareh-Nazari, B., Bachelerie, F. & Dargemont, C. Evidence for a Role of CRM1 in Signal-Mediated Nuclear Protein Export. *Science (80-.).* **278,** 141–144 (1997).

91. Kutay, U., Ralf Bischoff, F., Kostka, S., Kraft, R. & Görlich, D. Export of importin α from the nucleus is mediated by a specific nuclear transport factor. *Cell* **90,** 1061–1071 (1997).

92. Bohnsack, M. T., Czaplinski, K. & Görlich, D. Exportin 5 is a RanGTP-dependent

dsRNA-binding protein that mediates nuclear export of pre-miRNAs. *Rna* **10,** 185–191 (2004).

93. Stuven, T., Gorlich, D. & Hartmann, E. Exportin 6 : a novel nuclear export receptor that is specific for profilin.actin complexes. *EMBO J.* **22,** 5928–5940 (2003).

94. Mingot, J. M., Bohnsack, M. T., Jäkle, U. & Görlich, D. Exportin 7 defines a novel general nuclear export pathway. *EMBO J.* **23,** 3227–3236 (2004).

95. Arts, G. J., Kuersten, S., Romby, P., Ehresmann, B. & Mattaj, I. W. The role of exportin-t in selective nuclear export of mature tRNAs. *EMBO J.* **17,** 7430–7441 (1998).

96. Mingot, J. M., Kostka, S., Kraft, R., Hartmann, E. & Görlich, D. Importin 13: A novel mediator of nuclear import and export. *EMBO J.* **20,** 3685–3694 (2001).

97. Lipowsky, G. *et al.* Exportin 4: a mediator of a novel nuclear export pathway in higher eukaryotes. *EMBO J.* **19,** 4362–71 (2000).

98. Gontan, C. *et al.* Exportin 4 mediates a novel nuclear import pathway for Sox family transcription factors. *J. Cell Biol.* **185,** 27–34 (2009).

99. Hler, M. K. *et al.* Evidence for Distinct Substrate Specificities of Importin α Family Members in Nuclear Protein Import. *Mol. Cell. Biol.* **19,** 7782–7791 (1999).

100. Nakielny, S. & Dreyfuss, G. Transport of proteins and RNAs in and out of the nucleus. *Cell* **99,** 677–690 (1999).

101. Görlich, D. & Kutay, U. Transport between the cell nucleus and the cytoplasm. *Annu. Rev. Cell Dev. Biol.* **15,** 607–60 (1999).

102. Ribbeck, K., Lipowsky, G., Kent, H. M., Stewart, M. & Görlich, D. NTF2 mediates nuclear import of Ran. *EMBO J.* **17,** 6587–98 (1998).

103. Yuh, M. C. & Blobel, G. Karyopherins and nuclear import. *Curr. Opin. Struct. Biol.* **11,** 703–715 (2001).

104. Fukuda, M. *et al.* CRM1 is responsible for intracellular transport mediated by the nuclear export signal. *Nature* **390,** 308–311 (1997).

105. MBInfo. RanGTP regulates nucleocytoplasmic transport. (2014). Available at: https://www.mechanobio.info/what-is-mechanosignaling/what-are-small-gtpases/what-are-ran-gtpases/.

106. Kuusisto, H. V., Wagstaff, K. M., Alvisi, G., Roth, D. M. & Jans, D. A. Global enhancement of nuclear localization-dependent nuclear transport in transformed cells. *FASEB J.* **26,** 1181–1193 (2012).

107. Yang, W. & Musser, S. M. Nuclear import time and transport efficiency depend on importin β concentration. *J. Cell Biol.* **174,** 951–961 (2006).

108. Huang, W. Y. *et al.* Prognostic value of CRM1in pancreas cancer. *Clin. Investig. Med.*

32, 315–321 (2009).

109. Yao, Y. *et al.* The expression of CRM1 is associated with prognosis in human osteosarcoma. *Oncol. Rep.* **21,** 229–235 (2009).

110. Noske, A. *et al.* Expression of the nuclear export protein chromosomal region maintenance/exportin 1/Xpo1 is a prognostic factor in human ovarian cancer. *Cancer* **112,** 1733–1743 (2008).

111. Shen, A. *et al.* Expression of CRM1 in human gliomas and its significance in p27 expression and clinical prognosis. *Neurosurgery* **65,** 153–159 (2009).

112. Rensen, W. & Lavia, P. RAN (RAN, member RAS oncogene family). *Atlas Genet. Cytogenet. Oncol. Haematol.* **14,** 834–840 (2011).

113. Azuma, Y. & Dasso, M. The role of Ran in nuclear function. *Curr. Opin. Cell Biol.* **12,** 302–307 (2000).

114. Wang, C. I. *et al.* Importin subunit alpha-2 is identified as a potential biomarker for non-small cell lung cancer by integration of the cancer cell secretome and tissue transcriptome. *Int. J. Cancer* **128,** 2364–2372 (2011).

115. Ma, S. & Zhao, X. KPNA2 is a promising biomarker candidate for esophageal squamous cell carcinoma and correlates with cell proliferation. *Oncol. Rep.* **32,** 1631–1637 (2014).

116. Omenn, G. S., Lane, L., Lundberg, E. K., Overall, C. M. & Deutsch, E. W. Progress on the HUPO Draft Human Proteome: 2017 Metrics of the Human Proteome Project. *J. Proteome Res.* **16,** 4281–4287 (2017).

117. Ngounou Wetie, A. G. *et al.* Protein-protein interactions: Switch from classical methods to proteomics and bioinformatics-based approaches. *Cell. Mol. Life Sci.* **71,** 205–228 (2014).

118. Bonifacino, J. S., Dell'Angelica, E. C. & Springer, T. A. Immunoprecipitation. *Curr. Protoc. Immunol.* **41,** 8.3.1-8.3.28 (2001).

119. James, P. Mass spectrometry and the proteome. *Proteome Res. mass Spectrosc.* **33,** 1–9 (1961).

120. Price, P. Standard Definitions of Terms Relating to Mass Spectrometry: A report from the Committee on Measurements and Standards of the American Society for Mass Spectrometry. *J. Am. Soc. Mass Spectrom.* **2,** 336–348 (1991).

121. Yates, J. R., Ruse, C. I. & Nakorchevsky, A. Proteomics by Mass Spectrometry: Approaches, Advances, and Applications. *Annu. Rev. Biomed. Eng.* **11,** 49–79 (2009).

122. Lee, S. *et al.* Modern Mass Spectrometry. *Top. Curr. Chem.* **34,** 1–14 (2005).

123. Muller, P. Glossary of terms used in physical organic chemistry (IUPAC Recommendations 1994). *Pure Appl. Chem.* **66,** 1077–1184 (1994).

124. Karas, M., Bachmann, D., Bahr, U. & Hillenkamp, F. Matrix-assisted ultraviolet laser desorption of non-volantile compounds. *Int. J. Mass Spectrom. Ion Process* **78,** 53–68 (1987).

125. Yamashita, M. & Fenn, J. B. Electrospray ion source. Another variation on the free-jet theme. *J. Phys. Chem.* **88,** 4451–4459 (1984).

126. Dole, M. *et al.* Molecular Beams of Macroions. *J. Chem. Phys.* **49,** 2240–2249 (1968).

127. Karas, M., Bachmann, D. & Hillenkamp, F. Influence of the Wavelength in High-Irradiance Ultraviolet Laser Desorption Mass Spectrometry of Organic Molecules. *Anal. Chem.* **57,** 2935–2939 (1985).

128. Fenn, J. B. Electrospray ionization mass spectrometry: How it all began. *J. Biomol. Tech.* **13,** 101–118 (2002).

129. Römpp, A., Guenther, S., Takats, Z. & Spengler, B. Mass spectrometry imaging with high resolution in mass and space (HR 2 MSI) for reliable investigation of drug compound distributions on the cellular level. *Anal. Bioanal. Chem.* **401,** 65–73 (2011).

130. Forbes, D. J., Travesa, A., Nord, M. S. & Bernis, C. Nuclear transport factors: global regulation of mitosis. *Curr Opin Cell Biol* **35,** 78–90 (2015).

131. Ciciarello, M., Mangiacasale, R. & Lavia, P. Spatial control of mitosis by the GTPase Ran. *Cell. Mol. Life Sci.* **64,** 1891–1914 (2007).

132. Nachury, M. V. *et al.* Importin β is a mitotic target of the small GTPase ran in spindle assembly. *Cell* **104,** 95–106 (2001).

133. Harel, A. & Forbes, D. J. Importin beta: Conducting a much larger cellular symphony. *Mol. Cell* **16,** 319–330 (2004).

134. Samwer, M. *et al.* The nuclear F-actin interactome of Xenopus oocytes reveals an actin-bundling kinesin that is essential for meiotic cytokinesis. *EMBO J.* **32,** 1886–1902 (2013).

135. Zhong, Y. *et al.* Importin β interacts with the endoplasmic reticulum-associated degradation machinery and promotes ubiquitination and degradation of mutant α1-antitrypsin. *J. Biol. Chem.* **286,** 33921–33930 (2011).

136. Lowe, A. R. *et al.* Importin-β modulates the permeability of the nuclear pore complex in a Ran-dependent manner. *Elife* **2015,** 1–24 (2015).

137. Di Francesco, L. *et al.* Visualization of human karyopherin beta-1/importin beta-1 interactions with protein partners in mitotic cells by co-immunoprecipitation and proximity ligation assays. *Sci. Rep.* **8,** 1–15 (2018).

138. Schellhaus, A. K., Antonin, P. D. M. & Antonin, W. Nuclear reformation at the end of mitosis. *J. Mol. Biol. Mol Biol* **428,** 1962–1985 (2016).

139. Rosemarie Ungricht and Ulrike Kutay. Mechanisms and functions of nuclear envelope remodelling. *Nat. Rev. Mol. Cell Biol.* **18,** 229–245 (2017).

140. Kırlı, K. *et al.* A deep proteomics perspective on CRM1-mediated nuclear export and nucleocytoplasmic partitioning. *Elife* **4,** 1–28 (2015).

141. Masayoshi Nambak, Koji Nishitani, T. K. Characteristics of WI-38 cells (WI-38 CT-1) transformed by treatment with Co-60 gamma rays. *Gann* **71,** 300–307 (1980).

142. Jones, G. J., Heiss, N. S., Veale, R. B. & Thornley, A. L. Amplification and expression of the TGF-alpha, EGF receptor and c-myc genes in four human oesophageal squamous cell carcinoma lines. *Biosci. Rep.* **13,** 303–312 (1993).

143. Olson, B. J. S. C. & Markwell, J. Assays for Determination of Protein Concentration. *Curr. Protoc. Protein Sci.* **Chapter 3,** 3.4.1-3.4.29 (2007).

144. Brenner, A. J. & Harris, E. D. A Quantitative Test for Copper Using Bicinchoninic Acid. *Anal. Biochem.* **226,** 80–84 (1995).

145. Wiechelman, K. J., Braun, R. D. & Fitzpatrick, J. D. Investigation of the bicinchoninic acid protein assay: Identification of the groups responsible for color formation. *Anal. Biochem.* **175,** 231–237 (1988).

146. Miteva, Y. V., Budayeva, H. G. & Ileana, M. C. Proteomics-based methods for discovery, quantification, and validation of protein-protein interactions. *Anal. Chem.* **85,** 749–768 (2013).

147. Phizicky, E. M. & Fields, S. Protein-protein interactions: methods for detection and analysis. *Microbiol. Rev.* **59,** 94–123 (1995).

148. Gundry, R. L. *et al.* Preparation of Proteins and Peptides for Mass Spectrometry Analysis in a Bottom-Up Proteomics Workflow. *Curr. Protoc. Mol. Biol.* **77,** 342–355 (2010).

149. Mazzara, S. *et al.* CombiROC: An interactive web tool for selecting accurate marker combinations of omics data. *Sci. Rep.* **7,** 1–11 (2017).

150. Youden, W. J. Index for rating diagnostic tests. *Cancer* **3,** 32–35 (1950).

151. Habibzadeh, F., Habibzadeh, P. & Yadollahie, M. On determining the most appropriate test cut-off value: The case of tests with continuous results. *Biochem. Medica* **26,** 297–307 (2016).

152. Ignatchenko, V., Ignatchenko, A., Sinha, A., Boutros, P. C. & Kislinger, T. VennDIS: A JavaFX-based Venn and Euler diagram software to generate publication quality figures. *Proteomics* **15,** 1239–1244 (2015).

153. Szklarczyk, D. *et al.* STRING v10: Protein-protein interaction networks, integrated over the tree of life. *Nucleic Acids Res.* **43,** 447–452 (2015).

154. Jia Zhu, Yingying Wang, Hua Huang, Qichang Yang, Jing Cai, Qiuhong Wang, Xiaoling Gu, Pan Xu, Shusen Zhang, Manhua Li, Haifang Ding, L. Y. Upregulation of KPNβ1 in gastric cancer cell promotes tumor cell proliferation and predicts poor prognosis. *Tumour Biol.* **37,** 661–672 (2016).

155. Kuusisto, H. V. & Jans, D. A. Hyper-dependence of breast cancer cell types on the nuclear transporter Importin β1. *Biochim. Biophys. Acta - Mol. Cell Res.* **1853,** 1870–1878 (2015).

156. Zhang, Y. *et al.* Karyopherin alpha 2 is a novel prognostic marker and a potential therapeutic target for colon cancer. *J. Exp. Clin. Cancer Res.* **34,** 145 (2015).

157. Shi, B. *et al.* High expression of KPNA2 defines poor prognosis in patients with upper tract urothelial carcinoma treated with radical nephroureterectomy. *BMC Cancer* **15,** 1–11 (2015).

158. Altan, B. *et al.* Nuclear karyopherin-α2 expression in primary lesions and metastatic lymph nodes was associated with poor prognosis and progression in gastric cancer. *Carcinogenesis* **34,** 2314–2321 (2013).

159. Zheng, M. *et al.* Overexpression of Karyopherin-2 in Epithelial Ovarian Cancer and Correlation With Poor Prognosis. *Obstet. Gynecol.* **116,** 884–891 (2010).

160. Gousias, K., Niehusmann, P., Gielen, G. H. & Simon, M. Karyopherin a2 and chromosome region maintenance protein 1 expression in meningiomas: Novel biomarkers for recurrence and malignant progression. *J. Neurooncol.* **118,** 289–296 (2014).

161. Bar-Shira, A. *et al.* Multiple genes in human 20q13 chromosomal region are involved in an advanced prostate cancer xenograft. *Cancer Res* **62,** 6803–6807 (2002).

162. Shiraki, K. *et al.* Cellular apoptosis susceptibility protein and proliferation in human hepatocellular carcinoma. *Int J Mol Med* **18,** 77–81 (2006).

163. Huang, L. *et al.* KPNA2 is a potential diagnostic serum biomarker for epithelial ovarian cancer and correlates with poor prognosis. *Tumor Biol.* **39,** 1–5 (2017).

164. Tung, M.-C. *et al.* Higher prevalence of secretory CSE1L/CAS in sera of patients with metastatic cancer. *Cancer Epidemiol. Biomarkers Pre.* **18,** 1570–1577 (2009).

165. Kodama, M. *et al.* In vivo loss-of-function screens identify KPNB1 as a new druggable oncogene in epithelial ovarian cancer. *Proc. Natl. Acad. Sci.* 1–10 (2017). doi:10.1073/pnas.1705441114

166. Hajian-Tilaki, K. Receiver operating characteristic (ROC) curve analysis for medical diagnostic test evaluation. *Casp. J. Intern. Med.* **4,** 627–635 (2013).

167. Greiner, M., Pfeiffer, D. & Smith, R. D. Principles and practical application of the receiver-operating characteristic analysis for diagnostic tests. *Prev. Vet. Med.* **45,** 23–41 (2000).

168. Swets, J. A. Measuring the accuracy of diagnostic systems. *Science (80-.).* **240,** 1285–1293 (1988).

169. Stelma, T. *et al.* Targeting nuclear transporters in cancer: Diagnostic, prognostic and therapeutic potential. *IUBMB Life* **68,** 268–280 (2016).

170. Zannini, L. *et al.* Karyopherin-α2 Protein Interacts with Chk2 and Contributes to Its Nuclear Import. *J. Biol. Chem.* **278,** 42346–42351 (2003).

171. Narod, S. A. & Foulkes, W. D. BRCA1 and BRCA2: 1994 and beyond. *Nat. Rev. Cancer* **4,** 665–676 (2004).

172. Tseng, S. F., Chang, C. Y., Wu, K. J. & Teng, S. C. Importin KPNA2 is required for proper nuclear localization and multiple functions of NBS1. *J. Biol. Chem.* **280,** 39594–39600 (2005).

173. Sandrock, K., Bielek, H., Schradi, K., Schmidt, G. & Klugbauer, N. The nuclear import of the small GTPase Rac1 is mediated by the direct interaction with karyopherin α2. *Traffic* **11,** 198–209 (2010).

174. Waldmann, I., Wälde, S. & Kehlenbach, R. H. Nuclear import of c-Jun is mediated by multiple transport receptors. *J. Biol. Chem.* **282,** 27685–27692 (2007).

175. Le Roux, L. G. & Moroianu, J. Nuclear entry of high-risk human papillomavirus type 16 E6 oncoprotein occurs via several pathways. *J Virol* **77,** 2330–2337 (2003).

176. Wang, C.-I. *et al.* Quantitative Proteomics Reveals Regulation of Karyopherin Subunit Alpha-2 (KPNA2) and Its Potential Novel Cargo Proteins in Nonsmall Cell Lung Cancer. *Mol. Cell. Proteomics* **11,** 1105–1122 (2012).

177. Stelma, T. & Leaner, V. D. KPNB1-mediated nuclear import is required for motility and inflammatory transcription factor activity in cervical cancer cells. *Oncotarget* **8,** 32833–32847 (2017).

178. Yan, W., Li, R., He, J., Du, J. & Hou, J. Importin β1 mediates nuclear factor-κB signal transduction into the nuclei of myeloma cells and affects their proliferation and apoptosis. *Cell. Signal.* **27,** 851–859 (2015).

179. Forwood, J. K., Lam, M. H. & Jans, D. A. Nuclear import of Creb and AP-1 transcription factors requires importin-beta 1 and Ran but is independent of importin-alpha. *Biochemistry* **40,** 5208–17 (2001).

180. Wen, W., Meinkotht, J. L., Tsien, R. Y. & Taylor, S. S. Identification of a signal for rapid export of proteins from the nucleus. *Cell* **82,** 463–473 (1995).

181. Fischer, U., Huber, J., Boelens, W. C., Mattajt, L. W. & Lührmann, R. The HIV-1 Rev Activation Domain is a nuclear export signal that accesses an export pathway used by specific cellular RNAs. *Cell* **82,** 475–483 (1995).

182. Solsbacher, J., Maurer, P., Bischoff, F. R. & Schlenstedt, G. Cse1p is involved in export of yeast importin alpha from the nucleus. *Mol. Cell. Biol.* **18,** 6805–6815 (1998).

183. Kang, H. S. *et al.* Early growth response protein 1 upregulation and nuclear translocation by 2'-benzoyloxycinnamaldehyde induces prostate cancer cell death. *Cancer Lett.* **329,** 217–227 (2013).

184. Jäkel, S. *et al.* The importin β/importin 7 heterodimer is a functional nuclear import

receptor for histone H1. *EMBO J.* **18,** 2411–2423 (1999).

185. Xiao, Z., Liu, X., Henis, Y. I. & Lodish, H. F. A distinct nuclear localization signal in the N terminus of Smad 3 determines its ligand-induced nuclear translocation. *Proc. Natl. Acad. Sci. U. S. A.* **97,** 7853–7858 (2000).

186. Dolcet, X., Llobet, D., Pallares, J. & Matias-Guiu, X. NF-kB in development and progression of human cancer. *Virchows Arch* **446,** 475–482 (2005).

187. Kojima, M. *et al.* Increased Nuclear Factor-kB Activation in Human Colorectal Carcinoma and its Correlation with Tumor Progression. *Anticancer Res.* **24,** 675–681 (2004).

188. Matthews, C. P., Colburn, N. H. & Young, M. R. AP-1 a target for cancer prevention. *Curr. Cancer Drug Targets* **7,** 317–24 (2007).

189. Xia, F., Lee, C. W. & Altieri, D. C. Tumor cell dependence on Ran-GTP-directed mitosis. *Cancer Res.* **68,** 1826–1833 (2008).

190. Mor-Vaknin, N., Punturieri, A., Sitwala, K. & Markovitz, D. M. Vimentin is secreted by activated macrophages. *Nat. Cell Biol.* **5,** 59–63 (2003).

191. Satelli, A. & Li, S. Vimentin as a potential molecular target in cancer therapy. *Cell Mol Life Sci.* **68,** 3033–3046 (2011).

192. Wu, C.-C. *et al.* Candidate Serological Biomarkers for Cancer Identified from the Secretomes of 23 Cancer Cell Lines and the Human Protein Atlas. *Mol. Cell. Proteomics* **9,** 1100–1117 (2010).

193. Chi, N. C. & Adam, S. A. Functional domains in nuclear import factor p97 for binding the nuclear localization sequence receptor and the nuclear pore. *Mol. Biol. Cell* **8,** 945–56 (1997).

194. Kutay, U., Izaurralde, E., Bischoff, F. R., Mattaj, I. W. & Görlich, D. Dominant-negative mutants of importin-beta block multiple pathways of import and export through the nuclear pore complex. *EMBO J.* **16,** 1153–1163 (1997).

195. Cingolani, G., Petosa, C., Weis, K. & Müller, C. W. Structure of importin-β bound to the IBB domain of importin-α. *Nature* **399,** 221–229 (1999).

196. Trinkle-Mulcahy, L. *et al.* Identifying specific protein interaction partners using quantitative mass spectrometry and bead proteomes. *J. Cell Biol.* **183,** 223–239 (2008).

197. Have, S., Boulon, S., Ahmad, Y. & Lamond, A. I. Mass spectrometry-based immuno-precipitation proteomics – The user's guide. *Proteomics* **11,** 1153–1159 (2011).

198. Boulon, S. *et al.* Establishment of a Protein Frequency Library and Its Application in the Reliable Identification of Specific Protein Interaction Partners. *Mol. Cell. Proteomics* **9,** 861–879 (2010).

199. Tyanova, S. *et al.* The Perseus computational platform for comprehensive analysis of (prote)omics data. *Nat. Methods* **13,** 731–740 (2016).

200. Conlon, F. L. *et al.* Immunoisolation of Protein Complexes from Xenopus. *Methods Mol. Biol.* **917,** 369–390 (2012).

201. Seddon, A. M., Curnow, P. & Booth, P. J. Membrane proteins, lipids and detergents: Not just a soap opera. *Biochim. Biophys. Acta - Biomembr.* **1666,** 105–117 (2004).

202. Le Maire, M., Champeil, P. & Møller, J. V. Interaction of membrane proteins and lipids with solubilizing detergents. *Biochim. Biophys. Acta - Biomembr.* **1508,** 86–111 (2000).

203. Xia, Y., Shen, S. & Verma, M. I. NF-κB, an active player in human cancers. *Cancer Immunol Res* **2,** 823–830 (2014).

204. Blau, L. *et al.* Aberrant expression of c-Jun in glioblastoma by internal ribosome entry site (IRES)-mediated translational activation. *Proc. Natl. Acad. Sci.* **109,** E2875–E2884 (2012).

205. Moore, S. M. & Blobel, G. The GTP-binding protein Ran/TC4 is required for protein import into the nucleus. *Nature* **365,** 661–663 (1993).

206. Melchior, F., Paschal, B., Evans, J. & Gerace, L. Inhibition of nuclear protein import by nonhydrolyzable analogues of GTP and identification of the small GTPase Ran/TC4 as an essential transport factor. *J. Cell Biol.* **123,** 1649–1659 (1993).

207. Weis, K., Dingwall, C. & Lamond, A. I. Characterization of the nuclear protein import mechanism using Ran mutants with altered nucleotide binding specificities. *EMBO J.* **15,** 7120–8 (1996).

208. Izaurralde, E., Kutay, U., Von Kobbe, C., Mattaj, L. W. & Görlich, D. The asymmetric distribution of the constituents of the Ran system is essential for transport into and out of the nucleus. *EMBO J.* **16,** 6535–6547 (1997).

209. Xu, L., Kang, Y., Çöl, S. & Massagué, J. Smad2 nucleocytoplasmic shuttling by nucleoporins CAN/Nup214 and Nup153 feeds TGFβ signaling complexes in the cytoplasm and nucleus. *Mol. Cell* **10,** 271–282 (2002).

210. Hutten, S. & Kehlenbach, R. H. Nup214 Is Required for CRM1-Dependent Nuclear Protein Export In Vivo. *Mol. Cell. Biol.* **26,** 6772–6785 (2006).

211. Bayliss, R., Littlewood, T. & Stewart, M. Structural basis for the interaction between FxFG nucleoporin repeats and importin-beta in nuclear trafficking. *Cell* **102,** 99–108 (2000).

212. Kim, J. H. *et al.* CCAR1, a Key Regulator of Mediator Complex Recruitment to Nuclear Receptor Transcription Complexes. *Mol. Cell* **31,** 510–519 (2008).

213. Rishi, A. K. *et al.* Cell cycle- and apoptosis-regulatory protein-1 is involved in apoptosis signaling by epidermal growth factor receptor. *J. Biol. Chem.* **281,** 13188–13198 (2006).

214. Rüegsegger, U., Beyer, K. & Keller, W. Purification and characterization of human cleavage factor Im involved in the 3’ end processing of messenger RNA precursors. *J.*

Biol. Chem. **271,** 6107–6113 (1996).

215. Brown, K. M. & Gilmartin, G. M. A Mechanism for the Regulation of Pre-mRNA 3′ Processing by Human Cleavage Factor Im. *Mol. Cell* **12,** 1467–1476 (2003).

216. Yongsheng, S. *et al.* Molecular architecture of the human pre-mRNA 3′ processing complex. *Mol. Cell* **33,** 365–376 (2009).

217. Shi, Y. S., Chan, S. & Martinez-Santibanez, G. An up-close look at the pre-mRNA 3 ’-end processing complex. *Rna Biol.* **6,** 522–525 (2009).

218. Vinciguerra, P. & Stutz, F. mRNA export: An assembly line from genes to nuclear pores. *Curr. Opin. Cell Biol.* **16,** 285–292 (2004).

219. Mandel, C. R., Bai, Y. & Tong, L. Protein factors in pre-mRNA 3′-end processing. *Cell Mol Life Sci.* **65,** 1099–1122 (2008).

220. Huang, Y. & Carmichael, G. G. Role of polyadenylation in nucleocytoplasmic transport of mRNA. *Mol. Cell. Biol.* **16,** 1534–42 (1996).

221. Kaufmann, I., Martin, G., Friedlein, A., Langen, H. & Keller, W. Human Fip1 is a subunit of CPSF that binds to U-rich RNA elements and stimulates poly(A) polymerase. *EMBO J.* **23,** 616–626 (2004).

222. Nissen, P., Hansen, J., Ban, N., Moore, P. B. & Steitz, T. A. The structural basis of ribosomal activity in peptide bond synthesis. *Science (80-.).* **289,** 920–930 (2000).

223. Ruggero, D. & Pandolfi, P. P. Does the ribosome translate cancer? *Nat. Rev. Cancer* **3,** 179–192 (2003).

224. Wang, H. *et al.* Overexpression of ribosomal protein L15 is associated with cell proliferation in gastric cancer. *BMC Cancer* **6,** 1–8 (2006).

225. Mitchell, B. L., Yasui, Y., Li, C. I., Fitzpatrick, A. L. & Lampe, P. D. Impact of Freeze-thaw Cycles and Storage Time on Plasma Samples Used in Mass Spectrometry Based Biomarker Discovery Projects. *Cancer Inform.* **1,** 98–104 (2005).

APPENDIX I

A. List of protein hits identified in IP-MS experiments of Kpnβ1 from hTERT-RPE1 cell extracts

Majority protein IDs[a]	Protein names[b]	Gene Names[c]	Peptides[d]	Molecular weight (kDa)[e]	Score[f]	MS/MS count[g]	Intensity[h]	Sequence coverage (%)[i]	Sequence length[j]
Q14974	Importin subunit beta-1	KPNB1	6	97.169	45.552	11	2.1E+08	8.3	876
A0A087WUK2	Heterogeneous nuclear ribonucleoprotein D-like	HNRNPDL	8	40.04	56.539	15	5E+08	21.2	363
A0A087WZF1	Lipoma-preferred partner	LPP	4	63.382	28.419	7	57318000	11.4	590
A0A0A0MRA5	Heterogeneous nuclear ribonucleoprotein U-like protein 1	HNRNPUL1	14	85.939	103.11	30	6.02E+08	24	766
Q9HBD4	Transcription activator BRG1	SMARCA4	5	188.15	32.978	7	83380000	3.6	1679
A0A0A0MTH3	Integrin-linked protein kinase	ILK	4	54.611	25.752	4	31942000	9.3	483
A0A0B4J1Z1	Serine/arginine-rich splicing factor 7	SRSF7	3	15.763	21.454	7	78438000	29.2	137
A0A0D9SFB3	ATP-dependent RNA helicase DDX3X	DDX3X	27	70.839	247.23	51	1.17E+09	50.6	640
A0A0U1RRM4	Polypyrimidine tract-binding protein 1	PTBP1	11	62.463	83.541	21	3.04E+08	30.3	588
C9J2Y9	DNA-directed RNA polymerase	POLR2B	7	121.37	50.848	12	74673000	9.7	1067
A0A1X7SBZ2	Probable ATP-dependent RNA helicase DDX17	DDX17	25	80.253	252.69	70	2.1E+09	39.5	729
A0A286YFA2	D-3-phosphoglycerate dehydrogenase	PHGDH	4	25.638	24.151	6	30999000	19.7	239
A5YKK6	CCR4-NOT transcription complex subunit 1	CNOT1	11	266.94	65.446	18	1.48E+08	5.2	2376
B0QYK0	RNA-binding protein EWS	EWSR1	6	64.929	104.02	30	1.38E+09	13.9	618
B4DY09	Interleukin enhancer-binding factor 2	ILF2	6	38.91	58.341	21	3.38E+08	24.1	352
C9JSZ1	Far upstream element-binding protein 1	FUBP1	10	24.043	6.3042	3	97795000	62.5	232
C9JTN7	Nucleolysin TIAR	TIA1	5	16.794	11.699	4	36019000	34.9	152
D6R9P3	Heterogeneous nuclear ribonucleoprotein A/B	HNRNPAB	6	30.302	50.7	15	5.56E+08	25	280
D6RAN4	60S ribosomal protein L9	RPL9	4	20.775	30.838	13	1.25E+08	28.2	181
Q01085	Nucleolysin TIAR	TIAL1	6	14.616	54.853	13	4.12E+08	55.3	132
P62917	60S ribosomal protein L8	RPL8	3	22.389	20.347	8	1.25E+08	17.1	205
Q13435	Splicing factor 3B subunit 2	SF3B2	9	98.169	76.397	22	2.55E+08	17.2	878

P78406	mRNA export factor	RAE1	5	47.831	39.994	10	1.63E+08	22	437
F5H2B9	Uveal autoantigen with coiled-coil domains and ankyrin repeats	UACA	8	150.53	56.664	15	1.12E+08	7.8	1307
F5H2F4	C-1-tetrahydrofolate synthase, cytoplasmic	MTHFD1	7	110.61	42.425	9	89042000	8.2	1020
F5H365	Protein transport protein Sec23A	SEC23A	19	82.968	323.31	45	1.23E+09	36.1	736
P05388	60S acidic ribosomal protein P0	RPLP0	3	15.813	25.876	7	90313000	27.5	142
F8VV52	CCR4-NOT transcription complex subunit 2	CNOT2	5	58.62	32.169	9	1.21E+08	12.4	531
F8W8I6	Nucleolysin TIA-1 isoform p40	TIA1	4	42.835	7.2059	3	18956000	10.6	385
F8WJN3	Cleavage and polyadenylation specificity factor subunit 6	CPSF6	4	52.269	31.697	9	1.99E+08	9.4	478
G5EA31	Protein transport protein Sec24C	SEC24C	17	111.98	151.81	41	7.18E+08	24.3	1042
P38159	RNA-binding motif protein, X chromosome	RBMX	4	31.745	36.65	9	1.16E+08	16.8	292
Q8N1F7	Nuclear pore complex protein Nup93	NUP93	6	99.554	40.865	9	49972000	10.5	880
J3KTA4	Probable ATP-dependent RNA helicase DDX5	DDX5	10	69.086	44.233	17	3.14E+08	17.6	614
J3QK89	Calcium homeostasis endoplasmic reticulum protein	CHERP	5	104.93	32.55	7	86424000	7.3	927
J3QLE5	Small nuclear ribonucleoprotein-associated protein N	SNRPN	6	17.546	54.026	18	5.15E+08	26.6	169
K7ELC2	40S ribosomal protein S15	RPS15	3	17.723	27.452	8	29079000	44.7	152
M0R3D6	60S ribosomal protein L18a	RPL18A	4	16.714	24.158	9	90888000	24.1	141
P09012	U1 small nuclear ribonucleoprotein A	SNRPA	2	28.388	20.171	6	99423000	19.1	256
O14497	AT-rich interactive domain-containing protein 1A	ARID1A	12	242.04	75.102	14	1.8E+08	7.4	2285
O43390	Heterogeneous nuclear ribonucleoprotein R	HNRNPR	9	70.942	38.955	11	1.79E+08	18	633
O43809	Cleavage and polyadenylation specificity factor subunit 5	NUDT21	7	26.227	55.088	19	2.97E+08	39.6	227
U3KQK0	Histone H2B	HIST1H2BN	6	18.804	68.659	9	2.4E+08	31.3	166
O75369	Filamin-B	FLNB	12	278.16	32.522	4	36638000	4.4	2602
O96019	Actin-like protein 6A	ACTL6A	7	47.46	50.796	13	1.91E+08	26.8	429
P02751	Fibronectin	FN1	19	262.62	194.35	40	7.47E+08	11.9	2386
P05387	60S acidic ribosomal protein P2	RPLP2	2	11.665	21.395	7	1.06E+08	24.3	115
P08621	U1 small nuclear ribonucleoprotein 70 kDa	SNRNP70	5	51.556	46.723	13	1.54E+08	16	437
P09497	Clathrin light chain B	CLTB	5	25.19	30.58	8	2.46E+08	14.8	229
P13010	X-ray repair cross-complementing protein 5	XRCC5	7	82.704	45.729	7	76290000	19.7	732
P15880	40S ribosomal protein S2	RPS2	5	31.324	31.549	16	3.24E+08	18.8	293

P15924	Desmoplakin	DSP	13	331.77	96.576	15	1.49E+08	5.5	2871
P21980	Protein-glutamine gamma-glutamyltransferase 2	TGM2	12	77.328	95.152	28	8.31E+08	23.3	687
P23258	Tubulin gamma-1 chain	TUBG1	6	51.169	47.895	9	1.72E+08	18.4	451
P26196	Probable ATP-dependent RNA helicase DDX6	DDX6	11	54.416	122.28	23	3.15E+08	35.6	483
P27694	Replication protein A 70 kDa DNA-binding subunit	RPA1	5	68.137	29.946	7	80559000	9.9	616
P35637	RNA-binding protein FUS	FUS	11	53.425	142.88	38	2.58E+09	20.2	526
P39023	60S ribosomal protein L3	RPL3	5	46.108	38.42	12	2.06E+08	17.9	403
P52292	Importin subunit alpha-1	KPNA2	4	57.861	56.088	9	75556000	12.3	529
P53618	Coatomer subunit beta	COPB1	5	107.14	38.202	7	68544000	8.8	953
P55735	Protein SEC13 homolog	SEC13	5	35.54	139.67	18	9.9E+08	23	322
P60866	40S ribosomal protein S20	RPS20	2	13.373	17.474	8	90225000	22.7	119
P61353	60S ribosomal protein L27	RPL27	6	15.798	38.703	15	2.26E+08	45.6	136
Q5JR95	40S ribosomal protein S8	RPS8	5	21.879	43.431	12	2.8E+08	29.3	188
P62277	40S ribosomal protein S13	RPS13	3	17.222	18.167	8	1.05E+08	21.2	151
P62306	Small nuclear ribonucleoprotein F	SNRPF	2	9.7251	23.585	7	2.09E+08	39.5	86
P62314	Small nuclear ribonucleoprotein Sm D1	SNRPD1	4	13.281	37.388	17	2.46E+08	54.6	119
P62316	Small nuclear ribonucleoprotein Sm D2	SNRPD2	4	13.527	61.619	6	1.45E+08	30.5	118
P62318	Small nuclear ribonucleoprotein Sm D3	SNRPD3	2	13.916	17.834	5	4.27E+08	15.1	126
P62899	60S ribosomal protein L31	RPL31	3	14.463	23.504	6	1.42E+08	26.4	125
P98179	RNA-binding protein 3	RBM3	4	17.17	30.426	7	1.82E+08	47.8	157
Q02809	Procollagen-lysine,2-oxoglutarate 5-dioxygenase 1	PLOD1	11	83.549	87.323	21	1.87E+08	22.1	727
Q05048	Cleavage stimulation factor subunit 1	CSTF1	6	48.357	54.508	12	1.87E+08	20.6	431
Q10570	Cleavage and polyadenylation specificity factor subunit 1	CPSF1	5	160.88	40.954	6	39124000	3.8	1443
Q12906	Interleukin enhancer-binding factor 3	ILF3	10	95.337	100.71	14	2.44E+08	16.7	894
Q13151	Heterogeneous nuclear ribonucleoprotein A0	HNRNPA0	6	30.84	40.748	14	4.11E+08	23.6	305
Q14204	Cytoplasmic dynein 1 heavy chain 1	DYNC1H1	15	532.4	97.047	21	2.29E+08	4.4	4646
Q14444	Caprin-1	CAPRIN1	6	78.365	43.488	11	1.78E+08	15.7	709
Q15393	Splicing factor 3B subunit 3	SF3B3	11	135.58	108.29	15	4.54E+08	13	1217
Q15437	Protein transport protein Sec23B	SEC23B	6	86.478	48.549	6	38516000	10.6	767

Q15637	Splicing factor 1	SF1	8	68.329	73.775	19	2.92E+08	20.7	639
Q15717	ELAV-like protein 1	ELAVL1	5	36.091	40.345	13	1.43E+08	21.8	326
Q52LJ0	Protein FAM98B	FAM98B	6	37.19	131.83	15	2.57E+08	24.2	330
Q86X55	Histone-arginine methyltransferase CARM1	CARM1	9	65.853	69.129	18	4.03E+08	24.8	608
Q8NCA5	Protein FAM98A	FAM98A	5	55.4	35.894	9	2.34E+08	15.8	519
Q8TAQ2	SWI/SNF complex subunit SMARCC2	SMARCC2	9	132.88	125.11	19	2.66E+08	11.9	1214
Q8WXF1	Paraspeckle component 1	PSPC1	12	58.743	86.703	21	4.22E+08	27.5	523
Q92734	Protein TFG	TFG	11	43.447	312.34	40	1.68E+09	38	400
Q92804	TATA-binding protein-associated factor 2N	TAF15	5	61.829	22.338	9	1.62E+08	15.5	592
Q92922	SWI/SNF complex subunit SMARCC1	SMARCC1	5	122.87	13.685	3	36543000	4.9	1105
Q92945	Far upstream element-binding protein 2	KHSRP	29	73.114	323.31	103	4.91E+09	51.9	711
Q92973	Transportin-1	TNPO1	7	102.35	42.502	11	1.26E+08	10.2	898
Q969G3	SWI/SNF-related matrix-associated actin-dependent regulator of chromatin subfamily E member 1	SMARCE1	4	46.649	39.988	7	1.31E+08	18.5	411
Q96I24	Far upstream element-binding protein 3	FUBP3	12	61.64	89.592	20	3.92E+08	34.1	572
Q9BTL3	RNMT-activating mini protein	FAM103A1	2	14.381	14.568	3	1.03E+08	23.7	118
Q9BWJ5	Splicing factor 3B subunit 5	SF3B5	2	10.135	19.897	6	69418000	25.6	86
Q9H2D6	TRIO and F-actin-binding protein	TRIOBP	5	261.37	63.453	10	1.15E+08	2.7	2365
Q9Y224	UPF0568 protein C14orf166	C14orf166	9	28.068	140.04	33	1.31E+09	41.8	244
Q9Y3I0	tRNA-splicing ligase RtcB homolog	RTCB	20	55.21	216.51	58	2.66E+09	49.5	505
Q9Y678	Coatomer subunit gamma-1	COPG1	2	97.717	12.541	6	46360000	2.6	874
Q9Y6Y8	SEC23-interacting protein	SEC23IP	14	111.08	129.85	34	6.44E+08	20.9	1000

The definitions and parameters for each column are given in MaxQuant (version 1.5.4.1)

[a] Identifier(s) of major proteins possessing at least 50% of the peptides ascribed to a protein group.

[b] Name(s) of protein(s) contained within the protein group.

[c] Name(s) of the gene(s) associated to the proteins contained within the protein group.

[d] Total number of peptide sequences associated with all the proteins in the protein group. Only protein identifications made from at least 2 peptides were selected from the original data set.

[e] Molecular weight of the leading protein sequence contained in the protein group.

[f] Score for the protein identification which is derived from peptide posterior error probabilities. The higher the score, the more accurate the protein identification is.

[g] Number of MS/MS spectra reported for the peptide which was used to identify the peptide sequence ascribed to a protein group.

[h] Sum of eXtracted Ion Current (XIC) of all isotopic clusters associated with the identified amino acid sequence.

[i] Percentage of the sequence that is covered by the identified peptides of the best protein sequence contained in the group.

[j] the length of the identified amino acid sequence of the peptide.

B. List of protein hits identified in IP-MS experiments of Kpnβ1 from HeLa cell extracts

Majority protein IDs[a]	Protein names[b]	Gene Names[c]	Peptides[d]	Molecular weight (kDa)[e]	Score[f]	MS/MS count[g]	Intensity[h]	Sequence coverage (%)[i]	Sequence length[j]
Q14974	Importin subunit beta-1	KPNB1	11	97.169	109.62	24	3.75E+08	17.1	876
A0A024R4M0	40S ribosomal protein S9	RPS9	4	22.591	23.457	5	1.19E+08	17.5	194
A0A024R7W5	YTH domain-containing family protein 3	YTHDF3	4	58.311	32.34	10	1.3E+08	10.7	534
Q92804	TATA-binding protein-associated factor 2N	TAF15	4	48.839	26.82	5	1.27E+08	14.5	449
A0A087WUK2	Heterogeneous nuclear ribonucleoprotein D-like	HNRNPDL	7	40.04	66.24	14	6.24E+08	17.9	363
A0A087WV05	C-Myc-binding protein	MYCBP	3	12.755	20.741	7	1.21E+08	41.8	110
P27635	60S ribosomal protein L10	RPL10	5	18.565	43.631	10	2.1E+08	25.2	163
A0A087WVT6	Single-stranded DNA-binding protein 3	SSBP3	3	37.772	30.001	8	1.1E+08	11.9	361
A0A087X2D0	Serine/arginine-rich splicing factor 3	SRSF3	4	10.32	39.063	5	2.49E+08	42.1	95
A0A0A0MR66	RNA-binding protein 10	RBM10	7	110.36	51.44	12	1.13E+08	8.3	995
A0A0A0MRA5	Heterogeneous nuclear ribonucleoprotein U-like protein 1	HNRNPUL1	15	85.939	132.27	32	7.54E+08	26.1	766
Q05048	Cleavage stimulation factor subunit 1	CSTF1	6	38.448	122.61	13	2.17E+08	27.2	345
Q9HBD4	Transcription activator BRG1	SMARCA4	11	188.15	96.588	13	1.59E+08	8.2	1679
A0A0B4J1Z1	Serine/arginine-rich splicing factor 7	SRSF7	3	15.763	17.414	5	1.09E+08	29.2	137
A0A0B4J210	La-related protein 1	LARP1	4	69.746	26.034	8	91249000	8	610
A0A0D9SFB3	ATP-dependent RNA helicase DDX3X	DDX3X	23	70.839	268.18	61	1.49E+09	46.2	640
A0A0D9SF63	F-box-like/WD repeat-containing protein TBL1XR1	TBL1XR1	4	51.556	84.914	12	1.72E+08	14.3	474
A0A0U1RQF0	Fatty acid synthase	FASN	19	273.2	185.17	28	2.7E+08	10.9	2509
C9J2Y9	DNA-directed RNA polymerase	POLR2B	9	121.37	64.947	18	1.88E+08	11.5	1067
A0A1X7SBZ2	Probable ATP-dependent RNA helicase DDX17	DDX17	23	80.253	307.02	74	2.89E+09	37	729
A5YKK6	CCR4-NOT transcription complex subunit 1	CNOT1	13	266.94	82.884	22	2.32E+08	6.1	2376
J3KNE0	RanBP2-like and GRIP domain-containing protein 3	RGPD3	4	197.62	12.868	3	31087000	2.4	1760
B0QY90	Eukaryotic translation initiation factor 3 subunit L	EIF3L	2	55.161	25.729	3	19102000	4.9	466
B0QYK0	RNA-binding protein EWS	EWSR1	6	64.929	94.219	22	9.04E+08	13.9	618

B1AHC9	X-ray repair cross-complementing protein 6	XRCC6	10	64.283	85.374	21	2.32E+08	25.4	559
B1ANR0	Polyadenylate-binding protein	PABPC4	14	67.97	51.772	15	4.36E+08	25.2	615
G3V555	Heterogeneous nuclear ribonucleoproteins C1/C2	HNRNPC	8	28.916	119.18	30	1.35E+09	33.2	262
B4DY09	Interleukin enhancer-binding factor 2	ILF2	9	38.91	68.465	21	4.92E+08	42.3	352
P62826	GTP-binding nuclear protein Ran	RAN	4	26.224	38.535	9	1.72E+08	21.9	233
Q99613	Eukaryotic translation initiation factor 3 subunit C	EIF3C	3	105.34	32.858	7	54462000	4.2	913
F8W1R7	Myosin light polypeptide 6	MYL6	3	14.436	21.857	8	1.02E+08	33.8	130
B8ZZL3	Eukaryotic translation initiation factor 4E type 2	EIF4E2	2	23.248	13.821	3	32266000	11.5	200
C9J0K6	Sorcin	SRI	3	17.605	17.197	6	74773000	19.4	155
C9JSZ1	Far upstream element-binding protein 1	FUBP1	11	24.043	7.7765	3	1.35E+08	65.5	232
C9JTN7	Nucleolysin TIAR	TIA1	4	16.794	25.899	9	1.14E+08	29.6	152
D3YTB1	60S ribosomal protein L32	RPL32	2	15.616	12.525	4	43773000	17.3	133
D6R9P3	Heterogeneous nuclear ribonucleoprotein A/B	HNRNPAB	9	30.302	90.208	23	9.11E+08	32.5	280
D6RAN4	60S ribosomal protein L9	RPL9	4	20.775	43.128	15	2.29E+08	28.2	181
E7EPB3	60S ribosomal protein L14	RPL14	2	14.558	18.211	8	1.9E+08	19.4	124
E7EQG2	Eukaryotic initiation factor 4A-II	EIF4A2	4	41.29	6.2353	0	4314100	14.4	362
E7EQV9	Ribosomal protein L15	RPL15	3	20.51	33.956	10	2.42E+08	20.1	174
E7EWR4	Cleavage stimulation factor subunit 2	CSTF2	13	62.942	130.5	23	4.36E+08	32.8	597
E7EX17	Eukaryotic translation initiation factor 4B	EIF4B	4	69.697	24.049	7	2.16E+08	8.3	616
P62917	60S ribosomal protein L8	RPL8	4	22.389	28.487	10	2.1E+08	21	205
Q13435	Splicing factor 3B subunit 2	SF3B2	14	98.169	180.97	29	5.73E+08	27.3	878
F5H365	Protein transport protein Sec23A	SEC23A	17	82.968	323.31	39	1.07E+09	32.7	736
Q8N684	Cleavage and polyadenylation specificity factor subunit 7	CPSF7	9	41.265	87.814	20	3.3E+08	31.8	374
F8VV52	CCR4-NOT transcription complex subunit 2	CNOT2	6	58.62	41.41	10	1.31E+08	19.6	531
Q15366	Poly(rC)-binding protein 2	PCBP2	4	31.6	29.978	7	1.22E+08	23.3	301
F8W726	Ubiquitin-associated protein 2-like	UBAP2L	12	113.63	125.17	22	2.96E+08	20.7	1079
F8W8I6	Nucleolysin TIA-1 isoform p40	TIA1	3	42.835	6.4034	3	15533000	8.6	385
F8WJN3	Cleavage and polyadenylation specificity factor subunit 6	CPSF6	6	52.269	90.824	15	2.96E+08	19.5	478
G3V203	60S ribosomal protein L18	RPL18	4	18.756	56.795	7	2.14E+08	28.7	164

G5E9W3	Cleavage and polyadenylation specificity factor subunit 3	CPSF3	3	73.476	26.735	7	64287000	9	647
G5EA31	Protein transport protein Sec24C	SEC24C	10	111.98	94.729	26	3.04E+08	15.9	1042
H3BV80	RNA-binding protein with serine-rich domain 1	RNPS1	3	24.561	18.024	4	60923000	13.7	211
Q1KMD3	Heterogeneous nuclear ribonucleoprotein U-like protein 2	HNRNPUL2-BSCL2	5	84.69	38.607	7	82806000	9.5	746
Q8N1F7	Nuclear pore complex protein Nup93	NUP93	17	99.554	175	38	5.57E+08	26.5	880
P62277	40S ribosomal protein S13	RPS13	4	16.733	30.693	8	2.32E+08	25.7	148
J3KNL6	Protein transport protein Sec16A	SEC16A	12	251.89	99.859	26	2.9E+08	10.1	2357
J3KTA4	Probable ATP-dependent RNA helicase DDX5	DDX5	14	69.086	71.319	28	1.01E+09	20.7	614
J3KTL2	Serine/arginine-rich splicing factor 1	SRSF1	10	28.329	90.09	22	4.09E+08	39.1	253
J3QK89	Calcium homeostasis endoplasmic reticulum protein	CHERP	4	104.93	42.739	8	1.17E+08	8.7	927
J3QLE5	Small nuclear ribonucleoprotein-associated protein N	SNRPN	6	17.546	43.252	19	6.46E+08	26.6	169
J3QT28	Mitotic checkpoint protein BUB3	BUB3	3	31.703	52.297	11	1.93E+08	16.9	278
K7ELC2	40S ribosomal protein S15	RPS15	4	17.723	98.582	19	2.55E+08	53.3	152
M0R0F0	40S ribosomal protein S5	RPS5	4	22.391	30.181	9	1.19E+08	22	200
M0R3D6	60S ribosomal protein L18a	RPL18A	6	16.714	35.768	12	1.69E+08	26.2	141
O00303	Eukaryotic translation initiation factor 3 subunit F	EIF3F	5	37.563	42.639	13	73646000	25.8	357
O00425	Insulin-like growth factor 2 mRNA-binding protein 3	IGF2BP3	4	63.704	30.773	5	79788000	10.4	579
O43143	Pre-mRNA-splicing factor ATP-dependent RNA helicase DHX15	DHX15	10	90.932	86.972	21	2.81E+08	18.1	795
O43390	Heterogeneous nuclear ribonucleoprotein R	HNRNPR	15	70.942	160.01	36	8.91E+08	31	633
O43809	Cleavage and polyadenylation specificity factor subunit 5	NUDT21	10	26.227	110.37	30	8.31E+08	52	227
O60506	Heterogeneous nuclear ribonucleoprotein Q	SYNCRIP	8	69.602	53.446	12	2.36E+08	19.9	623
O75340	Programmed cell death protein 6	PDCD6	5	21.868	32.441	10	1.49E+08	27.7	191
M0QZC5	40S ribosomal protein S11	RPS11	7	13.997	31.63	8	1.10E+08	43.2	118
O75533	Splicing factor 3B subunit 1	SF3B1	19	145.83	165.89	26	3.43E+08	25	1304
O96019	Actin-like protein 6A	ACTL6A	9	47.46	112.33	17	5E+08	33.6	429
P05387	60S acidic ribosomal protein P2	RPLP2	6	11.665	73.644	14	2.74E+08	70.4	115
P05388	60S acidic ribosomal protein P0	RPLP0	5	34.273	75.437	5	1.56E+08	18.9	317
P08621	U1 small nuclear ribonucleoprotein 70 kDa	SNRNP70	6	51.556	51.948	20	3.09E+08	19.7	437

P08708	40S ribosomal protein S17	RPS17	4	15.55	37.126	8	1.77E+08	40.7	135
P09496	Clathrin light chain A	CLTA	6	27.076	39.124	17	1.5E+09	16.9	248
P09497	Clathrin light chain B	CLTB	6	25.19	36.757	9	2.79E+08	20.5	229
P0DN76	Splicing factor U2AF 35 kDa subunit	U2AF1	3	27.872	27.032	8	1.24E+08	17.9	240
P15880	40S ribosomal protein S2	RPS2	8	31.324	63.573	22	8.03E+08	28.3	293
P15927	Replication protein A 32 kDa subunit	RPA2	5	29.247	41.083	13	2.06E+08	36.3	270
P16403	Histone H1.2	HIST1H1C	4	21.364	30.472	8	1.36E+08	19.7	213
P18124	60S ribosomal protein L7	RPL7	5	29.225	33.342	9	1.94E+08	23.8	248
Q5HY54	Filamin-A	FLNA	39	276.55	323.31	99	1.97E+09	21.6	2607
P23258	Tubulin gamma-1 chain	TUBG1	9	51.169	125.18	16	2.42E+08	35.5	451
P23396	40S ribosomal protein S3	RPS3	12	26.688	101.53	30	1.46E+09	59.3	243
P25705	ATP synthase subunit alpha, mitochondrial	ATP5A1	3	59.75	20.802	6	56556000	6.1	553
P26196	Probable ATP-dependent RNA helicase DDX6	DDX6	12	54.416	233.99	31	4.92E+08	41.8	483
P27694	Replication protein A 70 kDa DNA-binding subunit	RPA1	9	68.137	102.62	18	4.22E+08	21.6	616
P31689	DnaJ homolog subfamily A member 1	DNAJA1	3	44.868	35.866	10	49725000	14.1	397
P31942	Heterogeneous nuclear ribonucleoprotein H3	HNRNPH3	11	36.926	223.95	33	1.41E+09	53.5	346
P35244	Replication protein A 14 kDa subunit	RPA3	4	13.569	59.904	13	2.03E+08	52.9	121
P35637	RNA-binding protein FUS	FUS	9	53.425	182.56	33	2.31E+09	20.2	526
P35658	Nuclear pore complex protein Nup214	NUP214	21	213.62	264.17	44	6.94E+08	17	2090
P37198	Nuclear pore glycoprotein p62	NUP62	5	53.254	66.281	16	2.19E+08	14.2	522
P38159	RNA-binding motif protein, X chromosome	RBMX	7	42.331	77.039	14	3.05E+08	22	391
P40227	T-complex protein 1 subunit zeta	CCT6A	5	58.024	36.206	8	67515000	14.5	531
P40429	60S ribosomal protein L13a	RPL13A	5	23.577	34.495	14	2.83E+08	22.2	203
P46060	Ran GTPase-activating protein 1	RANGAP1	6	63.541	58.495	12	2.57E+08	17.7	587
P46777	60S ribosomal protein L5	RPL5	4	34.362	31.681	12	1.68E+08	14.5	297
P49368	T-complex protein 1 subunit gamma	CCT3	4	60.533	30.043	6	53392000	10.3	545
P49792	E3 SUMO-protein ligase RanBP2	RANBP2	11	358.2	64.181	6	1.69E+08	4.8	3224
P52292	Importin subunit alpha-1	KPNA2	8	57.861	109.47	15	1.45E+08	29.3	529
P52907	F-actin-capping protein subunit alpha-1	CAPZA1	3	32.922	24.892	10	1.58E+08	15.4	286

P52948	Nuclear pore complex protein Nup98-Nup96	NUP98	9	197.58	91.445	19	4.05E+08	7.2	1817
P55072	Transitional endoplasmic reticulum ATPase	VCP	3	89.321	20.025	6	49642000	4.2	806
P55735	Protein SEC13 homolog	SEC13	3	35.54	124.17	10	6.47E+08	16.8	322
P60842	Eukaryotic initiation factor 4A-I	EIF4A1	4	46.153	40.047	7	1.17E+08	18.2	406
P62081	40S ribosomal protein S7	RPS7	6	22.127	49.69	15	3.39E+08	43.8	194
P62136	Serine/threonine-protein phosphatase PP1-alpha catalytic subunit	PPP1CA	3	37.512	20.918	7	56168000	11.8	330
P62140	Serine/threonine-protein phosphatase PP1-beta catalytic subunit	PPP1CB	2	37.186	14.781	3	34054000	8.3	327
P62263	40S ribosomal protein S14	RPS14	6	16.273	52.318	15	2.53E+08	39.7	151
P62314	Small nuclear ribonucleoprotein Sm D1	SNRPD1	4	13.281	71.951	21	4.84E+08	54.6	119
P62316	Small nuclear ribonucleoprotein Sm D2	SNRPD2	3	13.527	27.551	6	2.82E+08	30.5	118
P62318	Small nuclear ribonucleoprotein Sm D3	SNRPD3	2	13.916	23.461	6	5.29E+08	15.1	126
P62701	40S ribosomal protein S4, X isoform	RPS4X	7	29.597	47.309	16	2.5E+08	25.5	263
P62753	40S ribosomal protein S6	RPS6	3	28.68	42.005	8	3.28E+08	14.1	249
P62899	60S ribosomal protein L31	RPL31	4	14.463	37.042	9	3.06E+08	32.8	125
P62906	60S ribosomal protein L10a	RPL10A	6	24.831	41.302	9	1.48E+08	28.1	217
P63244	Guanine nucleotide-binding protein subunit beta-2-like 1	GNB2L1	5	35.076	34.607	7	1.49E+08	17.4	317
P78406	mRNA export factor	RAE1	7	40.968	142.15	15	4.22E+08	31	368
P98179	RNA-binding protein 3	RBM3	3	17.17	46.433	9	2.08E+08	38.2	157
Q02809	Procollagen-lysine,2-oxoglutarate 5-dioxygenase 1	PLOD1	6	83.549	55.058	8	1.11E+08	10	727
Q02878	60S ribosomal protein L6	RPL6	9	32.728	108.88	26	6.13E+08	39.2	288
Q07666	KH domain-containing, RNA-binding, signal transduction-associated protein 1	KHDRBS1	5	48.227	43.529	13	2.8E+08	15.3	443
Q09028	Histone-binding protein RBBP4	RBBP4	2	47.655	16.236	4	21311000	5.2	425
Q10570	Cleavage and polyadenylation specificity factor subunit 1	CPSF1	9	160.88	68.629	13	1.2E+08	7.7	1443
Q12906	Interleukin enhancer-binding factor 3	ILF3	16	95.337	122.7	25	4.24E+08	26.8	894
Q12996	Cleavage stimulation factor subunit 3	CSTF3	5	82.921	56.041	9	90749000	10.2	717
Q13085	Acetyl-CoA carboxylase 1	ACACA	6	265.55	44.522	4	67321000	3.8	2346
Q13151	Heterogeneous nuclear ribonucleoprotein A0	HNRNPA0	6	30.84	62.111	24	1.07E+09	23.6	305
Q13247	Serine/arginine-rich splicing factor 6	SRSF6	4	39.586	38.488	12	2.35E+08	12.5	344

Q13283	Ras GTPase-activating protein-binding protein 1	G3BP1	15	52.164	252.4	47	1.38E+09	44	466
Q13347	Eukaryotic translation initiation factor 3 subunit I	EIF3I	6	36.501	56.992	11	1.26E+08	25.2	325
Q14152	Eukaryotic translation initiation factor 3 subunit A	EIF3A	6	166.57	48.933	11	1.12E+08	5.3	1382
Q14247	Src substrate cortactin	CTTN	5	61.585	42.499	8	71658000	14.4	550
Q14315	Filamin-C	FLNC	13	291.02	15.054	18	8.28E+08	17.3	2725
Q14444	Caprin-1	CAPRIN1	12	78.365	155.8	32	1.22E+09	28.1	709
Q15365	Poly(rC)-binding protein 1	PCBP1	6	37.497	102.48	14	3.2E+08	29.8	356
Q15437	Protein transport protein Sec23B	SEC23B	8	86.478	38.9	9	90185000	14	767
Q15637	Splicing factor 1	SF1	13	68.329	197.33	31	1.01E+09	26.1	639
Q15717	ELAV-like protein 1	ELAVL1	5	36.091	38.561	11	1.4E+08	21.8	326
Q52LJ0	Protein FAM98B	FAM98B	8	37.19	133.73	17	3.53E+08	30	330
Q5BKZ1	DBIRD complex subunit ZNF326	ZNF326	7	65.653	44.599	9	94068000	17.7	582
Q5SRE5	Nucleoporin NUP188 homolog	NUP188	8	196.04	61.748	14	1.24E+08	6.5	1749
Q6P2Q9	Pre-mRNA-processing-splicing factor 8	PRPF8	3	273.6	17.379	4	22111000	1.7	2335
Q6UN15	Pre-mRNA 3-end-processing factor FIP1	FIP1L1	5	66.526	50.219	9	2.24E+08	14.1	594
Q86V81	THO complex subunit 4	ALYREF	4	26.888	38.609	7	53655000	32.3	257
Q86X55	Histone-arginine methyltransferase CARM1	CARM1	11	65.853	173.21	26	5.74E+08	28	608
Q8IX12	Cell division cycle and apoptosis regulator protein 1	CCAR1	11	132.82	124.33	22	3.29E+08	11.7	1150
Q8NC51	Plasminogen activator inhibitor 1 RNA-binding protein	SERBP1	4	44.965	31.658	9	1.25E+08	13	408
Q8NCA5	Protein FAM98A	FAM98A	7	55.4	44.008	9	2.32E+08	18.7	519
Q8TAQ2	SWI/SNF complex subunit SMARCC2	SMARCC2	6	132.88	47.005	7	75680000	6.1	1214
Q8WWM7	Ataxin-2-like protein	ATXN2L	8	113.37	61.185	16	2.86E+08	12.6	1075
Q8WX93	Palladin	PALLD	7	150.56	57.144	11	1.15E+08	8.9	1383
Q8WXF1	Paraspeckle component 1	PSPC1	10	58.743	124.27	27	4.94E+08	27.2	523
Q92734	Protein TFG	TFG	12	43.447	323.31	32	1.3E+09	37.5	400
Q92922	SWI/SNF complex subunit SMARCC1	SMARCC1	10	122.87	82.52	18	2.22E+08	12.4	1105
Q92973	Transportin-1	TNPO1	11	102.35	91.77	24	6.03E+08	15.7	898
Q969G3	SWI/SNF-related matrix-associated actin-dependent regulator of chromatin subfamily E member 1	SMARCE1	5	46.649	53.643	9	1.51E+08	20.9	411

Q96AE4	Far upstream element-binding protein 1	FUBP1	26	67.56	323.31	107	8.91E+09	49.2	644
Q96I24	Far upstream element-binding protein 3	FUBP3	10	61.64	73.998	14	3.38E+08	25.7	572
Q9BTL3	RNMT-activating mini protein	FAM103A1	3	14.381	20.184	3	75592000	39	118
Q9BWF3	RNA-binding protein 4	RBM4	3	40.313	55.113	8	50097000	14.8	364
Q9BWJ5	Splicing factor 3B subunit 5	SF3B5	2	10.135	32.855	6	1.02E+08	25.6	86
Q9NZB2	Constitutive coactivator of PPAR-gamma-like protein 1	FAM120A	3	121.89	19.07	6	64779000	3.8	1118
Q9UN86	Ras GTPase-activating protein-binding protein 2	G3BP2	9	54.12	70.576	17	2.41E+08	24.9	482
Q9Y224	UPF0568 protein C14orf166	C14orf166	10	28.068	160.75	35	1.72E+09	45.1	244
Q9Y2W1	Thyroid hormone receptor-associated protein 3	THRAP3	3	108.66	18.011	4	49141000	3.6	955
Q9Y383	Putative RNA-binding protein Luc7-like 2	LUC7L2	4	46.513	27.023	9	56435000	12	392
Q9Y3I0	tRNA-splicing ligase RtcB homolog	RTCB	21	55.21	282.27	65	3.41E+09	47.1	505
Q9Y5A9	YTH domain-containing family protein 2	YTHDF2	5	62.333	35.505	10	1.43E+08	15	579
Q9Y6Y8	SEC23-interacting protein	SEC23IP	9	111.08	74.654	13	1.89E+08	11.6	1000
Q9H0L4	Cleavage stimulation factor subunit 2	CSTF2T	8	62.942	22.61	13	2.17E+08	23.2	597

The definitions and parameters for each column are given in MaxQuant (version 1.5.4.1)
[a] Identifier(s) of major proteins possessing at least 50% of the peptides ascribed to a protein group.
[b] Name(s) of protein(s) contained within the protein group.
[c] Name(s) of the gene(s) associated to the proteins contained within the protein group.
[d] Total number of peptide sequences associated with all the proteins in the protein group. Only protein identifications made from at least 2 peptides were selected from the original data set.
[e] Molecular weight of the leading protein sequence contained in the protein group.
[f] Score for the protein identification which is derived from peptide posterior error probabilities. The higher the score, the more accurate the protein identification is.
[g] Number of MS/MS spectra reported for the peptide which was used to identify the peptide sequence ascribed to a protein group.
[h] Sum of eXtracted Ion Current (XIC) of all isotopic clusters associated with the identified amino acid sequence.
[i] Percentage of the sequence that is covered by the identified peptides of the best protein sequence contained in the group.
[j] the length of the identified amino acid sequence of the peptide.

C. List of protein hits identified in IP-MS experiments of Kpnβ1 from WHCO5 cell extracts

Majority protein IDs[a]	Protein names[b]	Gene Names[c]	Peptides[d]	Molecular weight (kDa)[e]	Score[f]	MS/MS count[g]	Intensity[h]	Sequence coverage (%)[i]	Sequence length[j]
Q14974	Importin subunit beta-1	KPNB1	6	97.169	44.051	13	1.49E+08	8.7	876
Q92804	TATA-binding protein-associated factor 2N	TAF15	4	48.839	27.718	9	2.59E+08	14.5	449
A0A087WUK2	Heterogeneous nuclear ribonucleoprotein D-like	HNRNPDL	8	40.04	57.498	15	4.05E+08	21.8	363
E7ETK0	40S ribosomal protein S24	RPS24	5	15.197	31.96	12	1.81E+08	35.9	131
Q5HY54	Filamin-A	FLNA	6	245.85	43.272	11	73648000	3.9	2315
A0A087X2D0	Serine/arginine-rich splicing factor 3	SRSF3	4	10.32	45.624	7	3.47E+08	49.5	95
A0A0A0MR66	RNA-binding protein 10	RBM10	4	110.36	25.857	6	43625000	5.5	995
A0A0A0MRA5	Heterogeneous nuclear ribonucleoprotein U-like protein 1	HNRNPUL1	9	85.939	73.085	19	2.93E+08	21.9	766
P35658	Nuclear pore complex protein Nup214	NUP214	9	152.57	101.43	17	2.07E+08	10.7	1519
Q9HBD4	Transcription activator BRG1	SMARCA4	13	188.15	120.95	22	2.23E+08	10.2	1679
Q15370	Transcription elongation factor B polypeptide 2	TCEB2	2	7.7561	6.449	3	4687900	12.1	66
A0A0D9SEJ5	Constitutive coactivator of peroxisome proliferator-activated receptor gamma	FAM120B	3	105.19	19.042	5	27905000	6.5	922
A0A0D9SFB3	ATP-dependent RNA helicase DDX3X	DDX3X	19	70.839	191.82	36	6.88E+08	37.2	640
A0A0U1RQF0	Fatty acid synthase	FASN	8	273.2	58.336	15	1.09E+08	5.3	2509
A0A0U1RRM4	Polypyrimidine tract-binding protein 1	PTBP1	9	56.51	107.06	28	6.22E+08	28.7	527
A0A1X7SBZ2	Probable ATP-dependent RNA helicase DDX17	DDX17	26	80.253	314.53	72	3.24E+09	40.3	729
A5YKK6	CCR4-NOT transcription complex subunit 1	CNOT1	21	266.94	139.87	34	5.02E+08	10.7	2376
H7BY10	60S ribosomal protein L23a	RPL23A	4	17.692	31.786	11	1.35E+08	29.7	158
B0QYK0	RNA-binding protein EWS	EWSR1	5	64.929	123.91	22	1.23E+09	11.8	618
B1AHC9	X-ray repair cross-complementing protein 6	XRCC6	5	64.283	30.89	8	60498000	12.5	559
B1ANR0	Polyadenylate-binding protein	PABPC4	26	67.97	323.31	69	2.68E+09	43.7	615
B4DY09	Interleukin enhancer-binding factor 2	ILF2	6	38.91	40.925	10	2.01E+08	20.7	352
P62826	GTP-binding nuclear protein Ran	RAN	2	26.224	14.666	6	70170000	10.7	233
F8W1R7	Myosin light polypeptide 6	MYL6	3	14.436	19.724	9	64428000	33.8	130

J3KMX2	SWI/SNF-related matrix-associated actin-dependent regulator of chromatin subfamily D member 2	SMARCD2	7	52.238	49.973	15	1.84E+08	22.8	456
C9J2Y9	DNA-directed RNA polymerase	POLR2B	12	133.06	123.55	27	2.87E+08	14.6	1167
D6R9P3	Heterogeneous nuclear ribonucleoprotein A/B	HNRNPAB	11	30.302	140.79	36	1.99E+09	36.1	280
D6RAN4	60S ribosomal protein L9	RPL9	4	20.775	33.939	16	1.86E+08	24.3	181
D6REX3	Protein transport protein Sec31A	SEC31A	11	136.22	71.841	22	2.44E+08	11	1251
E7EWR4	Cleavage stimulation factor subunit 2	CSTF2	12	62.942	169.99	27	4.68E+08	29.1	597
E9PLL6	60S ribosomal protein L27a	RPL27A	2	12.201	13.979	9	1.86E+08	22.2	108
F5H2F4	C-1-tetrahydrofolate synthase, cytoplasmic	MTHFD1	7	110.61	49.123	7	1.41E+08	8.2	1020
F5H365	Protein transport protein Sec23A	SEC23A	10	82.968	147.06	15	2.97E+08	15.6	736
Q8N684	Cleavage and polyadenylation specificity factor subunit 7	CPSF7	5	41.265	34.698	14	1.07E+08	21.7	374
F8VPD4	CAD protein	CAD	42	236.02	323.31	86	2.37E+09	30.2	2162
P05388	60S acidic ribosomal protein P0	RPLP0	4	15.813	30.779	3	1.12E+08	32.4	142
G3V203	60S ribosomal protein L18	RPL18	2	14.529	35.169	7	2.21E+08	20	130
F8VV52	CCR4-NOT transcription complex subunit 2	CNOT2	9	58.62	85.995	20	3.43E+08	35.6	531
Q15366	Poly(rC)-binding protein 2	PCBP2	4	31.6	52.563	9	1.93E+08	24.9	301
F8W930	Insulin-like growth factor 2 mRNA-binding protein 2	IGF2BP2	6	66.785	96.785	15	2.52E+08	12.9	605
F8WJN3	Cleavage and polyadenylation specificity factor subunit 6	CPSF6	4	52.269	29.908	9	1.22E+08	11.9	478
G5EA31	Protein transport protein Sec24C	SEC24C	15	111.98	132.31	31	4.96E+08	23.1	1042
Q1KMD3	Heterogeneous nuclear ribonucleoprotein U-like protein 2	HNRNPUL2-BSCL2	3	84.69	22.255	8	89518000	5.1	746
J3KNL6	Protein transport protein Sec16A	SEC16A	13	251.89	110.88	26	2.75E+08	10	2357
J3KTA4	Probable ATP-dependent RNA helicase DDX5	DDX5	14	69.086	67.013	25	7.41E+08	23.8	614
J3KTL2	Serine/arginine-rich splicing factor 1	SRSF1	6	28.329	44.474	17	2.17E+08	24.5	253
J3QK89	Calcium homeostasis endoplasmic reticulum protein	CHERP	7	104.93	64.541	13	2.01E+08	12.9	927
J3QLE5	Small nuclear ribonucleoprotein-associated protein N	SNRPN	6	17.546	54.513	23	7.28E+08	26.6	169
M0QZC5	40S ribosomal protein S11	RPS11	5	13.997	31.63	8	1.01E+08	43.2	118
M0R3D6	60S ribosomal protein L18a	RPL18A	5	16.714	30.82	11	1.16E+08	30.5	141
P09012	U1 small nuclear ribonucleoprotein A	SNRPA	4	28.388	45.992	10	1.79E+08	22.3	256
M0R2P6	SH3KBP1-binding protein 1	SHKBP1	6	73.707	47.705	9	1.05E+08	19.2	682

O14497	AT-rich interactive domain-containing protein 1A	ARID1A	17	242.04	125.65	32	3.99E+08	12	2285
O14980	Exportin-1	XPO1	4	123.38	26.326	7	62937000	5.4	1071
O15042	U2 snRNP-associated SURP motif-containing protein	U2SURP	7	118.29	46.299	14	1.66E+08	11.5	1029
O43148	mRNA cap guanine-N7 methyltransferase	RNMT	7	54.843	65.52	11	1.6E+08	19.7	476
O43390	Heterogeneous nuclear ribonucleoprotein R	HNRNPR	10	70.942	66.18	16	2.82E+08	21.3	633
O43809	Cleavage and polyadenylation specificity factor subunit 5	NUDT21	8	26.227	64.926	17	3.43E+08	45.4	227
O60506	Heterogeneous nuclear ribonucleoprotein Q	SYNCRIP	8	69.602	58.765	9	1.62E+08	23	623
O75369	Filamin-B	FLNB	9	278.16	77.044	13	1.29E+08	5.3	2602
O75533	Splicing factor 3B subunit 1	SF3B1	14	145.83	99.575	23	2.77E+08	17.7	1304
O96019	Actin-like protein 6A	ACTL6A	7	47.46	91.505	19	4.07E+08	28.7	429
P08621	U1 small nuclear ribonucleoprotein 70 kDa	SNRNP70	7	51.556	65.747	23	4.13E+08	27.9	437
P08708	40S ribosomal protein S17	RPS17	7	15.55	33.465	24	1.09E+09	45.9	135
P09496	Clathrin light chain A	CLTA	8	27.076	85.497	22	1.51E+09	20.6	248
P09497	Clathrin light chain B	CLTB	5	25.19	66.736	10	5.26E+08	16.6	229
P11940	Polyadenylate-binding protein 1	PABPC1	24	70.67	158.33	46	1.72E+09	48.1	636
P15924	Desmoplakin	DSP	69	331.77	323.31	141	2.55E+09	27.1	2871
P18124	60S ribosomal protein L7	RPL7	5	29.225	43.467	10	1.29E+08	22.6	248
P23258	Tubulin gamma-1 chain	TUBG1	5	51.169	45.454	8	1.53E+08	15.1	451
P24928	DNA-directed RNA polymerase II subunit RPB1	POLR2A	10	217.17	90.459	18	1.43E+08	9	1970
P26196	Probable ATP-dependent RNA helicase DDX6	DDX6	10	54.416	136.61	17	2.63E+08	35.4	483
P27635	60S ribosomal protein L10	RPL10	6	24.604	43.073	13	2.01E+08	22	214
P27694	Replication protein A 70 kDa DNA-binding subunit	RPA1	2	68.137	12.029	3	49312000	3.7	616
P30050	60S ribosomal protein L12	RPL12	3	17.818	26.749	6	1.39E+08	24.2	165
P31942	Heterogeneous nuclear ribonucleoprotein H3	HNRNPH3	12	36.926	323.31	35	1.4E+09	50	346
P35637	RNA-binding protein FUS	FUS	12	53.425	245.61	43	3.12E+09	22.2	526
P38159	RNA-binding motif protein, X chromosome	RBMX	8	42.331	77.799	19	3.95E+08	21.7	391
P40429	60S ribosomal protein L13a	RPL13A	4	23.577	27.938	8	1.07E+08	16.7	203
P46778	60S ribosomal protein L21	RPL21	5	18.565	40.885	13	2.43E+08	36.9	160
P49792	E3 SUMO-protein ligase RanBP2	RANBP2	7	358.2	52.425	9	1.36E+08	3.7	3224

P52597	Heterogeneous nuclear ribonucleoprotein F	HNRNPF	11	45.671	116.3	21	4.49E+08	43.4	415
P52948	Nuclear pore complex protein Nup98-Nup96	NUP98	8	197.58	63.095	15	3.14E+08	6.7	1817
P55735	Protein SEC13 homolog	SEC13	3	35.54	90.62	7	4.19E+08	15.5	322
P61978	Heterogeneous nuclear ribonucleoprotein K	HNRNPK	21	50.976	302.88	63	2.32E+09	47.3	463
P62277	40S ribosomal protein S13	RPS13	6	17.222	38.104	12	1.72E+08	30.5	151
P62304	Small nuclear ribonucleoprotein E	SNRPE	4	10.803	46.737	8	2.42E+08	42.4	92
P62306	Small nuclear ribonucleoprotein F	SNRPF	3	9.7251	40.348	8	2.91E+08	39.5	86
P62316	Small nuclear ribonucleoprotein Sm D2	SNRPD2	7	13.527	64.677	7	2.46E+08	48.3	118
P62318	Small nuclear ribonucleoprotein Sm D3	SNRPD3	3	13.916	32.378	7	7.17E+08	20.6	126
P62701	40S ribosomal protein S4, X isoform	RPS4X	9	29.597	64.376	14	2.31E+08	37.3	263
P62753	40S ribosomal protein S6	RPS6	5	28.68	64.9	10	3.88E+08	20.5	249
P62851	40S ribosomal protein S25	RPS25	2	13.742	12.706	9	4.37E+08	15.2	125
P62899	60S ribosomal protein L31	RPL31	4	14.463	41.901	8	2.46E+08	32.8	125
P63173	60S ribosomal protein L38	RPL38	3	8.2178	19.984	11	2.02E+08	50	70
P68366	Tubulin alpha-4A chain	TUBA4A	19	49.924	19.482	9	2.14E+08	40.2	448
P78406	mRNA export factor	RAE1	8	40.968	148.07	21	4.67E+08	35.3	368
P98179	RNA-binding protein 3	RBM3	3	17.17	25.389	6	1.54E+08	38.2	157
Q05048	Cleavage stimulation factor subunit 1	CSTF1	8	48.357	108.35	16	3.39E+08	28.1	431
Q10570	Cleavage and polyadenylation specificity factor subunit 1	CPSF1	9	160.88	80.442	19	1.58E+08	6.2	1443
Q12906	Interleukin enhancer-binding factor 3	ILF3	6	95.337	108.19	12	2.64E+08	11.1	894
Q12996	Cleavage stimulation factor subunit 3	CSTF3	6	82.921	68.996	12	1.46E+08	11.6	717
Q13151	Heterogeneous nuclear ribonucleoprotein A0	HNRNPA0	8	30.84	60.543	21	6.56E+08	24.9	305
Q13263	Transcription intermediary factor 1-beta	TRIM28	5	88.549	50.462	10	65402000	10.4	835
Q13435	Splicing factor 3B subunit 2	SF3B2	18	100.23	159.02	38	5.74E+08	28.9	895
Q14103	Heterogeneous nuclear ribonucleoprotein D0	HNRNPD	11	38.434	87.49	24	8.08E+08	25.9	355
Q14134	Tripartite motif-containing protein 29	TRIM29	14	65.834	144.67	27	4.56E+08	28.6	588
Q15149	Plectin	PLEC	9	531.78	70.022	15	1.07E+08	3.2	4684
Q15233	Non-POU domain-containing octamer-binding protein	NONO	26	54.231	323.31	117	5.91E+09	58.2	471
Q15365	Poly(rC)-binding protein 1	PCBP1	5	37.497	55.133	14	3.67E+08	27.5	356

Q15393	Splicing factor 3B subunit 3	SF3B3	10	135.58	98.475	13	5.04E+08	12.9	1217
Q15427	Splicing factor 3B subunit 4	SF3B4	2	44.385	14.784	6	82158000	8.7	424
Q15637	Splicing factor 1	SF1	11	68.329	182.69	25	6.71E+08	23.2	639
Q15717	ELAV-like protein 1	ELAVL1	6	36.091	49.962	16	2.76E+08	24.5	326
Q52LJ0	Protein FAM98B	FAM98B	6	37.19	136.72	13	2.73E+08	24.2	330
Q5BKZ1	DBIRD complex subunit ZNF326	ZNF326	10	65.653	77.29	18	2.33E+08	24.9	582
Q5QPM2	RNA-binding protein Raly	RALY	2	9.714	13.837	5	78386000	25.8	89
Q5SRE5	Nucleoporin NUP188 homolog	NUP188	6	196.04	39.154	8	43357000	4.9	1749
Q6P2E9	Enhancer of mRNA-decapping protein 4	EDC4	7	151.66	76.347	15	2.16E+08	7.9	1401
Q6UN15	Pre-mRNA 3-end-processing factor FIP1	FIP1L1	7	66.526	83.183	13	2.47E+08	19.4	594
Q86U42	Polyadenylate-binding protein 2	PABPN1	2	32.749	38.259	3	52242000	8.8	306
Q86X55	Histone-arginine methyltransferase CARM1	CARM1	10	65.853	95.542	25	5.06E+08	25.7	608
Q8IX12	Cell division cycle and apoptosis regulator protein 1	CCAR1	8	132.82	53.467	10	91222000	8.5	1150
Q8N163	Cell cycle and apoptosis regulator protein 2	CCAR2	3	102.9	21.923	5	47183000	4.3	923
Q8N1F7	Nuclear pore complex protein Nup93	NUP93	8	93.487	94.621	16	1.32E+08	15.9	819
Q8TAQ2	SWI/SNF complex subunit SMARCC2	SMARCC2	11	132.88	166.94	23	3.34E+08	14.3	1214
Q8WWM7	Ataxin-2-like protein	ATXN2L	3	113.37	19.755	4	36303000	4.6	1075
Q8WXF1	Paraspeckle component 1	PSPC1	17	58.743	197.28	42	1.25E+09	41.9	523
Q92499	ATP-dependent RNA helicase DDX1	DDX1	31	82.431	323.31	83	2.28E+09	44.2	740
Q92734	Protein TFG	TFG	8	43.447	241.88	19	7.18E+08	32.8	400
Q92797	Symplekin	SYMPK	6	141.15	55.914	9	87828000	8.6	1274
Q92945	Far upstream element-binding protein 2	KHSRP	32	73.114	323.31	121	6.62E+09	58.8	711
Q969G3	SWI/SNF-related matrix-associated actin-dependent regulator of chromatin subfamily E member 1	SMARCE1	4	46.649	56.141	11	2.06E+08	21.4	411
Q96AE4	Far upstream element-binding protein 1	FUBP1	30	67.56	323.31	96	7.03E+09	54.8	644
Q96I24	Far upstream element-binding protein 3	FUBP3	11	61.64	65.805	18	4.37E+08	25.2	572
Q96PK6	RNA-binding protein 14	RBM14	7	69.491	51.466	11	65612000	14.3	669
Q96RN5	Mediator of RNA polymerase II transcription subunit 15	MED15	7	86.753	50.721	7	94276000	9	788
Q9BTL3	RNMT-activating mini protein	FAM103A1	5	14.381	55.625	13	2.61E+08	64.4	118

Q9BUF5	Tubulin beta-6 chain	TUBB6	19	49.857	220.49	34	1.12E+09	50.9	446
Q9C005	Protein dpy-30 homolog	DPY30	4	11.25	44.066	13	85204000	76.8	99
Q9C0C2	182 kDa tankyrase-1-binding protein	TNKS1BP1	13	181.79	96.391	19	1.91E+08	13.1	1729
Q9C0J8	pre-mRNA 3 end processing protein WDR33	WDR33	9	145.89	81.3	16	1.89E+08	11.5	1336
Q9H3D4	Tumor protein 63	TP63	9	76.785	74.892	20	2.92E+08	16.8	680
Q9NZB2	Constitutive coactivator of PPAR-gamma-like protein 1	FAM120A	8	121.89	56.774	13	1.42E+08	12.1	1118
Q9Y224	UPF0568 protein C14orf166	C14orf166	10	28.068	178.66	36	1.47E+09	41.8	244
Q9Y230	RuvB-like 2	RUVBL2	5	51.156	44.854	9	1.01E+08	13.8	463
Q9Y3I0	tRNA-splicing ligase RtcB homolog	RTCB	23	55.21	306.27	63	2.98E+09	51.9	505
Q9Y6Y8	SEC23-interacting protein	SEC23IP	3	111.08	23.38	5	87829000	5.2	1000

The definitions and parameters for each column are given in MaxQuant (version 1.5.4.1)
[a] Identifier(s) of major proteins possessing at least 50% of the peptides ascribed to a protein group.
[b] Name(s) of protein(s) contained within the protein group.
[c] Name(s) of the gene(s) associated to the proteins contained within the protein group.
[d] Total number of peptide sequences associated with all the proteins in the protein group. Only protein identifications made from at least 2 peptides were selected from the original data set.
[e] Molecular weight of the leading protein sequence contained in the protein group.
[f] Score for the protein identification which is derived from peptide posterior error probabilities. The higher the score, the more accurate the protein identification is.
[g] Number of MS/MS spectra reported for the peptide which was used to identify the peptide sequence ascribed to a protein group.
[h] Sum of eXtracted Ion Current (XIC) of all isotopic clusters associated with the identified amino acid sequence.
[i] Percentage of the sequence that is covered by the identified peptides of the best protein sequence contained in the group.
[j] the length of the identified amino acid sequence of the peptide.

D. List of protein hits identified in IP-MS experiments of Kpnβ1 from KYSE30 cell extracts

Majority protein IDs[a]	Protein names[b]	Gene Names[c]	Peptides[d]	Molecular weight (kDa)[e]	Score[f]	MS/MS count[g]	Intensity[h]	Sequence coverage (%)[i]	Sequence length[j]
Q14974	Importin subunit beta-1	KPNB1	10	97.169	108.95	20	5.69E+08	13.1	876
A0A024R4M0	40S ribosomal protein S9	RPS9	11	22.591	72.175	21	1.07E+09	41.8	194
A0A024R7W5	YTH domain-containing family protein 3	YTHDF3	3	58.311	28.658	8	1.63E+08	7.7	534
G3V203	60S ribosomal protein L18	RPL18	4	15.639	54.743	9	7.12E+08	26.3	133
A0A087WUK2	Heterogeneous nuclear ribonucleoprotein D-like	HNRNPDL	6	40.04	45.491	13	5.79E+08	17.9	363
P27635	60S ribosomal protein L10	RPL10	7	18.565	66.494	18	6.8E+08	33.1	163
Q13148	TAR DNA-binding protein 43	TARDBP	5	26.743	97.564	14	4.68E+08	30.9	243
A0A087X2D0	Serine/arginine-rich splicing factor 3	SRSF3	4	10.32	102.73	11	7.63E+08	49.5	95
A0A0A0MRA5	Heterogeneous nuclear ribonucleoprotein U-like protein 1	HNRNPUL1	8	85.939	63.254	17	3.36E+08	18.7	766
A0A0A0MRR7	U1 small nuclear ribonucleoprotein C	SNRPC	2	19.687	48.123	6	3.62E+08	11.7	180
P35658	Nuclear pore complex protein Nup214	NUP214	3	152.57	20.549	6	71902000	3.2	1519
J3KR24	Isoleucine--tRNA ligase, cytoplasmic	IARS	6	131.76	37.956	6	2.57E+08	7	1152
Q05048	Cleavage stimulation factor subunit 1	CSTF1	2	38.448	42.981	6	1.34E+08	7	345
A0A0B4J1Z1	Serine/arginine-rich splicing factor 7	SRSF7	4	15.763	30.046	7	2.59E+08	37.2	137
A0A0D9SFB3	ATP-dependent RNA helicase DDX3X	DDX3X	7	70.839	55.715	14	2.09E+08	13.6	640
A0A1B0GTW1	Tight junction protein ZO-2	TJP2	6	140.73	51.977	9	1.56E+08	7.9	1249
A0A1X7SBZ2	Probable ATP-dependent RNA helicase DDX17	DDX17	20	80.253	169.65	44	1.64E+09	33.5	729
A5YKK6	CCR4-NOT transcription complex subunit 1	CNOT1	9	266.94	76.261	11	2.04E+08	4.1	2376
B0QY89	Eukaryotic translation initiation factor 3 subunit L	EIF3L	14	70.901	237.34	20	5.66E+08	23.1	607
B0QYK0	RNA-binding protein EWS	EWSR1	3	64.929	57.044	12	6.66E+08	8.6	618
B1AK87	F-actin-capping protein subunit beta	CAPZB	5	29.295	40.551	10	2.62E+08	26.9	260
P62826	GTP-binding nuclear protein Ran	RAN	3	26.224	24.568	8	2.33E+08	18.5	233
F8W1R7	Myosin light polypeptide 6	MYL6	4	16.29	38.631	10	3.79E+08	35.9	145
C9JXB8	60S ribosomal protein L24	RPL24	3	14.369	20.254	11	8.34E+08	24.8	121

C9JSZ1	Far upstream element-binding protein 1	FUBP1	9	24.043	8.3273	3	1.61E+08	65.1	232
C9JZR2	Catenin delta-1	CTNND1	5	104.85	57.57	12	86804000	9.2	938
D3YTB1	60S ribosomal protein L32	RPL32	5	15.616	33.517	8	2.71E+08	26.3	133
D6R9P3	Heterogeneous nuclear ribonucleoprotein A/B	HNRNPAB	8	30.302	87.955	31	2.13E+09	31.8	280
E7EQG2	Eukaryotic initiation factor 4A-II	EIF4A2	6	41.29	6.2259	0	26250000	20.7	362
E7EQV9	Ribosomal protein L15	RPL15	5	20.51	39.391	18	6.52E+08	32.2	174
E7EX17	Eukaryotic translation initiation factor 4B	EIF4B	12	69.697	237.95	34	1.24E+09	21.3	616
E7EX29	14-3-3 protein zeta/delta	YWHAZ	3	28.036	58.199	7	1.62E+08	13	246
Q86V81	THO complex subunit 4	ALYREF	3	27.557	41.373	7	75806000	26.5	264
P49458	Signal recognition particle 9 kDa protein	SRP9	2	7.6677	19.154	3	2.99E+08	28.8	66
E9PMW7	Elongation factor 1-delta	EEF1D	6	28.821	89.024	11	5.07E+08	32.2	261
F5H2B9	Uveal autoantigen with coiled-coil domains and ankyrin repeats	UACA	4	150.53	27.86	6	98600000	3.3	1307
F5H2F4	C-1-tetrahydrofolate synthase, cytoplasmic	MTHFD1	8	110.61	46.53	7	1.3E+08	9.7	1020
F5H365	Protein transport protein Sec23A	SEC23A	5	82.968	38.629	7	65691000	8.8	736
F8W822	ARF GTPase-activating protein GIT2	GIT2	3	46.988	21.397	5	28665000	15.9	421
F8W726	Ubiquitin-associated protein 2-like	UBAP2L	5	113.63	45.603	14	2.28E+08	7.2	1079
F8W930	Insulin-like growth factor 2 mRNA-binding protein 2	IGF2BP2	10	66.785	182.95	24	9.54E+08	23	605
F8WJN3	Cleavage and polyadenylation specificity factor subunit 6	CPSF6	4	52.269	43.329	10	1.71E+08	13.2	478
H0YCQ8	Eukaryotic translation initiation factor 3 subunit M	EIF3M	4	25.092	43.305	11	82589000	34.1	220
H0YEB6	Sjoegren syndrome/scleroderma autoantigen 1	SSSCA1	2	20.916	26.98	8	1.63E+08	11.9	193
H3BV80	RNA-binding protein with serine-rich domain 1	RNPS1	4	24.561	54.049	6	1.17E+08	29.4	211
J3QL05	Serine/arginine-rich splicing factor 2	SRSF2	2	15.156	66.546	6	2E+08	30.8	130
J3KTA4	Probable ATP-dependent RNA helicase DDX5	DDX5	9	69.086	40.441	13	6.68E+08	17.6	614
J3QR09	Ribosomal protein L19	RPL19	4	23.134	53.819	17	6.36E+08	18.1	193
J3KTL2	Serine/arginine-rich splicing factor 1	SRSF1	10	28.329	76.078	24	9.4E+08	35.2	253
J3QLE5	Small nuclear ribonucleoprotein-associated protein N	SNRPN	6	17.546	109.67	19	1.66E+09	26.6	169
J3QT28	Mitotic checkpoint protein BUB3	BUB3	5	31.703	48.913	17	6.09E+08	23.4	278
K7ES31	Eukaryotic translation initiation factor 3 subunit K	EIF3K	4	15.875	31.296	13	2.99E+08	40.9	137
M0QZC5	40S ribosomal protein S11	RPS11	6	13.997	38.635	10	3.23E+08	36.4	118

M0R0F0	40S ribosomal protein S5	RPS5	4	22.391	33.742	9	1.61E+08	33.5	200
M0R3D6	60S ribosomal protein L18a	RPL18A	6	16.714	37.08	12	4.23E+08	31.2	141
O00267	Transcription elongation factor SPT5	SUPT5H	5	121	72.308	6	1.98E+08	5.6	1087
O00425	Insulin-like growth factor 2 mRNA-binding protein 3	IGF2BP3	9	63.704	127.54	24	6.18E+08	19.9	579
O15371	Eukaryotic translation initiation factor 3 subunit D	EIF3D	7	63.972	65.791	11	3.68E+08	21.4	548
O43390	Heterogeneous nuclear ribonucleoprotein R	HNRNPR	5	70.942	31.019	10	2.35E+08	8.5	633
O43809	Cleavage and polyadenylation specificity factor subunit 5	NUDT21	10	26.227	86.171	36	1.09E+09	55.5	227
U3KQK0	Histone H2B	HIST1H2BN	3	18.804	51.74	9	5.46E+08	20.5	166
O60884	DnaJ homolog subfamily A member 2	DNAJA2	6	45.745	61.422	15	4.86E+08	22.6	412
O75534	Cold shock domain-containing protein E1	CSDE1	5	88.884	36.195	9	1.04E+08	10.3	798
O75821	Eukaryotic translation initiation factor 3 subunit G	EIF3G	8	35.611	116.4	22	6.8E+08	28.1	320
O94888	UBX domain-containing protein 7	UBXN7	6	54.862	44.96	14	2.83E+08	16.6	489
O95816	BAG family molecular chaperone regulator 2	BAG2	3	23.772	56	9	1.73E+08	20.9	211
O96019	Actin-like protein 6A	ACTL6A	7	47.46	67.984	11	3.81E+08	26.6	429
P02545	Prelamin-A/C	LMNA	13	74.139	183.96	26	7.94E+08	29.7	664
P05387	60S acidic ribosomal protein P2	RPLP2	11	11.665	222.29	34	2.85E+09	82.6	115
P07814	Bifunctional glutamate/proline--tRNA ligase	EPRS	14	170.59	115.48	28	6.68E+08	12.4	1512
P07900	Heat shock protein HSP 90-alpha	HSP90AA1	8	84.659	22.706	3	1.03E+08	14.3	732
P08579	U2 small nuclear ribonucleoprotein B	SNRPB2	4	25.486	23.216	6	77281000	25.3	225
P08621	U1 small nuclear ribonucleoprotein 70 kDa	SNRNP70	7	51.556	93.893	22	6.8E+08	21.7	437
P09012	U1 small nuclear ribonucleoprotein A	SNRPA	5	31.279	45.929	12	4.33E+08	24.8	282
P09661	U2 small nuclear ribonucleoprotein A	SNRPA1	4	28.415	44.697	5	1.56E+08	21.6	255
P10412	Histone H1.4	HIST1H1E	3	21.865	34.293	9	3.7E+08	19.2	219
P11908	Ribose-phosphate pyrophosphokinase 2	PRPS2	5	34.769	108.58	19	4.14E+08	24.2	318
P16401	Histone H1.5	HIST1H1B	3	22.58	30.076	10	3.95E+08	17.7	226
P16403	Histone H1.2	HIST1H1C	3	21.364	7.7382	3	95199000	17.8	213
P18077	60S ribosomal protein L35a	RPL35A	2	12.538	12.214	3	3.87E+08	13.6	110
P18124	60S ribosomal protein L7	RPL7	11	29.225	80.696	22	9.49E+08	36.7	248
P23246	Splicing factor, proline- and glutamine-rich	SFPQ	15	76.149	165.75	37	1.69E+09	27.3	707

P23258	Tubulin gamma-1 chain	TUBG1	5	51.169	34.796	11	2.39E+08	15.7	451
P23526	Adenosylhomocysteinase	AHCY	4	47.716	26.536	6	1.92E+08	9.5	432
P26196	Probable ATP-dependent RNA helicase DDX6	DDX6	8	54.416	128.77	13	2.18E+08	32.9	483
P26641	Elongation factor 1-gamma	EEF1G	3	50.118	28.794	6	1.87E+08	9.2	437
P27694	Replication protein A 70 kDa DNA-binding subunit	RPA1	4	68.137	26.775	6	1.95E+08	8	616
P30050	60S ribosomal protein L12	RPL12	3	17.818	74.942	13	1.32E+09	24.2	165
P30153	Serine/threonine-protein phosphatase 2A 65 kDa regulatory subunit A alpha isoform	PPP2R1A	7	65.308	49.756	11	1.23E+08	18.2	589
P31689	DnaJ homolog subfamily A member 1	DNAJA1	7	44.868	67.426	18	4.75E+08	30.2	397
P31942	Heterogeneous nuclear ribonucleoprotein H3	HNRNPH3	8	36.926	154.17	29	1.22E+09	42.2	346
P35637	RNA-binding protein FUS	FUS	9	53.425	139.85	33	1.48E+09	20.2	526
P40429	60S ribosomal protein L13a	RPL13A	5	23.577	34.833	14	4.91E+08	21.7	203
P42285	Superkiller viralicidic activity 2-like 2	SKIV2L2	11	117.8	76.936	17	2.11E+08	14.8	1042
Q5T4L4	40S ribosomal protein S27	RPS27	3	7.3564	24.481	6	3.33E+08	37.9	66
P43358	Melanoma-associated antigen 4	MAGEA4	5	34.899	126.07	16	3.73E+08	15.1	317
P46060	Ran GTPase-activating protein 1	RANGAP1	9	63.541	99.19	16	3.51E+08	24.2	587
P46777	60S ribosomal protein L5	RPL5	7	34.362	63.515	25	1.11E+09	23.2	297
P46778	60S ribosomal protein L21	RPL21	5	18.565	76.985	21	1.48E+09	36.9	160
P49368	T-complex protein 1 subunit gamma	CCT3	5	60.533	45.83	10	3.71E+08	13.8	545
P49756	RNA-binding protein 25	RBM25	5	100.18	31.872	9	87360000	10.1	843
P50991	T-complex protein 1 subunit delta	CCT4	5	57.924	100.81	14	2.25E+08	16.5	539
P52292	Importin subunit alpha-1	KPNA2	6	57.861	98.266	12	1.64E+08	17.8	529
P55735	Protein SEC13 homolog	SEC13	3	35.54	105.39	7	4.03E+08	15.5	322
P55884	Eukaryotic translation initiation factor 3 subunit B	EIF3B	17	92.48	182.69	27	8.33E+08	26.7	814
P60228	Eukaryotic translation initiation factor 3 subunit E	EIF3E	10	52.22	116.8	27	1.27E+09	28.5	445
P60842	Eukaryotic initiation factor 4A-I	EIF4A1	10	46.153	94.725	19	4.41E+08	36	406
P60866	40S ribosomal protein S20	RPS20	4	13.373	46.106	21	1.53E+09	25.2	119
Q5JR95	40S ribosomal protein S8	RPS8	5	21.879	143.67	13	9.04E+08	32.4	188
P62258	14-3-3 protein epsilon	YWHAE	3	29.174	6.8104	2	33024000	11.8	255

P62277	40S ribosomal protein S13	RPS13	6	17.222	44.919	14	5.98E+08	42.4	151
P62304	Small nuclear ribonucleoprotein E	SNRPE	3	10.803	36.231	4	4E+08	42.4	92
P62306	Small nuclear ribonucleoprotein F	SNRPF	4	9.7251	84.853	11	6.67E+08	80.2	86
P62314	Small nuclear ribonucleoprotein Sm D1	SNRPD1	4	13.281	72.499	27	9.11E+08	54.6	119
P62316	Small nuclear ribonucleoprotein Sm D2	SNRPD2	8	13.527	70.61	13	8.25E+08	54.2	118
P62318	Small nuclear ribonucleoprotein Sm D3	SNRPD3	2	13.916	29.092	8	1.3E+09	15.1	126
P62424	60S ribosomal protein L7a	RPL7A	9	29.995	87.518	23	1.63E+09	29.7	266
P62699	Protein yippee-like 5	YPEL5	2	13.841	12.659	6	58742000	19.8	121
P62701	40S ribosomal protein S4, X isoform	RPS4X	9	29.597	70.806	17	7.58E+08	40.7	263
P62753	40S ribosomal protein S6	RPS6	5	28.68	56.163	13	1.02E+09	18.9	249
P62877	E3 ubiquitin-protein ligase RBX1	RBX1	2	12.274	29.116	6	49316000	17.6	108
P62899	60S ribosomal protein L31	RPL31	4	14.463	38.022	9	5.79E+08	32.8	125
P62917	60S ribosomal protein L8	RPL8	6	28.024	60.113	13	6.97E+08	29.6	257
P78371	T-complex protein 1 subunit beta	CCT2	7	57.488	49.875	10	2.03E+08	21.7	535
Q07666	KH domain-containing, RNA-binding, signal transduction-associated protein 1	KHDRBS1	4	48.227	30.392	10	2.63E+08	12.2	443
Q09028	Histone-binding protein RBBP4	RBBP4	6	47.655	51.063	12	3.86E+08	28.5	425
Q13151	Heterogeneous nuclear ribonucleoprotein A0	HNRNPA0	5	30.84	70.148	14	7.3E+08	19	305
Q13247	Serine/arginine-rich splicing factor 6	SRSF6	5	39.586	37.144	14	7.88E+08	14.5	344
Q13263	Transcription intermediary factor 1-beta	TRIM28	7	88.549	94.196	16	4.96E+08	12.7	835
Q13283	Ras GTPase-activating protein-binding protein 1	G3BP1	13	52.164	139.37	35	1.1E+09	42.1	466
Q13435	Splicing factor 3B subunit 2	SF3B2	11	100.23	171.32	22	6.63E+08	21.3	895
Q13813	Spectrin alpha chain, non-erythrocytic 1	SPTAN1	12	284.54	92.418	17	4.63E+08	7.5	2472
Q14152	Eukaryotic translation initiation factor 3 subunit A	EIF3A	21	166.57	212.32	45	1.5E+09	18.2	1382
Q14247	Src substrate cortactin	CTTN	17	61.585	188.86	43	1.37E+09	33.8	550
Q14258	E3 ubiquitin/ISG15 ligase TRIM25	TRIM25	4	70.973	32.841	6	2.04E+08	7.9	630
Q14315	Filamin-C	FLNC	11	291.02	15.054	18	7.21E+08	15.6	2725
Q14444	Caprin-1	CAPRIN1	10	78.365	45.8	22	1.22E+09	25.1	709
Q15029	116 kDa U5 small nuclear ribonucleoprotein component	EFTUD2	11	109.43	93.553	22	4.9E+08	18.1	972

Q15046	Lysine--tRNA ligase	KARS	9	68.047	99.523	16	3.66E+08	22.9	597
Q15084	Protein disulfide-isomerase A6	PDIA6	4	48.121	44.438	9	3.95E+08	15.2	440
Q15149	Plectin	PLEC	5	531.78	31.331	2	54557000	1.9	4684
Q15427	Splicing factor 3B subunit 4	SF3B4	2	44.385	27.038	6	2.8E+08	8.7	424
Q15637	Splicing factor 1	SF1	7	68.329	96.365	21	8.29E+08	19.6	639
Q15717	ELAV-like protein 1	ELAVL1	4	36.091	30.562	8	2.19E+08	17.8	326
Q16777	Histone H2A type 2-C	HIST2H2AC	3	13.988	30.94	11	4.47E+08	44.2	129
Q1KMD3	Heterogeneous nuclear ribonucleoprotein U-like protein 2	HNRNPUL2	6	85.104	58.663	8	1.7E+08	13	747
Q6P2E9	Enhancer of mRNA-decapping protein 4	EDC4	6	151.66	98.107	15	3.03E+08	7.5	1401
Q6UN15	Pre-mRNA 3-end-processing factor FIP1	FIP1L1	5	66.526	42.993	9	1.66E+08	14.1	594
Q86X55	Histone-arginine methyltransferase CARM1	CARM1	9	65.853	88.945	19	6.65E+08	24.7	608
Q8IX12	Cell division cycle and apoptosis regulator protein 1	CCAR1	7	132.82	80.523	13	2.43E+08	11	1150
Q8IZ83	Aldehyde dehydrogenase family 16 member A1	ALDH16A1	5	85.126	51.368	7	89483000	7.9	802
Q8N163	Cell cycle and apoptosis regulator protein 2	CCAR2	19	102.9	201.25	36	1.29E+09	31.4	923
Q8N1F7	Nuclear pore complex protein Nup93	NUP93	6	93.487	55.296	10	65232000	12.2	819
Q8N684	Cleavage and polyadenylation specificity factor subunit 7	CPSF7	8	52.049	68.502	23	3.93E+08	24.4	471
Q8TAQ2	SWI/SNF complex subunit SMARCC2	SMARCC2	5	132.88	52.692	16	1.97E+08	5.8	1214
Q8WUF5	RelA-associated inhibitor	PPP1R13L	5	89.09	34.949	4	84870000	7.7	828
Q8WXF1	Paraspeckle component 1	PSPC1	11	58.743	107.71	23	9.09E+08	26	523
Q92734	Protein TFG	TFG	8	43.447	232.47	20	9.84E+08	28.5	400
Q92900	Regulator of nonsense transcripts 1	UPF1	5	124.34	32.778	11	1.64E+08	5.2	1129
Q92922	SWI/SNF complex subunit SMARCC1	SMARCC1	4	122.87	14.804	1	13410000	4.3	1105
Q92945	Far upstream element-binding protein 2	KHSRP	20	73.114	260.04	46	2.6E+09	40.6	711
Q96AE4	Far upstream element-binding protein 1	FUBP1	22	67.56	323.31	71	7.31E+09	48.6	644
Q96I24	Far upstream element-binding protein 3	FUBP3	3	61.64	12.622	4	65875000	7	572
Q96PK6	RNA-binding protein 14	RBM14	5	69.491	51.328	11	2.81E+08	10.9	669
Q96S59	Ran-binding protein 9	RANBP9	4	77.846	32.338	8	1.14E+08	7.5	729
Q99613	Eukaryotic translation initiation factor 3 subunit C	EIF3C	15	105.34	246.42	35	1.32E+09	18.4	913
Q9BWF3	RNA-binding protein 4	RBM4	3	40.313	84.522	6	1.22E+08	14.8	364

Q9C005	Protein dpy-30 homolog	DPY30	3	11.25	25.189	11	99985000	47.5	99
Q9NWU2	Glucose-induced degradation protein 8 homolog	GID8	3	26.748	30.322	5	1.44E+08	23.2	228
Q9NZI8	Insulin-like growth factor 2 mRNA-binding protein 1	IGF2BP1	3	63.48	20.011	5	92203000	6.9	577
Q9UHD9	Ubiquilin-2	UBQLN2	4	65.695	11.83	4	65545000	8.7	624
Q9ULW8	Protein-arginine deiminase type-3	PADI3	4	74.742	26.929	11	2.34E+08	10.2	664
Q9UMX0	Ubiquilin-1	UBQLN1	5	62.518	113.84	14	4.7E+08	14.4	589
Q9Y224	UPF0568 protein C14orf166	C14orf166	7	28.068	114.39	34	1.53E+09	37.7	244
Q9Y265	RuvB-like 1	RUVBL1	8	50.227	73.473	15	6.59E+08	27.6	456
Q9Y285	Phenylalanine--tRNA ligase alpha subunit	FARSA	3	57.563	18.876	5	57344000	7.1	508
Q9Y3F4	Serine-threonine kinase receptor-associated protein	STRAP	6	38.438	54.387	10	1.97E+08	26	350

The definitions and parameters for each column are given in MaxQuant (version 1.5.4.1)
[a] Identifier(s) of major proteins possessing at least 50% of the peptides ascribed to a protein group.
[b] Name(s) of protein(s) contained within the protein group.
[c] Name(s) of the gene(s) associated to the proteins contained within the protein group.
[d] Total number of peptide sequences associated with all the proteins in the protein group. Only protein identifications made from at least 2 peptides were selected from the original data set.
[e] Molecular weight of the leading protein sequence contained in the protein group.
[f] Score for the protein identification which is derived from peptide posterior error probabilities. The higher the score, the more accurate the protein identification is.
[g] Number of MS/MS spectra reported for the peptide which was used to identify the peptide sequence ascribed to a protein group.
[h] Sum of eXtracted Ion Current (XIC) of all isotopic clusters associated with the identified amino acid sequence.
[i] Percentage of the sequence that is covered by the identified peptides of the best protein sequence contained in the group.
[j] the length of the identified amino acid sequence of the peptide.

APPENDIX II

STRING interaction networks

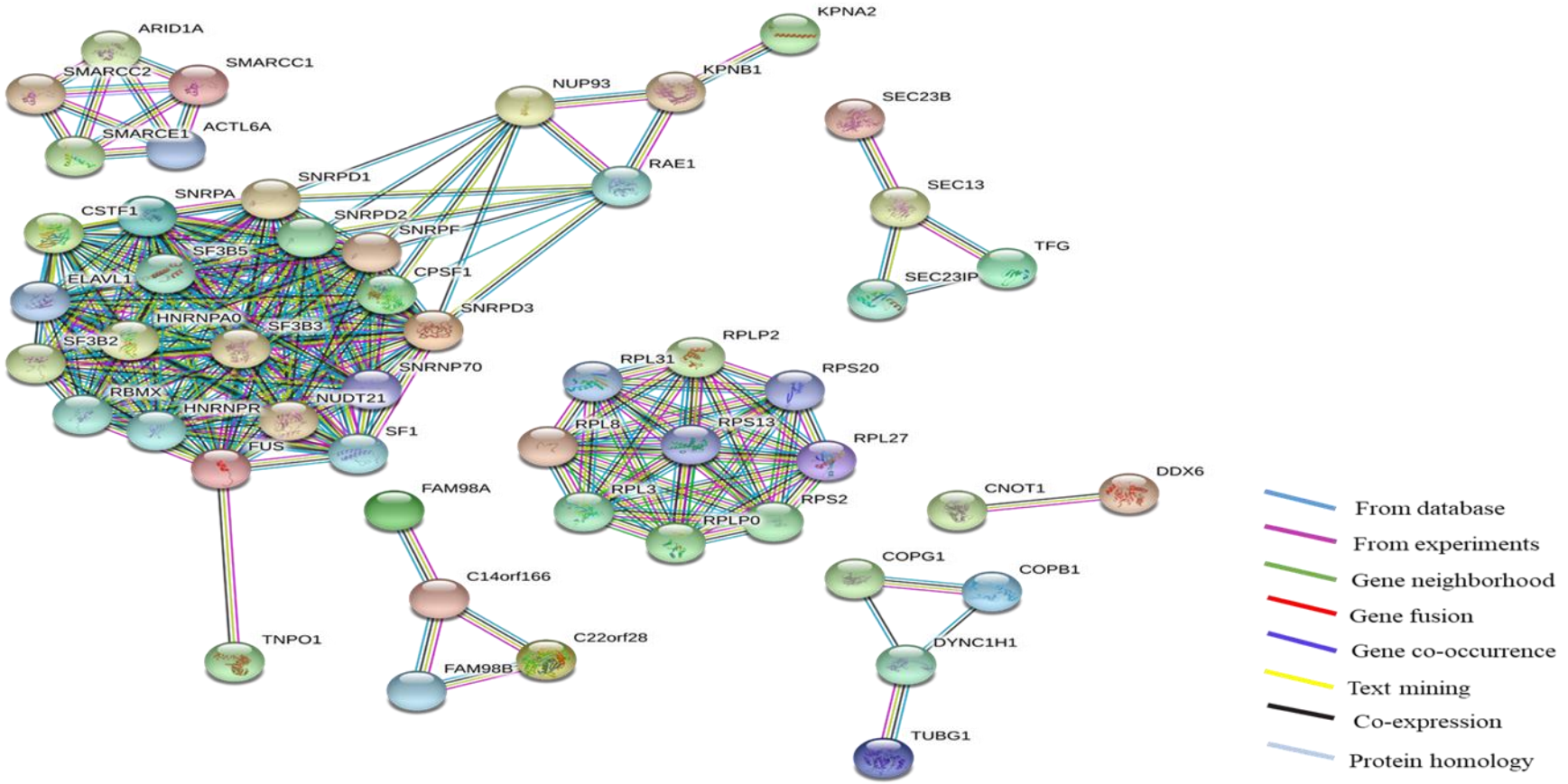

Figure A.1. STRING interaction network for the binding partners of Kpnβ1 in hTERT-RPE1 cell extracts

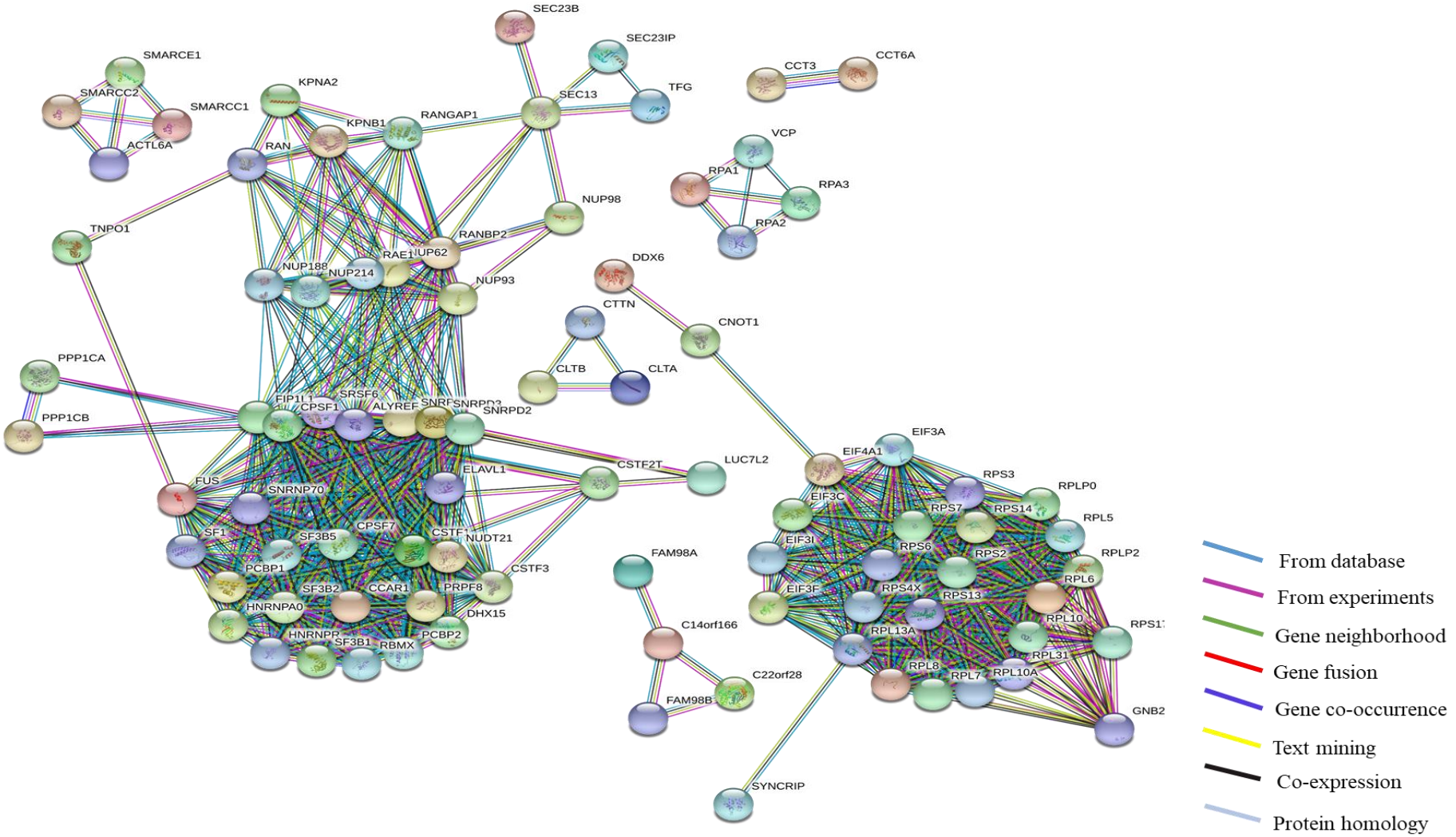

Figure A.2. STRING interaction network for the binding partners of Kpnβ1 in HeLa cell extracts

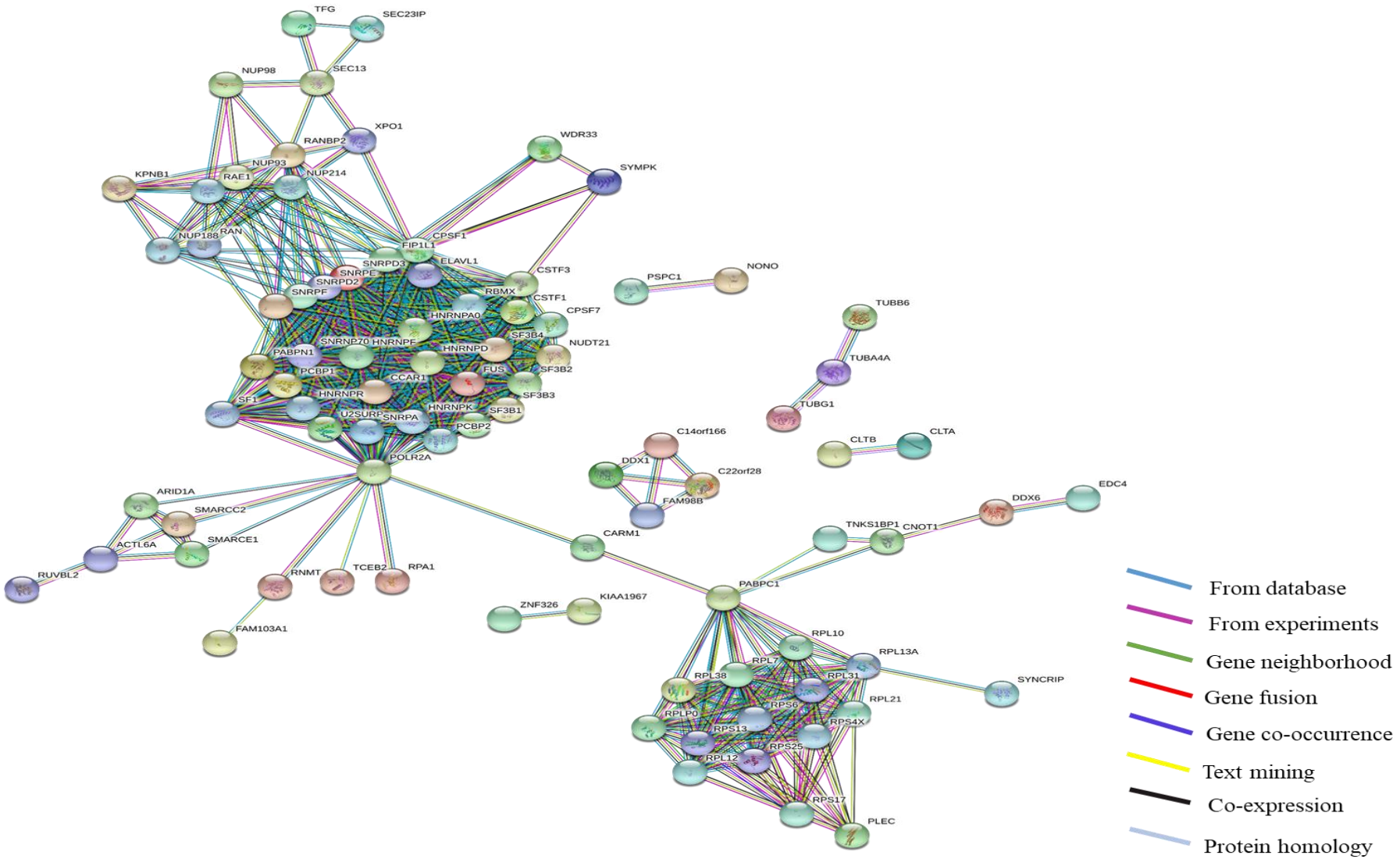

Figure A.3. STRING interaction network for the binding partners of Kpnβ1 in WHCO5 cell extracts

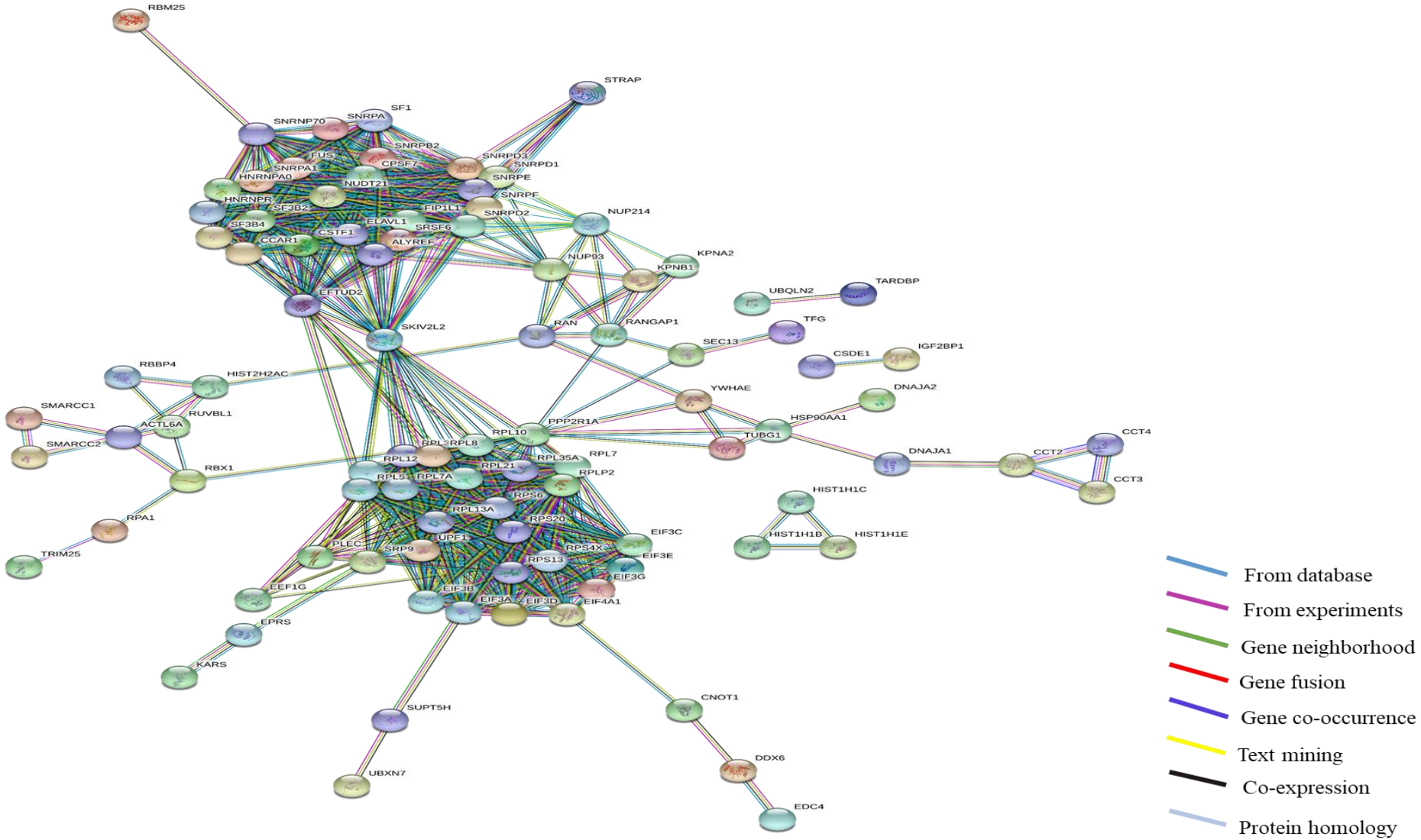

Figure A.4. STRING interaction network for the binding partners of Kpnβ1 in KYSE30 cell extracts

APPENDIX III

Buffers and solutions

Cell culture solutions

10x PBS

40 g NaCl

1 g KCl

3.82 g $Na_2HPO_4.2H_20$

1 g KH_2PO_4

Make up to 500 ml with dH_20 then autoclave

1x PBS

100 ml of 10x PBS

900 ml dH_2O

Trypsin-EDTA

0.5 g Trypsin

1.45 g $Na_2HPO_4.2H_20$

8 g NaCl

0.2 g $KHPO_4$

0.2 g KCl

10 mM EDTA, pH 8

Make up to 1 litre (L) with PBS, then autoclave

Freeze down medium

80% DMEM

10% FBS

10% DMSO

Protein solutions

RIPA buffer

150 mM NaCl

1% Triton-X-100

1% Sodium deoxycholate

0.1% SDS

10 mM Tris-Cl pH 7.5

Store at 4 °C

Western blot solutions

1 M Tris pH 6.8

Dissolve 121 g Tris base in 800 ml dH_2O. Adjust pH with concentrated HCl to pH 6.8. Make up to a final volume of 1 L with dH_2O, then autoclave.

1 M Tris pH 8.8 (1 L)

Dissolve 121 g Tris base in 800 ml dH_2O. Adjust pH with concentrated HCl to pH 8.8. Make up to a final volume of 1 L with dH_2O, then autoclave.

10% SDS in dH_2O (1 L)

Dissolve 100 g SDS in 800 ml dH_2O, then make up to a final volume of 1 L with dH_2O

Acrylamide/Bisacrylamide (37.5:1, 30%)

30 g Acrylamide

0.8 g Bisacrylamide

0.1 g SDS

Make up to 100 ml with dH_2O

10% Ammonium persulphate (APS)

Dissolve 0.1 g APS in 1 ml dH_2O

10% Separating gel

2.75 ml dH_2O

3.75 ml 1 M Tris-Cl, pH 8.8

3.35 ml 30 % Acrylamide

100 µl 10 % SDS

200 µl 10 % APS

20 µl Temed

4 % Stacking gel

3.65 ml dH2O

0.625 ml 1 M Tris-Cl, pH 6.8

0.65 ml 30 % Acrylamide

50 µl 10 % SDS

60 µl 10 % APS

6 µl Temed

4 X Laemmli loading dye

250 mM Tris-Cl, pH 6.8

6 % SDS

0.005 % Bromophenol Blue

40 % Glycerol

10 % β-mercaptoethanol

10x Running buffer

63.2 g Tris

40 g Glycine

10 g SDS

Dissolve in 800 ml dH_2O then make up to a final volume of 1 L with dH_2O

1x Running buffer

100 ml 10x Running buffer

900 ml dH_2O

10x Transfer buffer

38 g Tris

144 g Glycine

Dissolve in 800 ml dH_2O then make up to a final volume of 1 L with dH_2O, then autoclave.

1x Transfer buffer

100 ml 10x Transfer buffer

200 ml Methanol

700 ml dH_2O

10x TBS

24.33 g Tris base

80.06 g NaCl

Dissolve in 800 ml dH_2O. Adjust pH with concentrated HCl to pH 7.6. Make up to a final volume of 1 L with dH_2O, then autoclave.

1x TBST

100 ml of 10x TBS

900 ml dH_2O

1 ml TWEEN®20

5% milk blocking solution

2.5 g Fat-free powder milk

Dissolve in 40 ml TBST then make up to a final volume of 50 ml with TBST

Coomassie blue stain (1 litre)

0.5 g Coomassie brilliant blue

500 ml Methanol

100 ml Acetic acid

400 ml dH_2O

Coomassie destaining solution

50 ml Methanol

70 ml Acetic acid

880 ml dH_2O

Stripping buffer

10% Acetic acid

IP solutions

Non-denaturing lysis buffer

120mM NaCl

100 mM $CaCl_2$

250 mM Tris pH 7.4

Autoclave and store at 4°C

Wash buffer

1.2 g Na_2HPO_4

0.22 g $NaH_2PO_4.H_2O$

8.5 g NaCl

Dissolve in 800 ml in dH_2O. Adjust pH to pH 7.15. Make up to a final volume of 1 L with dH_2O

APPENDIX IV

Protein ladder

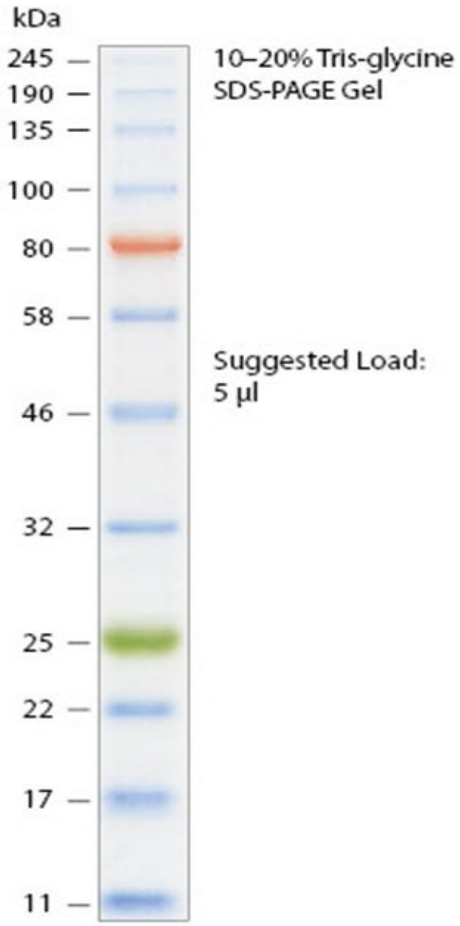

Figure B.1. Colour pre-stained protein standard broad range 11-245 kDa. The ladder was purchased from New England Biolabs (Cat. No. P7712, Ipswich, MA, USA)